

PhD THESIS

SIDERURGICAL AGGREGATES FOR THE MANUFACTURE OF CEMENT-
BASED MATERIALS

PhD CANDIDATE

GILBERTO DE JESUS GARCIA DEL ANGEL

SUPERVISORS

CARLOS THOMAS GARCIA

RENE BERNARDO ELIAS CABRERA CRUZ

UNIVERSITY OF CANTABRIA

Doctoral School of the University of Cantabria

Santander 2023

Preface

This doctoral thesis was developed at the E.T.S. de Caminos, Canales y Puertos in Santander, Spain, from 2019 to 2023. This section is written to show the achievements in the form of international stays, indexed articles, book chapters, and participation in conferences related to the Thesis topic.

This section contains four parts:

The first shows that an international stay at the Universidad Autónoma de Tamaulipas occurred. For this purpose, the certificate of the stay is attached.

The second part is the scientific publications related to this thesis, which consist of articles, book chapters, and conference papers.

The third part is acknowledging the institutions, thanks to which this work could be carried out.

The last part is the personal thanks to the people I consider closest to me; without their support, this work would not have been possible either.

International research stay certificate



Tampico Tamaulipas, a 28 de septiembre del 2021

A quien corresponda:

Por este medio, el que suscribe Jefe de la División de Estudios de Posgrado e Investigación de la Facultad de Ingeniería "Arturo Narro Siller" ubicada en el campus sur de la Universidad Autónoma de Tamaulipas certifica que el Mtro. Gilberto de Jesús García Del Ángel, doctorando en el programa de Doctorado en Ingeniería Civil por la Universidad de Cantabria, realizó su estancia de investigación desde el 22 de abril al 15 de septiembre del presente año.

Sin otro particular, queda de usted.

ATENTAMENTE
"VERDAD, BELLEZA, PROBIIDAD"

Dr. Julio César Rolón Aguilar
Jefe de la División de estudios de Posgrado

c.c.p. Archivo

Scientific publications

Articles published in JCR journals

1. García Del Angel, G.; Sainz-Aja, J.A.; Tamayo, P.; Cimentada, A.; Cabrera, R.; Pestana, L.R.; Thomas, C. Effect of Recycled Foundry Sand on the Workability and Mechanical Properties of Mortar. *Appl. Sci.* 2023, 13, 3436. <https://doi.org/10.3390/app13063436>
2. Del Angel, G.G.; Aghajanian, A.; Tamayo, P.; Rico, J.; Thomas, C. Siderurgical Aggregate Cement-Treated Bases and Concrete Using Foundry Sand. *Appl. Sci.* 2021, 11, 435. <https://doi.org/10.3390/app11010435>
3. Del Angel, G.G.; Aghajanian, A.; Cabrera, R.; Tamayo, P.; Sainz-Aja, J.A.; Thomas, C. Influence of Partial and Total Replacement of Used Foundry Sand in Self-Compacting Concrete. *Appl. Sci.* 2023, 13, 409. <https://doi.org/10.3390/app13010409>

Book chapters

Del Angel, G.G.; Thomas, C. 1 - The Use of Foundry Sand for Recycled Aggregate Concrete. In *The Structural Integrity of Recycled Aggregate Concrete Produced with Fillers and Pozzolans*; Awoyera, P.O., Thomas, C., Kirgiz, M.S., Eds.; *Woodhead Publishing Series in Civil and Structural Engineering*; Woodhead Publishing, 2022; pp. 3–24 ISBN 978-0-12-824105-9.

García Del Angel, G.; Thomas, C.; Cabrera R.; Rolón, J. 10 – Arena de fundición en hormigones como medida sustentable de construcción. In *La ingeniería y su impacto socioeconómico y medioambiental en zonas urbanas*; Pichardo, R., Treviño, J., Tobías, R.; Fomento editorial, 2021, pp. 151-165. ISBN Colofón: 978-607-635-274-8

Conferences presented at national and international congresses

García Del Angel, G., Thomas C. Viabilidad técnica de la gravacemento utilizando escorias de acería. XIX Congreso internacional, XXV Congreso internacional de Ciencias Ambientales (ANCA 2022). Tampico, México.

García Del Angel, G. Utilización de arena de fundición en materiales base cemento. 1st International Santander Conference Eco-Concrete (ISECC 2021), Santander, Spain.

García Del Ángel, G. Incorporation of foundry sand in cementitious materials. International Meeting of Civil Engineering Doctorates (EIDEIC 2021), Santander, Spain.

Acknowledgements to institutions



My deepest thanks to Carlos Thomas, who has placed his trust and knowledge in my training, allowing me to be part of the LADICIM concrete group, to whom I am also grateful for all the help and support throughout these years of work. Special thanks to Pablo Tamayo and Jose Adolfo Sainz-Aja, who guided me along this learning path.



Special thanks to Carlos Llovo from Reinosa Forgings and castings and Moises Puente from Rocacero for providing the materials used in this work. Also, special thanks to Jokin Rico from INGECID. Without the support of these companies, the research work would not have been possible.



To the Universidad Autónoma de Tamaulipas, especially to the Cuerpo Académico UAT- CA-29: Medio Ambiente y desarrollo sustentable, led by Dr. Julio César Rolón Aguilar, whom I also thank for his support. The present thesis is the culmination of years of work and experiences that would not have been possible without the support provided by Dr. René Cabrera, who encouraged me to reach greater achievements while I was studying for my degree.



Special acknowledgement



The PhD student, Gilberto de Jesús García Del Ángel, CVU 1133087, would like to give special thanks to the Consejo Nacional de Ciencia y Tecnología (CONACYT) for awarding the 2021 Northeast Regional Scholarship and an extension of the same. Without the invaluable support of the institution this work would not have been possible.

Acknowledgements

A todos y cada uno de los amigos y maravillosas personas que cruzaron mi camino por España, especialmente a Eneko Pedrazuela y Paulina Pérez, cuya amistad y apoyo me ayudaron a lo largo de este camino.

A mi padre Gilberto García, a mi madre Erika Del Angel y a mi familia, por ser los pilares que me sostuvieron en momentos donde la distancia era más fuerte que yo.

Muchas gracias.

Knowledge is meant to be shared.

Index

Preface.....	I
International research stay certificate.....	II
Scientific publications.....	III
Acknowledgements to institutions.....	IV
Special acknowledgement.....	V
Acknowledgements.....	VI
Index.....	VIII
Abstract.....	XIII
Abbreviations list.....	XV
Chapter 1. Introduction and objectives.....	1
1.1. Introduction.....	2
1.1.1. Recycled foundry sand.....	3
1.2. Objectives.....	11
1.3. Thesis structure.....	12
Chapter 2. The use of foundry sand in recycled aggregate concrete.....	17
2.1. Introduction.....	18
2.2. Foundry sand generation.....	19
2.3. Physical-chemical properties of foundry sand.....	20
2.4. Foundry sand in concrete.....	24
2.4.1. Fresh properties of concrete with foundry sand.....	25
2.4.2. Mechanical properties of concrete with foundry sand.....	26
2.4.2.1. Compressive strength.....	27
2.4.2.2. Flexural strength.....	30

2.4.3. Durability	31
2.4.3.1. Carbonation depth.....	31
2.4.3.2. Acid environment.....	32
2.4.3.3. Sulphate resistance	33
2.4.3.4. Rapid chloride penetration	34
2.5. Other applications of foundry sand.....	35
2.5.1. Foundry sand in road construction	35
2.5.2. Foundry sand in masonry elements	36
2.6. Conclusions.....	37
Chapter 3. Effect of recycled foundry sand on the workability and mechanical properties of mortar	41
3.1. Introduction.....	44
3.2. Materials.....	46
3.2.1. Cement and fine aggregates.....	46
3.2.2. Mix proportions	48
3.3. Methods.....	49
3.3.1. Workability	49
3.3.2. Physical properties	49
3.3.3. Mechanical properties.....	49
3.3.4. Wear resistance	50
3.3.5. Variable correlation.....	50
3.3.6. Microstructural characterization.....	50
3.4. Results and discussion.....	51
3.4.1. Workability	51
3.4.2. Physical characterization of mortars	54
3.4.3. Mechanical characterization of mortars.....	58

3.4.4. Mechanical durability	62
3.4.5. Variable correlation	63
3.4.6. Microstructural characterization	65
3.5. Conclusions and future work	68
Chapter 4. Siderurgical Aggregate Cement Treated Bases and Concrete Using Foundry Sand.....	71
4.1. Introduction	73
4.2. Materials and methods	76
4.2.1. Cement.....	76
4.2.2. Foundry sand	76
4.2.3. Siderurgical aggregates	77
4.2.4. Mix proportions	79
4.2.4.1. CTB Mix proportions	79
4.2.4.2. SAC Mix proportions.....	81
4.2.5. Physical properties of hardened concrete.....	83
4.2.6. Gas permeability.....	83
4.2.7. Depth of water penetration.....	83
4.2.8. Compressive strength	83
4.2.9. Modulus of elasticity.....	84
4.2.10. Flexural strength.....	84
4.3. Results and discussion.....	84
4.3.1. Physical properties of hardened concrete.....	84
4.3.2. Compressive strength	85
4.3.3. Modulus of elasticity.....	86
4.3.4. Flexural strength	87
4.4. Conclusions.....	87

Chapter 5. Influence of partial and total replacement of used foundry sand in self-compacting concrete.....	91
5.1. Introduction.....	93
5.2. Materials and methods.....	97
5.2.1. Materials.....	97
5.2.2. Mix proportions.....	98
5.2.3. Fresh state properties.....	100
5.3. Mechanical properties.....	101
5.4. Concrete microstructure.....	101
5.5. Results and discussion.....	102
5.5.1. Fresh state properties.....	102
5.5.2. Mechanical properties.....	105
5.5.3. Concrete microstructure.....	108
5.6. Conclusions.....	110
Chapter 6. General conclusions and future research work.....	113
6.1. General conclusions.....	114
6.2. Future research work.....	116
Chapter 7. References.....	117
Annexes.....	135
Index of tables and figures.....	136

Abstract

Foundry sand is a material composed of sand and natural or chemical binders. This compound is compacted to create moulds into which molten metal is poured. Once the solidification of the metal is complete, the foundry sand is broken down by mechanical means and reused until its properties are no longer suitable, creating a waste. The worldwide waste production of foundry sand is estimated at 100 Mt/year.

This thesis's main objective is to develop cement-based materials with partial and total replacement percentages of recycled foundry sand as fine aggregate.

In the first stage of this research, recycled foundry sand and natural aggregates were characterised by their particle size, and physical and chemical properties.

In the second stage, the influence of recycled foundry sand in manufacturing conventional mortars was analysed. The substitution percentages ranged from 25 to 100% by weight and the water/cement ratios varied from 0.5 to 0.7 depending on the percentage of substitution. Fresh properties, physical properties, mechanical properties, and durability were determined. It was concluded that while small substitution levels lead to a slight improvement of the mechanical properties, this trend is broken for high substitution levels due to the negative effect of the high w/c ratios required.

In the third stage, recycled foundry sand was used with untreated steel slags to manufacture cement-treated layers and concrete. The physical, mechanical, and durability characteristics of the aggregates were analysed. As for the concrete with steel aggregate, compressive strength, modulus of elasticity, and flexural strength tests were carried out; in general, the mechanical properties are adequate but the

durability was not satisfactory, so it is recommended that it be used as a clean-up concrete.

In the fourth stage, self-compacting concrete was manufactured with 50 and 100% replacement (by volume) of recycled foundry sand. The results showed that the workability of the concretes with recycled foundry sand is improved compared to the control concrete. Regarding compressive strength at 7 and 28 days, the self-compacting concrete with 50% replacement showed the best results. The microstructure analysis showed that incorporating recycled foundry sand improves the concrete, creating a denser and less porous matrix than the control concrete.

Abbreviations list

Due to the composition of this doctoral thesis comprising articles that were published during its development, the subsequent list of abbreviations aims to facilitate the reader's comprehension of each individual chapter.

Chapter	Abbreviation
1	CDW: Construction and demolition waste
	CFS: Chemical foundry sand
	CTM: Cement-treated material
	FS: Foundry sand
	GC: Gravel-cement
	GFS: Green foundry sand
	NS: Natural sand
	RFS: Recycled foundry sand
	SA: Siderurgical aggregates
	SCC: Self-compacting concrete
	SS: Steel slag
<hr/> w/c: Water/cement ratio <hr/>	
2	Al ₂ O ₃ : Aluminium oxide
	CC: Coal cinder
	C-S-H: Calcium-silica-hydrate gel
	EAFS: Electric Arc Furnace Slags
	FA: Fly ash
	Fe ₂ O ₃ : Iron oxide
	FUFS: Fungal treated UFS
	H ₂ SO ₄ : Sulfuric acid
	HMA: Hot Mix Asphalt
	HPC: High Performance concrete
	MgSO ₄ : Magnesium sulphate
	Na ₂ SO ₄ : Sodium sulphate
	RCPT: Rapid chloride permeability test
	RHA: Rice husk ash
	SFS: Spent foundry sand
	SiO ₂ : Silicon dioxide
	SO ₃ : Sulphur oxide
TUFS: Treated UFS	
UFS: Used foundry sand	

	UHPC: Ultra High Performance concrete
	WFS: Waste foundry sand
	<hr/>
	CFS: Chemical foundry sand
	FS: Foundry sand
	GFS: Green foundry sand
3	NS: Natural sand
	SEM: Scannign electron microscope
	SS: Silica sand
	UFS: Used foundry sand
	<hr/>
	CBR: California bearing ratio
	CTB: Cement-treated bases
	EAF: Electric Arc Furnace
	FS: Foundry sand
	NA: Natural aggregates
4	NS: Natural sand
	RA: Recycled aggregates
	RAC: Recycled aggregate concrete
	SA: Siderurgical aggregate
	SAC: Siderurgical aggregate concrete
	UCS: Unconfined compressive strength
	<hr/>
	CFS: Chemical foundry sand
	GFS: Green foundry sand
	LC: Limestone coarse aggregate
	LS: Limestone sand
5	SCC: Self-compacting concrete
	SS: Silica sand
	UFS: Used foundry sand
	WFS: Waste foundry sand
	<hr/>

Chapter 1. Introduction and objectives

1.1. Introduction

The construction industry is responsible for exploiting more than 50% of natural resources (coarse and fine aggregates) and 39% of CO₂ emissions. To counteract this, alternative materials have been investigated. Among the most notable alternative materials are the demolition and construction wastes (CDW). The CDW goes through a recovery process in which the first stage is its classification to separate the different materials (wood, plastic, metals, brick, concrete) to be recycled. In this section, the CDW on which the interest is focused is the one coming from the concrete elements. Subsequently, they go through a crushing and sieving process, which separates them into different sizes. Afterwards, contaminants such as wood, plastics and metal are removed by manual means or by screening. Finally, their tribological, physical and durability properties are evaluated for their use in cement-based materials. When these properties are suitable for their use in cement-based materials, they are known as recycled aggregates, which have been extensively valorised and studied in different cement-based materials, mainly in conventional and self-compacting concretes. However, there are steel slags (SS) and foundry sand (FS), known as siderurgical aggregates (SA), which come from foundry and steel processes. Like CDW, SS and FS undergoes a very similar valorization process. In the case of SS, when the slag is separated from the molten metal, it undergoes a slow cooling process which inertises the SS. Then it goes through a crush and sieve procedure. After crushing and screening, the SS is separated into different sizes, to finally characterize its tribological, physical and durability properties as with CDW. In the case of FS, once the sand is reused until its properties are no longer suitable for the foundry process, it is discarded and accumulated. Its valorization process consists of separating the traces of ferrous or non-ferrous materials by

means of sieves. Then, as with CDW and SS, its tribological and physical properties are evaluated for use as fine aggregate in cement-based materials. SA has similar characteristics to natural aggregates, however, comparing SS with natural aggregates, these have a higher density, higher strength, higher mechanical durability and higher porosity. As for FS, the density can be higher or lower than silica sand, this will depend on the foundry process and the type of binder used. FS has a higher absorption than natural aggregates, as well as chemical traces of other elements such as Co and Pb, which are not present in natural sand. In general, these physicochemical characteristics depend on the foundry process and the material being manufactured. . The effect that these SA have on cement-based materials will depend on different variables such as their substitution percentage, water/cement ratio (w/c), characteristics of the aggregates, etc. Using SA in cement-based materials favours the use of potential aggregates that, if not used, would be taken to landfills, ending their useful life. By using them, not only is their helpful life prolonged, but the exploitation of natural resources is avoided, and in parallel, a cement-based material is created with characteristics similar to those made with natural aggregates.

1.1.1. Recycled foundry sand

Sand casting is a traditional method that is used in the automotive industry, aerospace, machine component manufacturing, etc. [1], this system is the most common process for casting ferrous materials (iron and steel) and non-ferrous materials (brass, bronze, and aluminium). Foundry sand (FS) is the material used for the manufacture of sand moulding boxes; these boxes are manufactured by compacting two moulds (one upper and one lower) of agglomerated sand against a solid object, generally made of wood, plastic, or metal [2], this object is a reproduction of the part to be manufactured. When the compaction procedure is complete, the moulds are removed momentarily to remove the part, and the moulds are reattached to form a single mould

with a cavity inside. Subsequently, the molten metal is poured into the moulding box, the metal solidifies, and the sand box is removed and broken up by mechanical means for subsequent reuse. Depending on the binder used in the casting process, two types of FS are distinguished; green foundry sand (GFS), which is dark or grey in colour and consists of 85-95% silica, 0%-10% bentonite clay as a binder, 2%-10% water and 5% carbonaceous additive to improve the finish of the casting, controlling the strength and permeability [3,4]. Chemical foundry sand (CFS), which is off-white to medium tan in colour, consists mainly of silica, between 93%-99% and between 1%-3% chemical additives such as furfuryl alcohol, sodium silicates, phenolic urethanes, and phenolic formaldehyde [5-7]. Chemical bonding systems are most commonly used to manufacture cores and moulds for non-ferrous castings [8].

It is estimated that the generation of discarded FS is 100 Mt annually [9] and that for 1 t of steel produced, 0.60 t of discarded FS is generated [10]. To prevent FS from being taken to landfills, researchers have analysed its physical and chemical properties to use it in other composite materials, with which recycled foundry sand (RFS) is generated. According to Sabour et al. [11], the three primary producers of RFS are China, India, and the United States, producing 48.75, 11.49 and 11.30 Mt annually, respectively. On the other hand, Brazil is reported to generate 3 Mt annually [12], South Africa around 1 Mt [13], and Spain and Poland around 1 and 0.70 Mt [14].

The physical properties of RFS depend on variables such as the type of casting process, the type and amount of additives used for moulding, the number of times the sand has been recycled, the industry sector, differences in sand shape, fines content, particle size, and mineralogy [15-18]. For example, Dayton et al. [19] studied RFS from 39 foundries, finding that generally, the grain size varies between 0.05 - 2 mm. The

physical properties of RFS reported by different authors it is shown in Table 1.1:

Table 1.1. Physical properties of RFS according to different authors.

Authors	Specific gravity (g/cm ³)	Absorption (%)	Modulus of fineness
FIRST [4]	2.60-2.80	-	-
Smarzewski [14]	2.67	1.40	1.80
Sandhu & Siddique [20]	2.65	0.62	1.93
Priyadarshini & Prakash [21]	2.55	1.70	1.80
Ashish & Verma [22]	2.64	0.75	-

The chemical properties of RFS depend on the type of molten metal cast, the binder, and the additives used [23], as can be seen from the main component is silicon dioxide (SiO₂), whose range varies between 81.85%-91.20%, followed by aluminium oxide (Al₂O₃), with values between 2.30%-11.82% and iron oxide (Fe₂O₃), whose range varies between 1.20%-1.82% [24–28].

Within the valorisation process, one concern is leaching, being the binder system is the primary source of organic contaminants in the RFS; the GFS smelting process has a lower potential to leach organic compounds than chemically bonded systems [5]. However, several metallic elements are found in RFS, a study reported by Miguel et al. [6] in which it was analysed different RFS samples found that the elevated Co and Pb concentrations are due to the sand binder being an alkyd urethane. The authors also reported that the concentrations of Cr, Mo, Ni, and Ti are bound in the silica matrix and therefore do not represent a problem. Table 1.2 shows the chemical composition of the RFS according to different authors in the literature.

Table 1.2. Chemical composition of RFS (% by weight) according to different authors.

Constituent	Alekseev et al. [24]	Alonso-Santurde et al. [25]	Apithanyasa i, Supakata & Papong. [26]	Arulrajah et al. [27]	Basar & Deveci [28]
SiO ₂	91.20	85.4	83.60	84.15	81.85
Al ₂ O ₃	2.30	3.64	2.91	11.82	10.41
Fe ₂ O ₃	1.20	1.45	1.71	1.53	1.82
SO ₃	0.70	-	-	0.45	0.84
CaO	0.10	0.49	0.42	1.51	1.21
Na ₂ O	0.30	0.48	0.37	-	0.76
K ₂ O	0.10	0.38	0.53	0.29	0.49
MnO	0.00	0.03	-	-	-
TiO ₂	0.10	0.16	-	0.26	-
P ₂ O ₃	-	0.06	-	-	-
MgO	-	0.66	0.99	-	1.97
LOI	3.70	6.87	-	-	6.93

With the above, it can be concluded that the high generation of RFS, its physicochemical properties, the increased awareness of the environmental problems this waste could cause, and the search for alternative aggregates have led researchers to study its viability.

It is well known that mortar is composed of three materials, cement, sand and water, which form a greyish paste when mixed together. On the other hand, in masonry, mortar is defined as a mixture of one or more inorganic binders, water, and additives or admixtures [29]. The difference between concrete and mortar is that mortar uses only sand, while concrete comprises the materials above and coarse aggregates. However, mortar is still one of the most popular construction materials, its ease of application, mechanical properties, and durability

have made it one of the most reliable materials for everything from the most straightforward projects to large-scale works.

Regarding mortars with RFS, Monosi, Sani and Tittarelli [30] used a replacement of up to 30% of natural sand (NS) by RFS with a fixed w/c ratio of 0.5, reporting a decrease of the workability of 8, 19 and 22% as the RFS content increased by 10, 20 and 30% respectively. At 28 days, the compressive strength of the mortars decreased when the replacement was higher than 20%, which was attributed to the presence of fine powder carbon and clay within the binder, causing a loosening of contacts and links between the aggregates and cement matrix [30]. However, with up to 10% RFS replacement, the mortar's compressive strength was not affected significantly. Vázquez et al. [31] used RFS from an aluminium foundry as a total replacement for NS in manufacturing mortars. The compressive strength results at 7, 14, and 28 days reported that the total inclusion of RFS decreased the compressive strength by 71, 77, and 76% compared to the control mortar. This was attributed to the reaction of cement with aluminium, which produces hydrogen gas that creates microcracks in the cementitious matrix [31]. Çevik et al. [23] manufactured mortars with up to 60% replacement (in steps of 15%) of NS by RFS and a fixed w/c ratio of 0.5. Compressive strength results at three days showed an increase of 13 and 12% when 15 and 30% of RFS were used, respectively. However, at 28 days, the compressive strength of the mortars decreased compared to the control mortar. Matos et al. [32] studied the replacement of NS by 50 and 100% of RFS. Workability results indicated that, compared with the control mortar, the replacement by RFS decreased the workability by 22 and 39%, which was attributed to the presence of pulverized coal and fine particles of bentonite, increasing the absorption of water, thus decreasing the workability [32]. As for the reduction of compressive strength, it was due to the lower compaction of the mix because of the reduction of workability and to the excess of fine material in the RFS, which

impedes the proper bonding between the aggregates and the cement paste as stated by Siddique and Noumowe [33].

As can be observed, the use of RFS in mortars has taken a conservative line in which low percentages of substitution are used. Even those works using complete RFS substitution are scarce. Therefore, this research proposes the total use of RFS in manufacturing mortars, analysing their physical and mechanical properties and their durability, as well as complementing the study with SEM analysis.

Gravel-cement (GC), is a cement-treated material (CTM), which is used as a structural layer in road pavements. CTM are characterised by being a mixture of coarse aggregates, with a minimum amount of cement (3.5-5%) and an adequate amount of water for compaction and hydration of the cement [34,35].

CTM consists of granular materials, cement, water, and additives if is necessary. In the particular case of GC, artificial aggregate obtained from combining two or more aggregate particle size fractions is used [36]. The aggregates must provide the GC with adequate adhesion to the cement paste, absence of leachates, volumetric stability, and a compatible and non-separable mineral skeleton [37]. The aggregates to be used in a GC must be crushed materials from a quarry or gravel pit, industrial or mining by-products [36], construction and demolition waste (CDW), or inert waste products [37].

Regarding RFS, Li et al. [38] reported that the incorporation of up to 20% RFS reduces the mechanical properties of CTM. Vinoth et al. [39] studied ten different RFS samples from different foundries, and reported that the Proctor density is between 1.24 -1.83 g/cm³ and the optimum moisture content between 20-25%. The lower densities and moisture percentages are attributed to the carbon content in the RFS, making it more absorbent. It also reported that compressive strengths

of CTM with RFS appear to be influenced by the aggregate size and cement content. Bhardwaj and Sharma [40], reported that the inclusion of 10 to 40% RFS increases the optimum moisture content from 16 to 18.3% due to the bentonite particles making more water required as for density, it increased from 1.71 to 1.84 g/cm³ due to the higher specific surface area and density of RFS compared to natural aggregate. Almost similarly, Iqbal et al. [41] reported that increased RFS replacement increases the optimum moisture content due to the natural moisture content of RFS, while the variation in maximum density is due to the mineralogy, grain size, shape, and fines content of RFS.

A study reported the use of steel slags and RFS for manufacturing CTM, proving that using these recycled aggregates can achieve the requirements of a CTM [42]. Though there is evidence of the replacement of natural aggregates for steel slags and RFS in concretes, there is not much information about the combination of those by-products in the concrete and CTM-making process

The concept of self-compacting concrete (SCC) was first proposed in Japan in 1986 by Okamura [43], and subsequently, the prototype was developed by Ozawa in 1988 [44]. SCC differs from conventional concrete in that it can settle under its weight, i.e., it does not require external vibration. Its advantages, in addition to those mentioned above, are that it decreases construction and labour times, reduces noise pollution, improves the filling capacity of heavily reinforced structures, improves the interfacial transition zone between the paste and the aggregate, and decreases permeability [45].

SCC does not require vibration to be compacted; it can flow under its own weight and, even in the presence of congested reinforcements, fills and compacts the formwork [46]. Moreover, it has been studied with other by-products, such as electric arc furnace slags [47,48], showing adequate fresh state properties and mechanical behaviour. Likewise, SCC with recycled aggregates of precast concrete as coarse aggregates

has displayed mechanical properties [49] and durability [50], similar to SCC with natural aggregates. Moreover, SCC with recycled aggregates from railway wastes has shown adequate fresh-state properties, mechanical properties, and durability [51].

Regarding RFS in SCC, Siddique and Sandhu [52] studied SCC with 5, 10, and 15% replacement of natural sand by RFS, reporting an increase in compressive strength and splitting tensile strength at all ages (7, 28, and 56 days). The slump flow increases by 3% with 10% and 15% RFS replacement. By contrast, Parashar et al. [53] reported decreases in fresh state properties, SCC's behaviour, and mechanical properties when increasing replacement percentages up to 40%. Ashis and Verma [22] studied SCC with up to 50% replacement of RFS at intervals of 10%. The results indicated that the incorporation of RFS does not affect the passing ability and viscosity but negatively affects the flowability as the RFS replacement proportion increases. A decrease in the segregation of the SCC was also reported with an increase in RFS incorporation due to the low specific density of the RFS, avoiding settling [22]. In the same study [22], it was reported that RFS negatively affects compressive strength at early ages, but for longer ageing it does the contrary. This is due to a high silica content which slows down the pozzolanic reactions [22] however, with more extended aging, an improvement in compressive strength was observed. Sandhu and Siddique [54] analysed the replacement rate from 5% to 30% of RFS in SCC. It was reported that the fresh state and mechanical properties decreased as the replacement rate increased due to the increase in the specific surface area of RFS, leading to improper hydration and the formation of voids. Makul [55] concluded that RFS could be used in ready-mixed concrete plants and precast concrete yards. Moreover, it has been reported that using RFS led to 50–60% cost savings compared to natural sand [56]. A 100% replacement of fine natural aggregate by RFS can be proposed as a solution to landfill disposal and, at the same time, result in eco-efficient concrete

As described above, the use of RFS in SCC follows a certain conservatism by not using higher replacement percentages, so this work aims to investigate the effects of total RFS substitution in the manufacture of SCC, analysing its fresh state properties and its mechanical properties.

Therefore, this research proposes the partial and full replacement of the recycled foundry sand in manufacturing mortars, cement-treated bases, and self-compacting concretes. This will lengthen the life cycle chain of this SA and produce more environmentally friendly cement-based materials.

1.2. Objectives

This thesis aims to use siderurgical aggregates as a replacement for natural aggregates and cement in the manufacture of cement-based materials. To achieve this, several objectives have been set out, which are presented below:

1. Valorisation of the recycled foundry sand: Determine its grading, physical, and chemical properties.
2. Use of recycled foundry sand to manufacture mortars: Manufacture mortars with different replacement percentages and analyse their properties in the fresh state, hardened state, and resistance to abrasion.
3. Use of the recycled foundry sand to manufacture cement-treated bases: determine the maximum density and optimum moisture content through the modified Proctor test and study its mechanical properties.
4. Use of recycled foundry sand to manufacture self-compacting concrete: Study the behaviour in the fresh and hardened state of self-compacting concrete with different replacement percentages.

1.3. Thesis structure

This doctoral thesis consists of 7 chapters, which are described below:

Chapter 1. Introduction and objectives:

This chapter generally shows the problems to be solved with the doctoral thesis and the justification of the subject. In this same chapter, the main objective and the specific objectives are described.

Chapter 2. The use of foundry sand in recycled aggregate concrete:

This chapter is one of the results of the research carried out during this doctoral thesis. It deals more broadly with the generation of foundry sand, its physic-chemical properties, the fresh and hardened properties of concretes with recycled foundry sand, durability, and other applications in the construction industry. This book chapter has been published in the book "The Structural Integrity of Recycled Aggregate Concrete Produced with Fillers and Pozzolans," published by Elsevier with the same name as this chapter.

Chapter 3. Effect of recycled foundry sand on the workability and mechanical properties of mortar:

The use of recycled foundry sand in the manufacture of mortars is investigated. It is mainly studied how the degree of substitution (0-100%) of the material influences the workability, physical properties, mechanical properties (flexural and compressive strength), and durability. In addition, the microstructure of the mortar was also studied. This article has been published in *Applied Sciences*, with the same title as the chapter.

Chapter 4. Siderurgical Aggregate Cement Treated Bases and Concrete Using Foundry Sand: In this work, the effect of recycled foundry sand on the mechanical properties of a cement-treated layer and a conventional concrete was investigated:

The particle-size skeleton was made with untreated steel slag and recycled foundry sand. The maximum density and optimum moisture content were determined. A 2, 3, and 4% cement-to-aggregate weight ratio was used to manufacture the specimens. The compressive strength at seven days was carried out according to PG-3, and the results were compared with Spanish and international standards. As for the concrete was manufactured with the same materials as the cement-treated base, and its physical properties, mechanical properties, and durability were determined. This article has been published in *Applied Sciences*, with the same title as this chapter.

Chapter 5. Influence of partial and total replacement of used foundry sand in self-compacting concrete:

This chapter used recycled foundry sand as partial (50%wt.) and total (100%wt.) replacement of silica sand. A new mixture method was used in which the aggregates were mixed for a longer time, allowing a better homogenisation. The workability of the self-compacting concrete was studied and compared between the different substitution grades. The compressive strength and microstructure were also studied and compared between the different concretes. This article has been published in *Applied Sciences*, with the same title as this chapter.

Chapter 6. General conclusions and future research lines:

This chapter describes the main conclusions derived from the results of the research articles. It also sets out the future lines of research that have been proposed.

Chapter 7. References:

This chapter shows the literature used for the writing of the articles as well as the standards for the tests.

It should be mentioned that the structure of chapters 2 to 5 have been adapted from published articles. Finally, it is mentioned that chapters

3 to 5 contain the following sections: Abstract, Introduction, Materials and Methods, Results, Discussion and Partial conclusions.

The purpose of Figure 1.1 is to present a comprehensive overview of the research activities conducted during the development of this Doctoral Thesis. This figure serves as a visual aid to guide the reader through the stages and processes involved in the research. Its aim is to provide a clear outline of the methodology employed and the progression of the study.

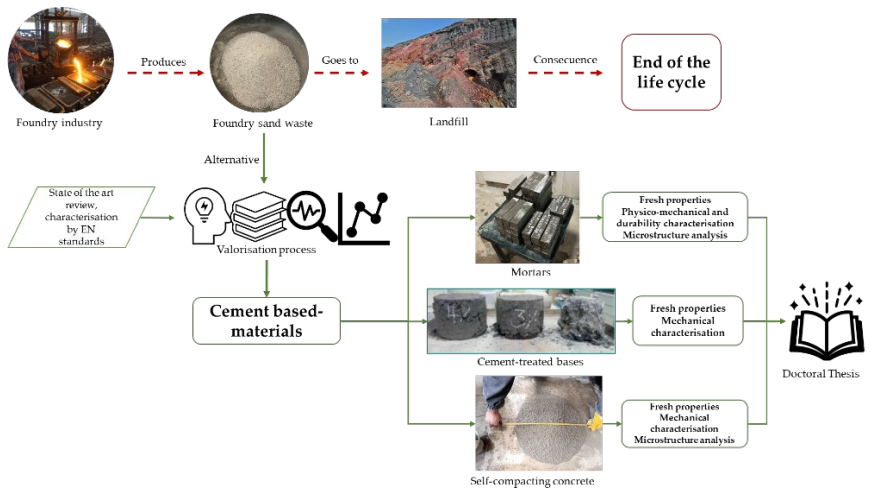


Figure 1.1. Doctoral Thesis outline

Chapter 2. The use of foundry sand in recycled aggregate concrete

Elsevier published this book chapter, it is part of the book "The Structural Integrity of Recycled Aggregate Concrete Produced with Fillers and Pozzolans". This book chapter is the result of extensive literature research on foundry sand. Including it as a chapter is to provide a broader background of this waste. The reference of this book chapter is presented below:

Del Angel, G.G.; Thomas, C. 1 - The Use of Foundry Sand for Recycled Aggregate Concrete. In *The Structural Integrity of Recycled Aggregate Concrete Produced with Fillers and Pozzolans*; Awoyera, P.O., Thomas, C., Kirgiz, M.S., Eds.; Woodhead Publishing Series in Civil and Structural Engineering; Woodhead Publishing, 2022; pp. 3–24 ISBN 978-0-12-824105-9.

The use of foundry sand in recycled aggregate concrete

Gilberto García Del Angel and Carlos Thomas

2.1. Introduction

Approximately 100 million tons of used foundry sand (UFS) is annually generated worldwide by foundry industry [17], in countries like Turkey, Poland, Spain, India, Brazil and the United States, foundries generate about 0.3, 0.7, 1, 1.7, 3 and 8 million metric tons of UFS per year, respectively [14,57]. In USA, only 10% of the waste material is used outside the foundries, the rest it is disposed in landfills, but the inconvenient is the leaching of heavy metals such as chromium, nickel, zinc, copper, iron and cadmium, creating soil pollution [58], other environmental issues due the UFS are saturation of landfills, CO₂ emissions (due the transport of the UFS from the foundry to the landfill), consumption of virgin raw materials and early closure of the material life cycle [17]. The increasing awareness of the environmental problems due the industrial activity has led to enforce regulations for the management of waste materials products from manufacturing industries, through a valorisation process, waste materials, now named by-products, can be used as replacement material for different applications. The viability of using UFS in the civil engineer branch in order to reduce the environmental issues caused by raw material extraction, transportation and land filling has been studied, proving that the UFS could be use as replacement of natural sand (NS) in soil improvement, blocks and bricks manufacturing, ceramics, road construction and concrete. Thus, the high production of UFS and the low reuse of it have open a gap where many researches have experiment the incorporation of the UFS in the civil engineer field, from road construction [59], concrete [60], self-compacting concrete (SCC) [52] fill material, fine aggregate replacement for concrete,

asphalt concrete pavements, Portland cement kiln feed, bituminous mixtures, rock wool silica and alumina additive [61].

2.2. Foundry sand generation

In the foundry industry, sand casting is a traditional metal forming method and an essential, necessary process, whose products are widely used in automotive, aerospace, machine tool components, etc., [1]. In the metal casting process of ferrous (steel and iron) and non-ferrous materials (aluminium, copper and brass) the sand cast system is the most common process, this system needs a high-quality silica sand with good shape and thermal conductivity properties, this high-quality sand will be used, shaped and compacted according to the mould pattern selected. As shown in Figure 2.1 through the production cycles, the foundry sand (FS) it is reuse until it is no longer suitable for the manufacturing process, when this happens, this by-product is known as UFS, Waste Foundry Sand (WFS) or Spent Foundry Sand (SFS) [5].



Figure 2.1. Foundry sand generation.

There are two types of FS depending of the binder that is use; green foundry sand (GFS) that consist up to 85-95% silica, 0-10% of bentonite clay as binder, 2-10% of water and 5% sea coal as carbonaceous additive to improve the casting finish, controlling the strength and permeability [62–64], generally is black, or grey colour (Figure 2.2 left). There are other additives used to prevent expansion defects and absorb moisture, those are cellulosic additives like rice hulls, wood flour,

pecan shells, oat hulls and aqueous emulsion [6,58]. When the FS use polymers as binders to create “cores” receive the name of chemical foundry sand (CFS), that consists of 93-99% silica and 1-3% chemical binder [4] like furfuryl alcohol, sodium silicates, phenolic-urethanes and phenol-formaldehyde [5–7], as shown in Figure 2.2 (right), CFS has a typically medium tan or off-white colour [5] and a very low moisture absorption [8]. The temperature of the mould-metal interface approaches 1000°C. As a result, all organic materials (binders, additives, coatings) have oxidation and thermal degradation (burning). Residual organic compounds in UFS are found only in small quantities, typically does not contain organic contaminants above regulatory threshold levels [8].



Figure 2.2. Green foundry sand (left) and Chemical foundry sand. Source: [65].

2.3.Physical-chemical properties of foundry sand

The physical properties are an important parameter when study an aggregate because those properties will determine the possible uses in any field required. The physical properties of the UFS depends of such variables as the type of casting process, the type and amount of additives used for moulding, number of times that the sand was recycled, the industry sector, differences in shape, fines content, particles and mineralogy [15–18]. Dayton et al. [19] studied UFS from 39 foundries, finding that sand with grain size of 0.05 mm–2 mm was

the dominant size fraction of the UFS, ranging with a median of 90.3%. The particle shape is typically sub angular to round and it does not meet the gradation requirements for fine aggregates as per ASTM C33 [66]. The grain size distribution of UFS is very uniform, with approximately 85 to 95% of the material between 0.6 mm and 0.15 mm sieve sizes. While 5 to 20 % of FS can be expected to be smaller than 0.075 mm [5,15]. The sand wastes from the green sand systems are typically characterized by specific gravity (2.39-2.69 g/cm³), permeability (10-3 to 10-6 cm/sec), and moisture content (0.1 to 10 %). Density often ranges between 2.20 and 2.70 g/cm³, unit weight between 1052 and 1554 kg/m³, it has low absorption capacity (0.38% to 4.15%) and is non-plastic [17]. The values of absorption of UFS can vary, generally are higher compared to normal sand, the presence of binders and additives can be the main reason [15]. The specific gravity of UFS has been found to vary from 2.20 to 2.80 [4,5,14,53,57,62,67–69], meanwhile other studies shown values from 2.39 to 2.55, this variability can be attributed because the fines and additive contents [15]. Different researchers had study the physical properties of the UFS (Table 2.1) finding bulk density values from 1.28 to 1.48 t/m³, density values from 2.45 to 2.65 kg/m³, water absorption percent from 0.86 to 1.4 %, moisture percent from 3.25 to 10% and fineness modulus from 1.74 to 3.07 [4,5,14,53,57,62,67–69]. The plastic behaviour can depend on the clay content, for FS with 6 to 10% clay, a liquid limit (LL) greater than 20 and a plastic index (PI) greater than 2 are typical [4].

Table 2.1. Physical properties of UFS according to several authors.

Property	Bulk density (t/m ³)	Specific gravity	Density (kg/m ³)	Water absorption (%)	Fineness modulus
Siddique et al. [5]	-	2.61	-	1.30	1.78
Siddique et al.[62]	-	2.20	-	0.86	2.50
FIRST [4]	1.28	2.60-2.80	-	-	-
Guney et al. [57]	-	2.45	-	-	-
Matos et al. [67]	-	-	2.650	-	3.07
Gurumoorthy & Arunachalam [68]	1.40	2.32	-	-	1.74
Parashar et al. [53]	-	2.24	-	-	-
Gholampour et al. [69]	1.48	-	2.450	1.20	2.40

Depending upon the type of metal, type of binder, combustible used and foundry processing stage, the chemical composition of UFS may vary [15]. As it shown in Table 2.1 researches had found that the main constituents of UFS is silicon dioxide (SiO₂) in a range from 70.02 to 98.00 %, aluminium oxide (Al₂O₃) in a range from 0.80 to 11.99% and iron oxide (Fe₂O₃) from 0.70 to 5.06 %. Traces of MgO, K₂O, and TiO₂ also can be found, as reported by FIRST[4].

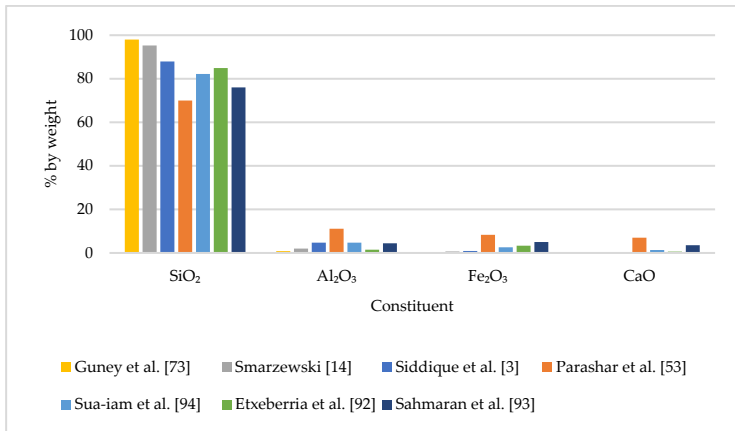


Figure 2.3. Chemical composition of UFS (%wt.) according to different authors.

A concern in the valorisation of UFS is the possible elevated concentrations of metals that can be harmful for human and animal health if leached [17]. The added organic and inorganic additives in the FS are the main source of organic contaminants [15]. The binder system is the primary source of organic contaminants in sand, the green sand casting process has lower potential leaching organic compounds than chemically bonded systems (depending upon the curing and pouring process) [5]. Under incomplete combustion conditions the organic compounds used in resins and binders can be transformed into hazardous compounds, however, these reactive compounds are not found at significant concentrations in sand [4].

Metal elements commonly found in UFS include Ag, Al, Ba, Be, Cd, Co, Cr, Cu, Fe, Li, Mg, Mn, Mo, Ni, Pb, Sb, Ti, Te, Tl, V, and Zn, Zr [6,17,70]. Miguel et al. [6] compared samples of UFS and virgin sands, finding that in UFS the content of Ba is commonly elevated as result of additives added, while high concentrations of Zr are found in some samples because it is the main constituent of paints used in the casting moulds. Pb is due to either bronze casting or the use of this metal in

alkyd urethane resin, also Co concentrations are high when alkyd urethane resin is used [6,70]. Cr, Mo, Ni, and Tl concentrations associated with the virgin sand should not be an issue since these metals are bound within the silica sand matrix [6]. The majority of UFS are categorized as non-hazardous [15], it is observed that because the low metal concentrations in UFS, this could be used beneficially in other applications posing no environmental or human health risk [6,8], providing an environmental friendly solution [17].

In summary, the main component in FS are SiO_2 , Al_2O_3 and Fe_2O_3 , the chemical properties of FS depend on the type of binder used, the combustion conditions and casting moulds, which can influence in the content of metals. It has been studied that the concentrations of metals in UFS are low and do not represent a risk for human health, thus their use in other applications is considerate.

2.4. Foundry sand in concrete

The high produced quantities of FS and UFS, their adequate physical and chemical properties and the increased concern of the environmental issues that this by-product could produce has lead the researchers to investigate the feasibility of the utilization of this by-product in conventional concrete with partial or total replacement of regular sand [5,15,32,33,62,71–75]. Concrete with Electric Arc Furnace Slags (EAFS) and UFS has been studied [76]. Some studies have proved the feasibility of FS and UFS in self-compacting concrete (SCC) and SCC with other additions such fly ash (FA), rice husk ash (RHA) and metakaolin [22,53,55,77–79]. In addition, High Performance concrete (HPC) and Ultra High Performance Concrete (UHPC) with incorporation of FS has been studied [14,18].

2.4.1. Fresh properties of concrete with foundry sand

One of the main characteristics that will demonstrate if concrete will have a good workability is the slump test. Siddique et al. [62] reported a control mix slump value of 90 mm, the slump test value decreased when replaced NS for UFS in 10%, 20% and 30% by weight, observing a loss in the slump value from 85 to 80 mm. Naik et al. [71] studied the replacement of NS for FS and UFS by 25% and 35%, slump values when UFS was used were 32 and 29 mm, respectively, from a control mix with a slump value of 152 mm.

Guney et al. [57] reported a control mix with a slump value of 160 mm, when 5%, 10% and 15% replacement of NS for GFS was used, the slump value decrease to 150 mm, 110 mm and 600 mm respectively. Khatib et al. [73] reported that there is systematic loss in workability as the percentage of UFS content increases due to the increased fineness of fine aggregate. Etxeberria et al. [76] reported slump values of concrete with natural coarse aggregates and UFS of 150 mm (CFS) and 750 mm (GFS). The lower slump values are attributed to the presence of binders that increased the water demand such as ashes, clay-type fine materials and impurities in UFS [15].

Monosi et al. [16] studied the effect of two different types of UFS, the first type was recovered directly from the moulds disposal (*) and the second one from the aspiration process (**). It was reported a decrease of the slump test of 20% when using 20% of replacement of NS by both UFS from a control concrete with 160 mm of slump. Also, when using 30% of replacement, the UFS from the moulds disposal presented a 150 mm slump meanwhile the UFS from the aspiration process result in a slump of 120 mm, a decrease of 6.25% and 25% respectively. This means that, as the replacement rate is higher, due the finer particles of the UFS there is a decrease in the workability [16].

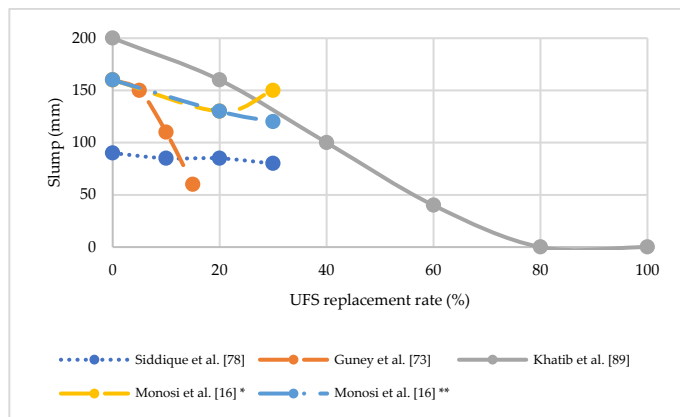


Figure 2.4. Slump test results according to different authors.

In SCC, slump values parameters could vary depending the standard of each country, The European Guidelines for SCC limit V-funnel flow time to a maximum of 25 s and slump flow diameter to a minimum of 550 mm [80]. Based on that guidelines, a study reported the replacement by weight of NS for UFS by 10%, 20%, 30% and 40% and the use of FA in addition with cement, proving that all the mixes qualified as SCC but the flow class and viscosity class varied depending on the UFS content in the mix [53]. Another study shown that SCC with a replace up to 100% of NS with UFS and up to 70% cement with FA can achieve proper fresh properties, enable manufacturing green, lower cost SCC [77]. SCC mixtures exhibited acceptable V-funnel performance at replacement levels of RHA and UFS not more than 10 and 30 wt.% [78].

2.4.2. Mechanical properties of concrete with foundry sand

In this section the compressive strength, flexural strength and modulus of elasticity of concrete, SCC, HPC and UHPC with incorporation of different replacement percent of UFS will be reviewed.

2.4.2.1. Compressive strength

In the Table 2.2, the concrete compression strength at 28 days with different replacement percent of UFS by different authors is presented. It can be observed that in some studies the increase of substitution of UFS decrease the compressive strength of concrete in relation with the control mix. On the other hand, it is observed that the compressive strength increase as the substitution rate of sand for UFS is higher. This could be due the variability of the composition of FS.

Table 2.2. Compressive strength (MPa) with different replacement percent of UFS at 28 days according to different authors.

UFS % by volume	0	10	20	30	40	50	60	100
Siddique et al. [62]	28.50	29.70	30.00	31.30	-	-	-	-
Gholampour et al. [69]	43.20	-	-	-	-	31.00	-	16.50
Siddique et al. [74]	36.27	31.05	32.52	38.03	36.42	37.14	23.86	-
Khatib et al. [73]	43.60	-	40.00	-	38.00	-	-	26.00
Martins et al. [72]	41.00	39.70	42.00	42.50	46.00	44.00	-	-
Kaur et al. [75]	31.10	33.76	27.80	-	-	-	-	-
Kaur et al. [75]	31.10	36.10	32.80	-	-	-	-	-
Parashar et al. [53]	34.40	32.40	26.40	21.80	21.50	-	-	-
Smarzewski [14]	122.20	116.40	-	-	-	-	-	-
Basar & Deveci [81]	43.20	41.70	40.02	36.60	31.00	-	-	-
Ganesh et al. [60]	33.14	33.24	32.58	31.24	29.48	25.23	-	-
Monosi et al. [30]	45.00	-	38.00	35.00	-	-	-	-

The increase or decrease of the compressive strength can vary depending on the substitution rate, the type of UFS used, the type of concrete and if there is or not a previous treatment. As reported by Siddique et al. [62] the increase of the compressive strength could be

related to the fact that UFS is finer than regular sand creating a denser matrix due a large formation of calcium-silica-hydrate gel, C-S-H [74] and due the high silica content [62]. Results shown an increase of the compressive strength with a substitution from 10%-30% of sand by UFS which represents an increase of 4%, 5% and 10% respectively. [62]. Another work by Siddique et al. [74] showed that with a substitution from 30%-50% of NS for UFS the compressive strength increase between 2%-5%. Martins et al. [72] reported an increase of the compressive strength from 2%-12% with a substitution by 20%-50% of NS for UFS, the increase of the compressive strength was also attributed to the amount of silica content and the fine and regular shape of UFS [72]. Kaur et al.[75] reported an increase of the compressive strength when a substitution rate of 10%, 15% and 20% of fungal treated UFS (FUFS) was used, the higher increase was reported with 10% substitution of NS by FUFS, increasing the compressive strength 16%. This increase is due a formation of calcified filaments and biomineral formations which acts as filling material reducing the water absorption and porosity [75].

The decrease of the compressive strength is attributed to the high surface area of FS particles which led to the reduction of the water cement gel in matrix, resulting in a poor bonding between aggregates and cement paste as reported by Gholampour et al. [69] and Naik et al. [71] reported that the depending the type of binder in the UFS, weakens the interfacial transition zone in the concrete reducing the compressive strength [71], a similar conclusion is reported by Monosi et al. [30], it can be attributed to the presence of binders within the UFS which have fine powder of carbon and clay and causes a loose of contacts and links between the cement paste and the aggregate. Basar & Deveci [81] reported that the decrease of compressive strength is due to the higher surface area of fine particles which led to the reduction of the water cement gel in the matrix.

Diverse authors [72,74,81] had studied the substitution of 10% NS for UFS in conventional concrete, results presented a decrease in the compressive strength from 3%-14% as reported by Martins et al.[72], Basar & Deveci [81] and Siddique et al. [74]. With a 20% substitution of NS for UFS the compressive strength decrease is in the order of 7%-16% as reported by Siddique et al. [74], Khatib et al. [73], Kaur et al.[75], Basar & Deveci [81], Ganesh et al. [60] and Monosi et al. [30].

The effect of the compressive strength decrease with the substitution of 30% of NS by UFS has been studied and results shown that the decrease values are between 6%-22% as reported by Ganesh et al. [60], Basar & Deveci [81] and Monosi et al. [30]. The decrease of compressive strength with a substitution of 40% of NS by UFS was studied by Ganesh et al. [60], Khatib et al. [73] and Basar & Deveci [81], results reported a decrease value between 11%-28%. The use of 50% replacement of NS by UFS resulted in a decrease of the compressive strength 24% and 28% as reported by Ganesh et al. [60] and Gholampour et al. [69].

Few studies reported the substitution of 60% replacement of fine aggregate by UFS, in this case, Siddique et al. [74] reported a decrease value of 18% of the compressive strength. Finally, the total substitution of NS by UFS has shown a decrease of the compressive strength by 40% and 62% as reported by Khatib et al. [73] and Gholampour et al. [69].

In the case of UHPC, Smarzewski [14] studied mixtures with cement, silica fume, quartz sand, basalt and UFS. The study reported an increase of 11% of the compressive strength with the substitution of 5% of quartz sand for UFS due the formation of calcium-silica-hydrate gel, C-S-H. On the other hand, a decrease of 5% and 12% of the compressive strength was reported when the substitution of NS by UFS was 10% and 15% respectively, this decrease it can be attributed to some UFS impurities affecting the rheology and density of UHPC as the WFS substitution increases [14]. Smarzewski and Barnat-Hunek [18] studied

the compressive resistance of HPC with additions of coal cinder (CC), gravel, granite and UFS, the substitution of 5% of sand by UFS did not represent a significant increase of the compressive strength (0.2%) and the substitution of 15% of sand by UFS decrease the compressive strength by 1.3%.

2.4.2.2. Flexural strength

Ganesh et al. [60] studied the incorporation of FS from an aluminium casting industry as a replacement of NS from 10% to 50% in a conventional concrete. Results show that the incorporation of FS from 10% to 30% decrease the flexural strength 2.47%, 2.42% and 5.08% respectively, beyond 20% substitution it was presented a decrease of the flexural strength due fineness and the presence of clay, wood flour and sawdust in the FS. A similar case was reported by Gholampour et al. [69], results showed a decrease of 19.92% and 18.86% on the flexural strength with mixes containing 50% replacement of NS for UFS compared with conventional concrete.

On the other hand, Siddique et al. [62] obtained an increase of the flexural strength at 28 days with 10%, 20% and 30% substitution of NS for UFS, the reported increase compared with the control mix was 2.0%, 5.6% and 9% respectively. Smarzewski & Barnat-Hunek [18] obtained a decrease of 5% and 37% on the flexural strength when substituted 5% and 10% of quartz sand by UFS. Kumar et al. [82] experimented with quarry dust and UFS by mixing these materials in a 80/20 and 70/30 proportion. Results shown that with a 30% replacement of UFS the flexural strength decrease 14%, meanwhile, the mixture with 20% replacement of UFS presented a decrease of 21%.

Table 2.3. Flexural strength (MPa) with different replacement percent of UFS at 28 days according to different authors.

UFS % by volume	0	5	10	20	30	40	50
Smarzewski & Barnat-Hunek [18]	6.40	6.05	4.03	-	-	-	-
Ganesh et al. [60]	4.09	-	3.98	3.98	3.87	3.69	3.66
Gholampour et al. [69]	5.62	-	-	-	-	-	4.50
Siddique et al. [62]	3.41	-	4.00	4.10	4.18	-	-
Kumar et al. [82]	3.13	-	-	3.78	3.57	-	-

It is observed that the flexural strength trend to decrease as the FS replacement increase, this could be attributed to the poor bonding between the aggregates and cement paste

2.4.3. Durability

Although it is true that a good concrete is one that has good mechanical characteristics, its durability properties should not be lost of sight, since these will determine the behaviour of the concrete with respect to external agents. Such external agents that will be discussed in this section are; Carbonation, which it is associated with the corrosion effect in steel reinforcement; Acid environment; Sulphate resistance, which is a function of its physical and chemical resistance of the concrete to the penetration of sulphate ions and Chloride penetration, which can tell us how concrete behaves in a marine environment and how it can affect steel reinforcement.

2.4.3.1. Carbonation depth

There is not much information about carbonation depth in concrete containing UFS, a study presented by Siddique et al. [74] analysed the carbonation effects in concretes with a replacement rate of UFS from

10%-60% at the age of 90 days and 365 days. Results shown carbonation depth increases with the age and with the UFS replacement, reaching a carbonation penetration of 2.17 mm at 90 days and 5 mm at 365 days with a concrete mix containing 60% of UFS, this penetration is far less than the cover of reinforcing steel bars to cause corrosion. Ganesh et al. [83] also studied the carbonation depth at 180 and 365 days with a replacement rate of UFS from 10%-50%, results shown that the carbonation depth increases with the substitution rate, this could be due the poor workability of the concrete as the substitution rate increases, resulting in a deficient compactness and a porous system.

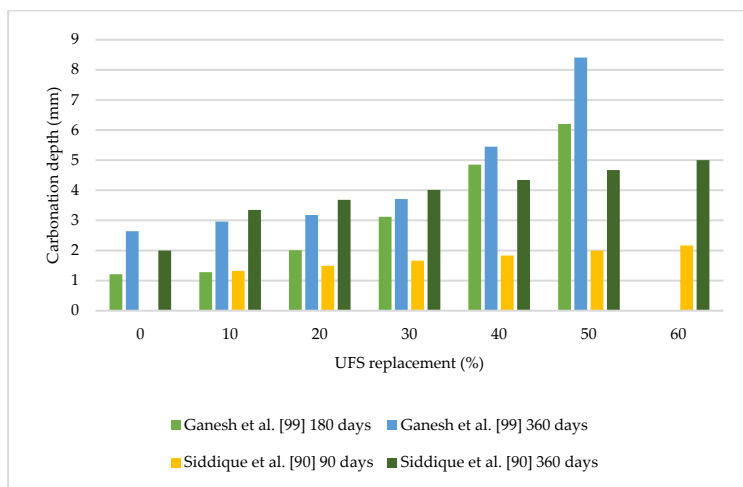


Figure 2.5. Carbonation depth of concrete with different UFS replacements according to different authors.

2.4.3.2. Acid environment

There have been few studies in this regard; among the few studies that exist, the works of Gurumoorthy and Arunachalam [23] who studied the effect of treated UFS (TUFs) as partial replacement of sand in various percentages (0–40%), on exposure to acid environment

(sulphuric acid and hydrochloric acid). Results from sulfuric acid (H_2SO_4) environment and HCl environment proved that the concrete mixture with 30% replacement of NS with TUFs showed the minimum weight loss and compressive strength loss compared with the control concrete. In the H_2SO_4 environment the percentage of weight loss of the concrete with a substitution of 30% of sand by TUFs is from 3.79% to 20.95% between 7 and 90 days, this is an improvement compared with the control concrete which reported weight loss values from 5.15% to 25.13% at the same ages. The HCl environment results shown a weight loss at 90 days of 3.45% with a concrete with substitution of 30% of sand by TUFs which is lower, compared with the loss weight of the control concrete value, which was 4.82% at the same age. Strength loss of concrete with 30% of TUFs was 24.53% at 90 days; meanwhile the control concrete reported a strength loss of 33.5%. This is explained due TUFs is finer than NS, which fills the pores in the concrete impeding the reduction of the concrete porosity and therefore the weight loss and due the TUFs have a rich silica content than NS, which make a more durable concrete in acid exposure [23].

2.4.3.3. Sulphate resistance

Few studies had analysed this durability property, Siddique et al. [52] analysed the compression strength of concrete immersed in a Magnesium sulphate solution of 50 g/l in concrete specimens at 7, 28 and 56 days with a replacement rate of 10%, 15% and 20% of UFS and concrete specimens immersed in water at the same ages. Results shown that the concrete containing 10% UFS had higher compressive strength at all ages, it is also reported that when the UFS replacement increase to 15% and 20%, the compressive strength tends to decrease [52].

Gurumoorthy and Arunachalam [68] studied the weight loss and strength loss of concrete immersed in a sodium sulphate environment (Na_2SO_4) as per ASTM C1012 [84]. The weight loss of the control

concrete was from 0.12% to 1.03 between 7 and 90 days, concrete with 30% of TUFs showed a lower weight loss values at the same ages, from 0.02% to 0.69% respectively. The loss of compressive strength in the control concrete was 1.95% at 90 days; meanwhile the concrete with 30% of TUFs reported a compressive strength value of 1.51 % at the same age [68], it is shown that TUFs as replacement material in concrete enhances the sulphate resistance.

On the other hand, Ganesh et al. [83] reported that the presence of FS reduces the sulphate resistance of concrete, and when the replacement rate increases, this effect is further enhanced. In this case, this is due the FS presented traces of sulphur, the presence of sulphur oxide (SO₃) can increase the strength of NaSO₄ and magnesium sulphate (MgSO₄) solutions and enhance the formation of ettringite, causing concrete deterioration [83].

2.4.3.4. Rapid chloride penetration

Gurumoorthy and Arunachalam [23] studied the rapid chloride permeability test (RCPT) value in a concrete with 30% of TUFs, results showed higher resistance to chloride permeability than control concrete at 28 days, those values were 1249 and 1739 C respectively, which indicates a low chloride ion permeability as per ASTM C 1202-2012 [85]. It is reported that with the increase of TUFs the C value decreased [68]. This decrease in the RCPT could be due the finer particles of TUFs act as a good filler material, reducing the voids between the components of the concrete mixture and creating a stronger internal structure [68]. According to Siddique et al. [74] it has also been observed that cement type, w/c ratio, curing conditions and test age have an effect on the chloride permeability of concrete [74]. Siddique et al. [52] also reported that the coulomb value of a concrete mixture containing 15% UFS decreased, which indicates that the

concrete is denser due the fine particles of UFS act like a good filling material to make the internal structure of concrete stronger [52].

2.5. Other applications of foundry sand

FS does not only limited to concrete, due the good physical and chemical properties it can be used directly as a fill material in embankments, sand replacement in hot mix asphalt (HMA), flowable fills, Portland cement concrete production, asphalt pavers, road sub-base, etc. [4]. In this section, diverse uses of FS in road construction and masonry elements it is reviewed.

2.5.1. Foundry sand in road construction

A study performed by the US EPA [86] indicates that reusing 1 t of UFS in road construction and manufactured soil could avoid 34.67 kWh of energy consumption, 0.08 m³ of water consumption, and 10.86 kg of CO₂ emissions. It is estimated that 1.4–4.7 million t of UFS were generated in 2014 and if fully reused in road construction and manufactured soil, it would have saved 50–162 GWh of energy, 0.12–0.37 million m³ of water, and 17,280–55,904 t of CO₂ emissions [87].

UFS have potential for use as a soil amendment or a component of manufactured soils because contain plant nutrients, organic carbon, clay and their sandy texture provides for good drainage, making them useful for enhancing soil blend physical and chemical properties and attractive components in manufactured soils [19].

The environmental characterization of leaching and solubilization of HMA with a 100% of UFS it has been studied, concluded that substances present in the UFS were encapsulated definitively by the HMA asphalt matrix, making environmentally inert [88]. FS must be free of coatings of mould additives, binders and burn carbon because these constituents can inhibit the adhesion of the asphalt cement binder

to the FS [89]. The feasibility for UFS as a fine aggregate in asphalt concrete has been examined, the results showed that the replacing proportion of 15% give satisfactory performances for hot mix pavement. When this proportion is higher, the asphalt mix become more sensitive to moist damage thus the use of antistripping additives is recommended [59]. From geotechnical standpoint, the FS treated with a 5.5% of hydraulic binder (cement) gives acceptable mechanical performances and do not shows environmental impacts for sub-base layers. However, the setting up and the final performances depend on the water content, and need material homogeneity [59]. Pasetto and Baldo [42] have given an experimental study concerning hydraulically bound mixtures for road foundations, with the aggregate skeleton fully composed by FS and steel slags. The best mechanical results are achieved for the mixture 80/20 (steel slag - FS), at 7 days uniaxial compressive strength and indirect tensile strength values up to 5.6 and 0.72 MPa, respectively.

2.5.2. Foundry sand in masonry elements

The possibility of producing new red ceramics composites from FS and red mud of hazardous bauxite waste replacing the traditional clay-sand mix was studied, these ceramics exhibit high physical properties after sintering at 1150°C, the developed materials reach complete neutralization from both industrial wastes heavy metals [24]. Another use that is given to the UFS is their implementation for manufacture blocks and bricks, [25,26,32,90,91]. Matos et al. [32] proved the feasibility to fabricate blocks with 100% UFS, reaching similar strength values from concretes up to 20 MPa. Jitendra and Khed [90] manufactured blocks with fly ash (FA) and FS, results shown that the strength of the concrete blocks increased and chloride ion penetration and water absorption in concrete blocks decreased with a 50% replacement of cement for FA and 15% replacement of sand with FS.

Apithanyasai et al.[26] studied the optimal ratio of UFS, FA and EAFS for production of geopolymer bricks, which is 40%, 30% and 30% respectively, reaching a compressive strength of 25.76 MPa at 28 days, leaching test were made, proving that the geopolymer bricks can be classified as non-hazardous waste.

Clay fired bricks with 50% of UFS can be used as single storied load bearing structures, and also in the construction of infill walls in multi-storied framed structures [91]. It is possible to obtain ceramic bricks with 35% of green sand and 25% of core sand accomplishing the technological standards for traditional bricks, the addition of the FS to the ceramic matrix decreases the firing shrinkage and increase the water absorption [25].



Figure 2.6. Bricks manufactured with UFS. Source: [91].

2.6. Partial conclusions

Overall, the incorporation of FS as a partial replacement in concrete has proven to improve the mechanical and durability properties, therefore the following conclusions are presented:

- There are two types of FS: Green sand, which it is made up to 85-95% silica, 0-10% bentonite clay as binder, 2-10% water and

5% sea coal. Chemical Foundry Sand that consists of 93-99% silica and 1-3% chemical binder.

- The physical and chemical properties of FS are generally good due the sand used is of high quality, these properties depend on the type of metal casted and the type of binders used.
- The slump value will decrease as long the replacement of NS by FS increase, the loss of workability is attributed to the binders like clay-type fine materials that increase water demand.
- Regarding the compressive strength, the increase of this mechanical property with the addition of FS it is because the high silica content and the finer particles than regular sand, which create a denser matrix.
- The decrease of the compressive strength is attributed to the high surface area of FS particles, which led to the reduction of the water cement gel in the concrete matrix, resulting in a poor bonding between aggregates and cement paste, other explanation it is the presence of binders like fine powder carbon and clay.
- Very little information was finding about flexural strength in concrete with FS, finding suggest that in most cases, the flexural strength decrease as the replacement increase
- Carbonation depth increase as the FS replacement increase, this could be due de poor workability of concrete as the substitution increases, creating a porous system due the deficient compactness.
- Concrete with 30% of TUFs showed a minimum weight loss and compressive loss in H₂SO₄ and HCl environment, this is because the TUFs is finer than NS, filling the pores which reduce the porosity and therefore, weight loss.
- The sulphate resistance tends to increase with 10%-30% of FS, reducing the weight and compressive strength loss; this will

depend of the type of FS and the previous or post treatment.
The decrease of the sulphate resistance when FS

- The incorporation of 15%-30% of FS in concrete also decrease the rapid chloride penetration, this is because the FS create a denser matrix due the fine particles of the sand.

Chapter 3. Effect of recycled foundry sand on the workability and mechanical properties of mortar

This chapter is the result of the experimental campaign to manufacture mortars with foundry sand residue using different percentages of fine aggregate substitution. This article has been published in the journal Applied Sciences and its reference is presented below:

García Del Angel, G.; Sainz-Aja, J.A.; Tamayo, P.; Cimentada, A.; Cabrera, R.; Pestana, L.R.; Thomas, C. Effect of Recycled Foundry Sand on the Workability and Mechanical Properties of Mortar. Appl. Sci. 2023, 13, 3436. <https://doi.org/10.3390/app13063436>

Effect of recycled foundry sand on the workability and mechanical properties of mortar

Gilberto García Del Angel¹, Jose A. Sainz-Aja¹, Pablo Tamayo¹, Ana Cimentada¹, René Cabrera², Luis Ruiz Pestaña³ and Carlos Thomas¹

1. LADICIM (Laboratory of Materials Science and Engineering), University of Cantabria, E.T.S. de Ingenieros de Caminos, Canales y Puertos, Av./Los Castros 44, 39005 Santander, Spain
2. FI (Faculty of Engineering), Autonomous University of Tamaulipas, Centro Universitario, Tampico 89336, Mexico
3. Department of Civil and Architectural Engineering, University of Miami, Coral Gables, FL 33146, USA

Abstract: Modern society requires a large number of metal components manufactured by sand casting, which involves the generation of a waste product known as Used Foundry Sand (UFS), of which approximately 100 Mt are generated on an annual basis. Virtually all UFS is currently landfilled, despite the economic and environmental cost overruns that this entails. Here, the recovery of UFS as fine aggregates for the manufacture of concrete is proposed. Since the presence of UFS will mainly affect the mortar that binds the aggregates in the manufacture of concrete, it was decided to isolate this fraction and study only the effect of UFS in mortars. This study evaluated a total of 32 different mixes combining different w/c ratios varying between 0.5 and 0.7 with 5 replacement ratios of natural sand by UFS: 0, 25, 50, 75 and 100% respectively. The combined effect was evaluated of the w/c ratio and the replacement ratio on the workability, physical properties, mechanical properties, mechanical durability, and microstructure of the mortars. The incorporation of UFS decreases the workability of the mortars due to the absorption of the residue. As for the physical properties of the mortars, density decreased and porosity and absorption increased at all replacement percentages. Flexural and compressive strength decreased when the replacement percentage is higher than 25 wt.%. In terms of mechanical durability, the mortars with UFS showed abrasion marks within the limits of the EN-1338 standard. From the results obtained, it is possible to conclude that the

mortars with UFS requires a higher amount of water. Therefore, while small replacement levels lead to a slight improvement in the mechanical properties, this trend breaks down for high replacement levels due to the negative effect of the high w/c ratios required. The authors recommend that for replacements higher than 25 wt.% of UFS, the w/c ratio has to be taken into consideration to obtain the same workability as the control mortar although this decreases the mechanical properties.

Keywords: Used foundry sand; mortar; workability; mechanical properties; wear resistance; w/c ratio.

3.1. Introduction

Foundry sand (FS) is the material used in manufacturing of mould boxes in the sand-casting process of ferrous and nonferrous materials. The main constituents of FS are silica sand and binders, which can be of natural or chemical origin [92]. When organic binders such as bentonite clays are used along with carbon powder to enhance the cast surface, the FS is called green foundry sand (GFS). When chemical binders are used instead, such as phenolic-urethanes, epoxy resins, or sodium silicates, the FS is called chemical foundry sand (CFS) [4]. The GFS or CFS is compacted against a mould which will leave a cavity in the shape of the part required and then molten metal is poured into it. Once the metal has cooled, the sand box is broken up by the "shakeout" method. By means of vacuum belts, a magnet collects the metal debris and the sand is used again several times in the manufacture of moulds until its properties are no longer suitable for the casting process, creating a by-product known as used foundry sand (UFS) [30].

The construction industry is responsible for 39% of CO₂ emissions and for more than 50% of the extracted natural resources [93]. In this regard, the use of alternative cementitious materials [94] and the reuse of solid waste from the construction, steel and foundry industry benefits the environment by reducing the exploitation of natural aggregates, reducing CO₂ emissions emitted by the machinery and transport of aggregates from the quarry to the construction site. Also, the use of waste tire [95,96], marble [97,98], waste lathe fibres [99], waste lathe scraps [100], waste glass [101,102], coal bottom ash [103] and PET [104] has been studied as a substitute of coarse and fine aggregates in the concrete manufacturing towards a more eco-friendly material.

According to Tittarelli [105], 100 Mt of UFS are generated annually and mostly landfilled, thus creating an environmental cost [106]. The

physical and chemical properties of UFS vary depending on the foundry process or the metal and the binder used [92]. However, it has been reported that most of the UFS is categorized as non-hazardous [15] and its physical properties are suitable for use in cement-based materials such as low strength materials [33], cement-treated bases [107], conventional concrete [16,108] and self-compacting concrete [52,54].

Regarding mortars, diverse authors have experiment with UFS and additions such ceramic moulds shells and paraffin waxes wastes [109], polyurethane residues [110] and high phenolic contents [111] geopolymers [112]. Monosi, Sani and Tittarelli [30] used a replacement of up to 30% of natural sand (NS) by UFS with a fixed w/c ratio of 0.5, reporting a decrease of the workability of 8, 19 and 22% as the UFS content increased by 10, 20 and 30% respectively. At 28 days the compressive strength of the mortars decreased when the replacement was higher than 20%, which was attributed to the presence of fine powder carbon and clay within the binder, causing a loosening of contacts and links between the aggregates and cement matrix [30]. However, with up to 10% replacement of UFS the compressive strength of the mortar was not affected significantly. Vázquez et al. [31] used UFS from an aluminium foundry as a total replacement for NS in the manufacture of mortars. The compressive strength results at 7, 14 and 28 days reported that the total inclusion of UFS decreased the compressive strength by 71, 77 and 76% compared to the control mortar. This was attributed to the reaction of cement with aluminium, which produces hydrogen gas that creates microcracks in the cementitious matrix [31]. Çevik et al. [23] manufactured mortars with up to 60% replacement (in steps of 15%) of NS by UFS and a fixed w/c ratio of 0.5. Compressive strength results at 3 days showed an increase of 13 and 12% when 15 and 30% of UFS were used respectively. However, at 28 days, the compressive strength of the mortars decreased compared to the control mortar. Matos et al. [32] studied the

replacement of NS by 50 and 100% of UFS. Workability results indicated that, compared with the control mortar, the replacement by UFS decreased the workability by 22 and 39%, which was attributed to the presence of pulverized coal and fine particles of bentonite, increasing the absorption of water thus decreasing the workability [32]. As for the reduction of compressive strength, it was due to the lower compaction of the mix because of the reduction of workability and to the excess of fine material in the UFS, which impedes the proper bonding between the aggregates and the cement paste as stated by Siddique and Noumowe [33].

The value of this research lies in the study of the physical-mechanical properties and statistical analysis of the effects of incorporation of UFS in mortar to achieve more sustainable materials, following the research line of low carbon footprint materials as other authors have developed [113]. Most studies use low UFS replacements and a fixed w/c ratio. This paper investigates in depth the influence between higher UFS replacements and w/c ratio. Also, the mechanical durability will be analysed. The total use of UFS as an aggregate in mortars is an alternative to avoid the exploitation of natural resources and increase the life cycle of a material that is perceived as waste.

3.2. Materials

3.2.1. Cement and fine aggregates

A CEM I-52.5 R type cement according to EN 197-1 [114] was used with a density of 3.05 g/cm³ determined according to UNE 80103 [115] and a Blaine specific surface of 4447.2 cm²/g obtained according to EN 196-6 [116]. The chemical composition of the cement is given in Table 3.1.

Table 3.1. Cement chemical composition.

Composition (wt.%)								
CaO	SiO ₂	Al ₂ O ₃	Fe ₂ O ₃	SO ₃	K ₂ O	MgO	TiO ₂	C
69.6	18.65	3.15	2.66	3.22	0.54	1.17	0.17	0.47

The UFS and silica sand (SS) grading curve and images can be observed in Figure 3.1 and Figure 3.2, respectively. The aggregates grading curve were obtained by EN-933-2.

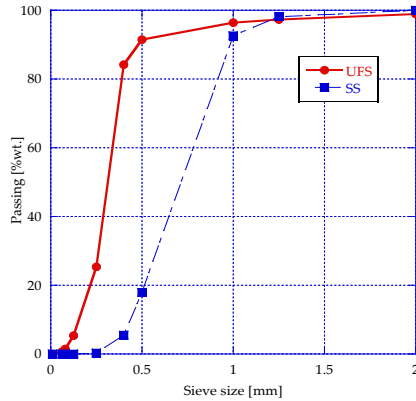


Figure 3.1. Aggregates grading curve.



Figure 3.2. Used foundry (a) sand and silica sand (b).

The UFS was proportioned by a foundry company in Reinosa, Spain. Table 3.2 and Table 3.3 show the absorption of the sands used in this study and the chemical composition of the UFS respectively. It can be observed that the UFS presents a higher absorption than the SS, which

is in concordance with findings in the literature [92]. Also, it is observed that the main components of the UFS are SiO₂, CaO and Al₂O₃ as reported by other authors [53,92,117].

Table 3.2. Physical properties of the aggregates used.

Component	Density [g/cm ³]	Absorption [%]
SS	2.58	0.35
UFS	2.58	3.37

Table 3.3. UFS chemical composition.

Composition (wt.%)										
CaO	SiO ₂	Al ₂ O ₃	Cr ₂ O ₃	Fe ₂ O ₃	SO ₃	K ₂ O	MgO	TiO ₂	P ₂ O ₅	Others
7.83	83.9	2.87	1.67	1.4	0.72	0.7	0.53	0.13	0.06	<0.05

3.2.2. Mix proportions

Table 3.4 shows a description of the 32 different mix proportions used in this research work. For all the mixes the cement content was fixed at 500 g. The design of these dosages is to investigate the effect of UFS on workability, physical and mechanical properties and mechanical durability.

Table 3.4. Mortar mix proportion descriptions.

UFS replacement [%]	0 %	25 %	50 %	75 %	100 %
	0.50(*)(**)	0.50(*)	0.50	0.57(*)	0.60
	0.55	0.51(*)(**)	0.52(*)	0.59(*)	0.65
	0.60	0.52(*)	0.55(*)	0.60(*)	0.67(*)
	0.65	0.55	0.56(*)	0.62(*)(**)	0.69(*)
w/c	0.70	0.60	0.57(*)(**)	0.65	0.70(*)(**)
		0.65	0.58(*)	0.70	
		0.70	0.60		
			0.65		
			0.70		

Mixes tested for physical properties (*) and wear resistance test (**)

3.3. Methods

3.3.1. Workability

The workability of all the mortars was tested on the flow table as described in EN-1015-3 standard [118]. The objective of this test was to analyse the influence of the w/c ratio as UFS% increased, based on the workability of the control mortar (0% UFS and 0.50 w/c ratio).

3.3.2. Physical properties

The evolution of specific gravity, dry density and bulk density were obtained according to EN 12390-7 [119] on the mortar specimens (*). The accessible porosity and the absorption coefficient were obtained according to UNE 83980 [120] on the same specimens (*).

3.3.3. Mechanical properties

At 28 days, the flexural strength of the 32 mixes was tested according to EN-1015-11 [121] on standardized mortar specimens of 40x160x160 mm. After the flexural strength test was performed, the two halves of the mortar were tested for compressive strength according to the same standard [121]. Figure 3.3 shows the setup of the respective mechanical test.

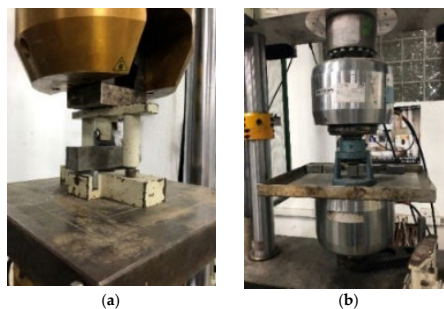


Figure 3.3. Set up of the flexural (a) and compression strength test (b).

3.3.4. Wear resistance

The mortar specimens were previously painted black in order to better appreciate the abrasion marks. The wear resistance test was performed according to EN-1338 [122] (Annex G) on the 3 faces of the standardized mortar specimens (**) at the age of 28 days (Figure 3.4).



Figure 3.4. Set up of the abrasion wear resistance test.

3.3.5. Variable correlation

In order to perform the statistical analysis, a colour code matrix was made using the Pearson correlation coefficient (r) parameter with the use of Python [123]. If this parameter is close to 1, it implies that both variables are highly correlated in a directly proportional way. If this value is close to -1, it implies that they are strongly correlated in an inversely proportional way. If this value is close to 0, it implies that there is no strong linear correlation between the two variables.

3.3.6. Microstructural characterization

A scanning electron microscope (SEM) equipped with X-ray energy dispersive microanalysis capabilities was used to study the microstructure of select samples. As there are several water-cement ratios in each one of the mortar mixtures, an intermediate ratio was taken, in this case 0.6, taking 5 different samples in total. Prior to

analysis under the microscope, the 5 samples were taken and left in the oven for 24 h, then removed and metallized as shown in Figure 3.5 to facilitate their observation in the SEM. The samples were sprayed with a thin layer of gold in a pulverisation process in order to increase its conductive properties. It is necessary because mortars are not good conductive materials.

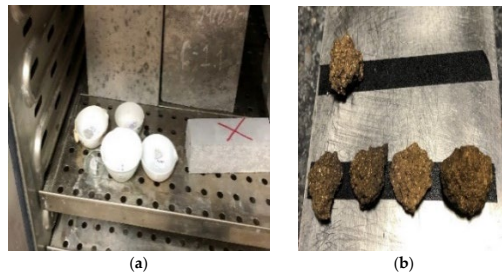


Figure 3.5. Sample preparation for SEM analysis. (a) oven drying at 70 °C. (b) Samples after metallization.

3.4. Results and discussion

3.4.1. Workability

Figure 3.6a show the effect of both the w/c ratio and the UFS on the slump table result test. The fitting equations for each UFS replacement percentage show that, in general, there is a linear relationship between increasing w/c ratio and slump. If the methodology is replicated in another study, validated results can be guaranteed for each replacement percentage. It also shows that the higher the UFS replacement, the higher the w/c ratio to obtain the same workability Figure 6b shows an example of the visual appearance of two of the tests carried out, namely the 50% UFS case, but for w/c ratios of 0.52 and 0.57, respectively.

As shown in Figure 3.6b, the high absorption of the UFS influences the workability of the mortar. It can be observed that with a w/c ratio of

0.52, the slump diameter is 100 mm, i.e., the lower diameter of the cone. For a w/c ratio of 0.57, a higher workability is obtained, resulting in a slump diameter of 150 mm. It is also possible to conclude that to obtain similar workability, increasing the UFS requires an increase in the amount of water. In particular, to obtain workability similar to that obtained in the reference mortar with a w/c ratio of 0.5 in the case of a UFS replacement equal to 50%, the w/c ratio should be 0.57, and 0.7 in the case of a UFS replacement of 100 %.

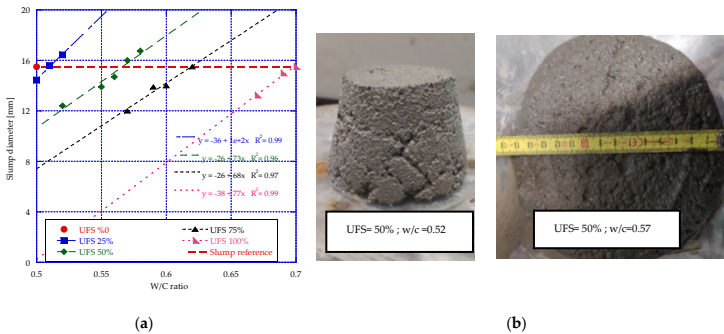


Figure 3.6. Mortar workability: slump table test results in cm (a) and comparative example for a fixed UFS value (b).

From the results shown in Figure 3.7a, it is worth noting that there are no data for high UFS values and low w/c ratios. This is because these mixes were too dry, and it was not possible to achieve acceptable workability. The reduction in workability with the increase in UFS was also observed in other studies [16,32,92]. In this regard, Figure 3.7b shows that for the same w/c (0.5), the slump diameter decreases with higher UFS replacement; from UFS 50 onwards, there is no slump, so the diameter is the same that the flow mould (10 cm). This reduction in workability for high UFS replacement is justified because UFS has a much higher absorption than SS [30,124]. From Figure 3.7a, it is also possible to see that, in general, a high w/c ratio and low UFS values

increase workability. However, the maximum workability values are found with a UFS of 25%. This is because the smaller UFS particle size facilitates particle mobility. Therefore, it is possible to conclude that the presence of UFS has two opposing effects: on the one hand, the particle geometry improves the workability of the mixes, as stated by de Barros et al. [72], and on the other hand, the higher absorption of UFS means that, especially for high UFS replacements, larger quantities of water are required to obtain similar workability.

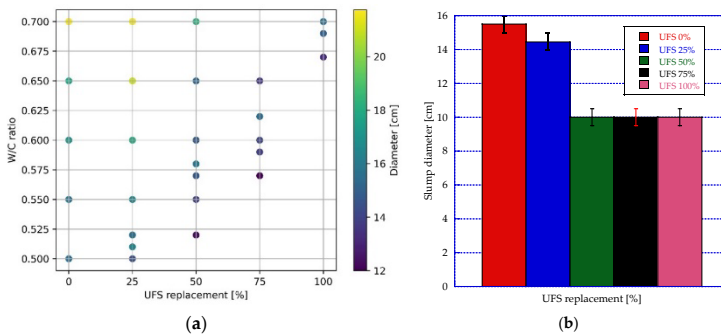


Figure 3.7 Mortar workability: slump table test results in cm (a); effect of UFS in mortar workability with $w/c = 0.5$ (b).

In Figure 3.8, the effect of modifying the UFS replacement is observed; as mentioned in the previous paragraph, the UFS has a strong influence on the mortar workability. The reduction in the workability is because of the high absorption of the UFS. This prevents the proper workability of mortars with low w/c ratios; in consequence, higher w/c ratios are necessary to obtain the same workability as the control mortar. This loss of workability is more evident as the percentage of replacement increases.



Figure 3.8. Mortar workability: slump table test results. Comparative example for a fixed w/c ratio.

3.4.2. Physical characterization of mortars

Figures 3.9–3.11 show the evolution of apparent specific gravity, dry density and bulk density as a function of UFS replacement and w/c ratio.

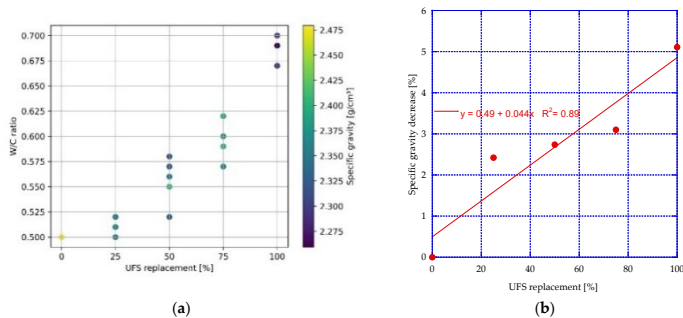


Figure 3.9. Specific gravity (g/cm³) of the mortar mixes (a) and decrease in the specific gravity (%) (b).

Figure 3.9a show that increasing the UFS decreases the specific gravity of the mortars, which is because, as previously stated, to increase the

workability, the w/c should be increased. This increase generates air voids within the matrix, generating a loss of density. In general, it can be observed that mortars with UFS of 100% and w/c of 0.7 showed the lowest densities compared to the control mortar. Figure 3.9b shows the percentual decrease in the specific gravity between the mortar mixes with UFS 25, 50, 75 and 100% compared with the reference mix (UFS 0%). It is observed that there is a minimal difference between the decrease in UFS 25% and UFS 50% mortars, but as the UFS increases up to 100%, it is evident that the decrease in the specific gravity is higher because the higher w/c ratios needed to manufacture the mortars.

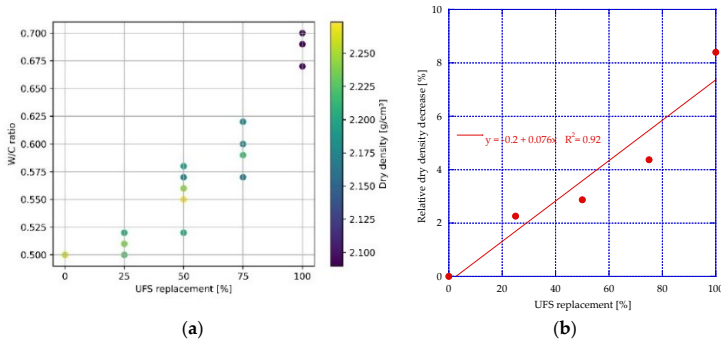


Figure 3.10. Dry density (g/cm^3) of the mortar mixes (a) and dry density decrease (%) (b).

Figure 3.10a show the influence of increasing UFS and w/c on dry density. As in the previous figure, it can be observed that the mortar with UFS of 100% presents the lowest densities with a w/c of 0.7. On the other hand, mortars with UFS of 25% and w/c up to 0.57 present dry densities similar to those of the control mortar. Figure 3.10b shows the percentual decrease in the dry density as the UFS increases; this is because the higher w/c ratios form voids within the mortar matrix, creating a more porous and lighter structure.

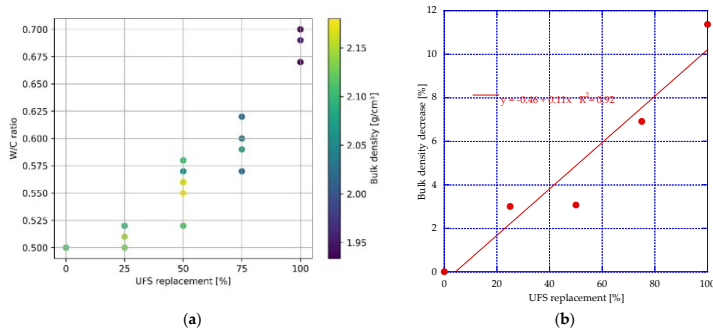


Figure 3.11. Bulk density of the mortar mixes (g/cm^3) (a) and bulk density decrease (%) (b).

Figure 3.11a show that mortars with UFS of 25% and w/c up to 0.53 achieved similar bulk saturated densities to the control mortar. For mortars with UFS of 50% and w/c between 0.55 and 0.57, a similar behaviour is observed, while for the mortars with UFS of 100%, a decrease in bulk density is observed. Figure 11b shows a similar behaviour as the previous plot; the decrease difference between UFS 25% and UFS 50% is minimal, but as the UFS increases, the percentual decrease in the bulk density is higher because of the higher w/c ratio.

Figure 3.12 shows the results for the porosity of mortars with different percentages of UFS and w/c ratios. It is observed that, compared to the control mortar, the porosity of mortars with UFS of 25 and 50% is very similar even with higher w/c ratios; this may be due to the fact that FS contains a higher proportion of fines than SS, creating a denser matrix as stated by other authors [62]. On the other hand, mortars with UFS of 75 and 100% present a higher porosity than the control mortar; this is because although the UFS presents more fines, increases in the w/c ratio increase the air void content within the matrix, making it more porous.

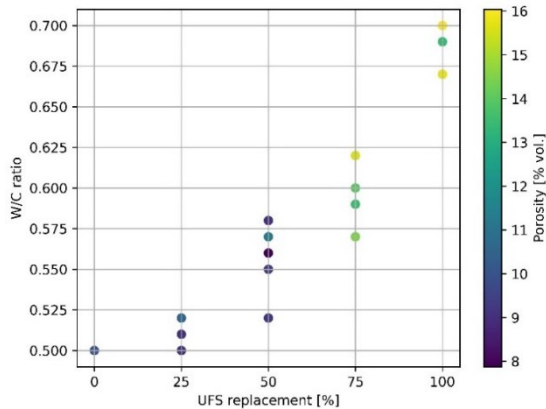


Figure 3.12. Accessible porosity of mortars with UFS (% vol.).

Figure 3.13 presents the absorption results in relation to the UFS and w/c ratio. It is well known that porosity is directly related to absorption, so an explanation similar to the one presented in the previous figure is applied in this case. In general, mortars with UFS replacement up to 50% and w/c ratios up to 0.58 show absorptions similar to those of the control mortar.

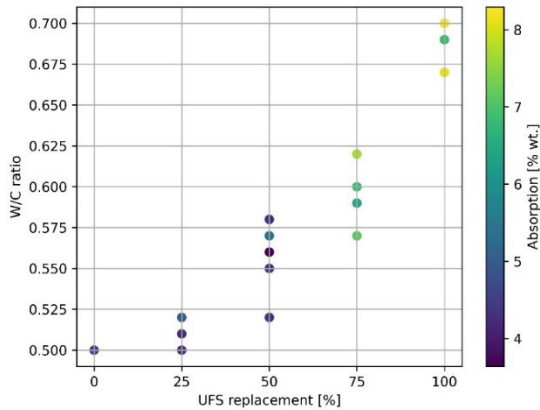


Figure 3.13. Absorption coefficient of mortars with UFS (% wt.).

3.4.3. Mechanical characterization of mortars

Figure 3.14 shows the flexural strength results as a function of the w/c ratio and the UFS replacement, while Figure 3.15 shows the values of compressive strength as a function of the same two parameters.

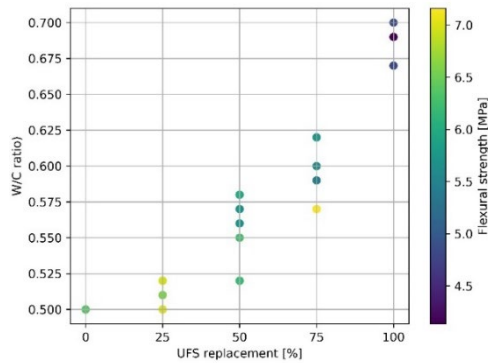


Figure 3.14. Flexural strength (MPa) as function of w/c ratio and UFS replacement.

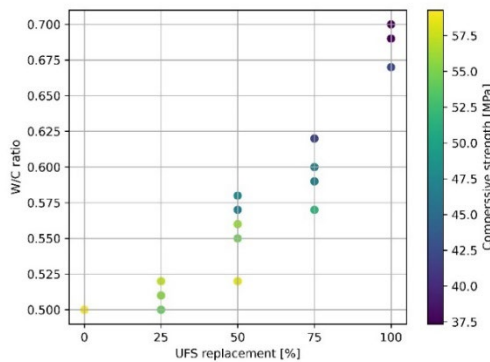


Figure 3.15. Compressive Strength (MPa) as function of w/c ratio and UFS replacement.

From the results shown in Figure 3.14 and Figure 3.15, it can be concluded that for high w/c ratios and/or high UFS replacements, the mechanical properties of the mortars are reduced. The effect of increasing the w/c ratio on the mechanical properties is clearly documented. From these results, robust conclusions cannot be drawn on the effect of UFS replacement on compressive strength, as there are no case studies with the same w/c ratios and different UFS values. For this reason, these results were completed with the second batch of

mixes, which enables the comparison of test specimens (Figure 3.16) with the same w/c ratio and different UFS replacements. These results are shown in Figure 3.17a.



Figure 3.16. Mortar specimens with UFS, from 0 to 100%.

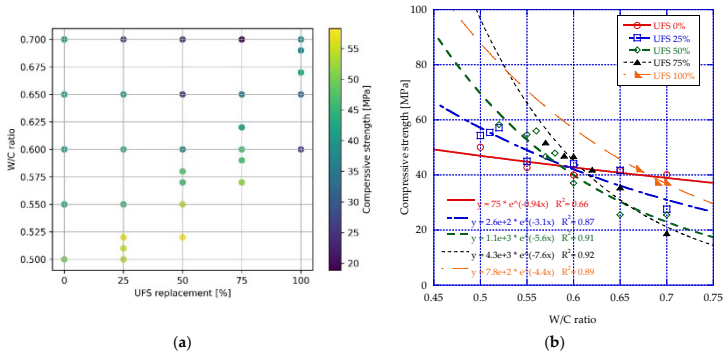


Figure 3.17. Compressive strength of mortars (MPa) (a) and w/c ratio influence on compressive strength of UFS mortars (b).

As previously stated, Figure 3.17a confirms that increasing the w/c ratio generally decreases the mechanical performance of the mortars. An exception occurs for a UFS replacement of 100%, where the lowest compressive strength is observed for a w/c ratio of 0.6, and it increases with the w/c ratio. This is because, in the case of 100% UFS and a w/c ratio of 0.6, the workability of the specimens was very low, the mortar was too dry, and the specimens had defects that were detrimental to their strength. Regarding the effect of the UFS replacement on the compressive strength for constant w/c values, there is no uniform trend for all cases. This is because, as previously stated, there are two

phenomena that have opposite effects on the strength of the mortars. In general, given a fixed w/c ratio, an increase in UFS replacement reduces the mechanical properties of the mortars, as also reported by other authors [16,32,92,125]. However, as UFS has a higher absorption than the SS, this water absorption can, in some cases, lead to an increase in the mechanical properties of mortar and concrete, as reported by other authors [23,126], because the finer particles of the UFS fill the pores of the mortar matrix, resulting in a denser material. This is especially seen in cases of very high w/c ratios and UFS replacements. This phenomenon is similar to recycled concrete, where recycled aggregates from concrete also have a higher absorption [127].

Figure 3.17b shows the influence of the w/c ratio on the compressive strength of mortars with UFS. In general, it is observed that there is a trend in the loss of compressive strength as the UFS replacement increases, as reported in the literature. The fitting equations for each UFS replacement percentage show the relationship between increasing w/c ratio and decreasing compressive strengths. It is observed that a small variation in the w/c ratio has a major influence on compressive strength when higher percentages of UFS are used. Moreover, it is observed that the slope increases with increasing UFS. For low w/c ratios (0.5–0.52), UFS 25% mortars present an initial tendency to increase their compressive strength up to 5%, but at high w/c ratios (0.55 to 0.7), there is a loss of compressive strength of 17, 19, 23 and 49%, respectively. The UFS 50% mortars show similar behaviour, and it is observed that with a w/c ratio of 0.52, the compressive strength is slightly higher than that of UFS 25% (2%); at a w/c ratio of 0.55, this increase is 22%. However, as the w/c increases from 0.6 to 0.7, the compressive strength losses are 32 and 53%, respectively. In the case of UFS 75% mortars, as in the other two cases, there is a tendency to lose compressive strength. It is worth mentioning that there are no w/c ratios of 0.5 and 0.55 in these mortars because the high absorption of UFS makes it difficult to make specimens, so higher w/c ratios were

used. By comparing the compressive strength of the UFS 75% with a w/c ratio of 0.57 (51.75 MPa), it was observed that the increase in w/c ratio decreases the compressive strengths by 10, 32 and 64% as the w/c is 0.6, 0.65 and 0.7, respectively. The loss of compressive strength is due to the high w/c ratios necessary to produce mortars with the same workability as the control mortar. These high w/c ratios in mortars with higher UFS replacements create a porous material, resulting in a less dense and less resistant matrix.

3.4.4. Mechanical durability

Figure 3.18 shows the wear results as a function of the UFS replacement amount for samples with the same workability. This parameter evaluates the mechanical durability of the mortars.

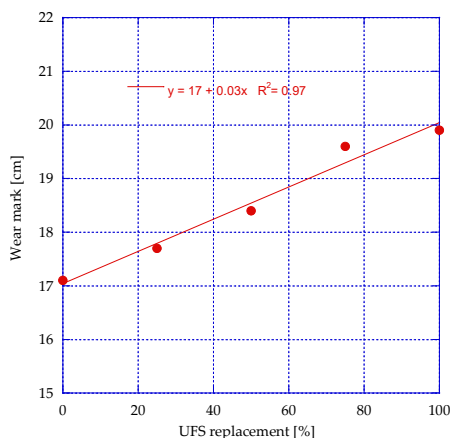


Figure 3.18. Wear resistance.

From the results shown in Figure 3.18, it can be concluded that increasing the FSR increases the wear value obtained in the test. The mechanical durability of mortars decreases with increasing UFS replacement. This is because mortars need a high w/c ratio to achieve the same workability. This results in a more porous material, which

could be because it creates a loss of bond between the aggregates and the cement, as mentioned by other authors [128–130]. Nevertheless, even with an FSR of 100%, the values obtained remain below the most restrictive value defined in EN-1338 [122], which is 20 mm. Figure 19 shows examples of the specimens' appearance after the wear resistance tests.

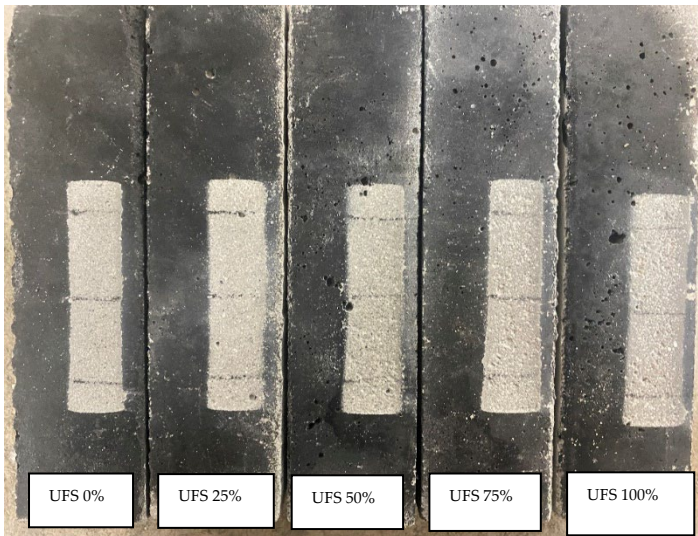


Figure 3.19. Examples of the specimen surface after the wear resistance tests.

3.4.5. Variable correlation

Figure 20 shows the correlation matrix of the results obtained in this work.

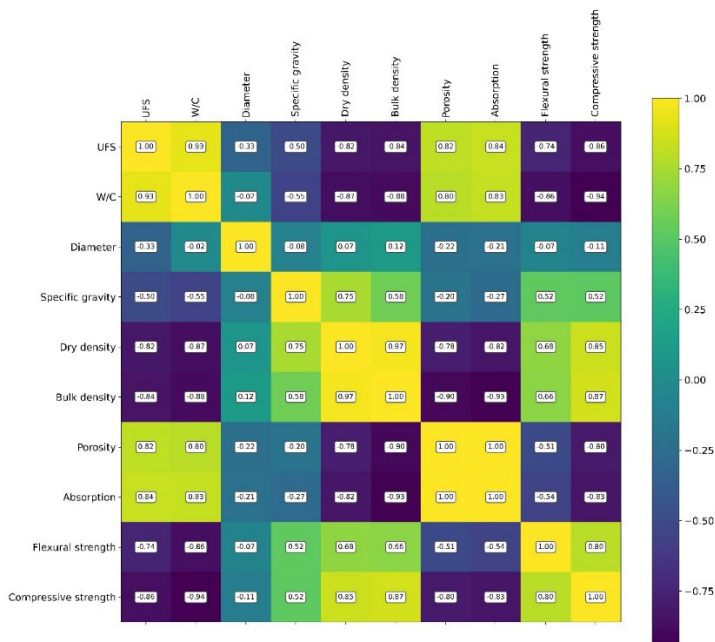


Figure 3.20. Correlation matrix of analysed parameters.

The properties of the mortars can be grouped into four families or blocks: (1) workability, which includes “diameter”; (2) densities, which includes specific gravity, dry density and bulk density; (3) compactness, which includes both porosity and absorption; and (4) mechanical properties, which includes flexural strength and compressive strength. Figure 3.20 shows that there is a high linear correlation between the quantities in each family. There is no clear correlation between workability and any of the other three families of properties. However, the properties in the density family are anti-correlated to the properties in the compactness family and relatively well-correlated to the mechanical properties. Finally, an inverse

correlation between the compactness and mechanical properties of blocks is also observed.

Regarding the effect of FSR and w/c on the workability block, we can see that there is no clear trend in relation to either of these two variables. This is because it is a parameter that depends on both variables simultaneously, and each one has an inverse effect. The greater the amount of water, the greater the diameter, but the greater the FSR, the smaller the diameter. For this reason, it can be said that there is one effect that cancels out the other.

Regarding the density block, it can be observed that there is an inverse relationship between the density values and both FSR and w/c. Moreover, it can be stated that this inversely proportional relationship is clearer in the case of dry density and bulk density than in the case of specific gravity.

Regarding the compactness block, it can be observed that there is a directly proportional correlation; the higher the FSR or w/c, the higher the values of voids.

Finally, in the case of mechanical properties, it can be concluded that, as with densities, the higher the values of both FSR and w/c, the lower the values of the mechanical properties.

3.4.6. Microstructural characterization

Figure 3.21 shows microstructural figures of samples with a w/c ratio of 0.6 and different UFS replacement ratios for 25× magnifications.

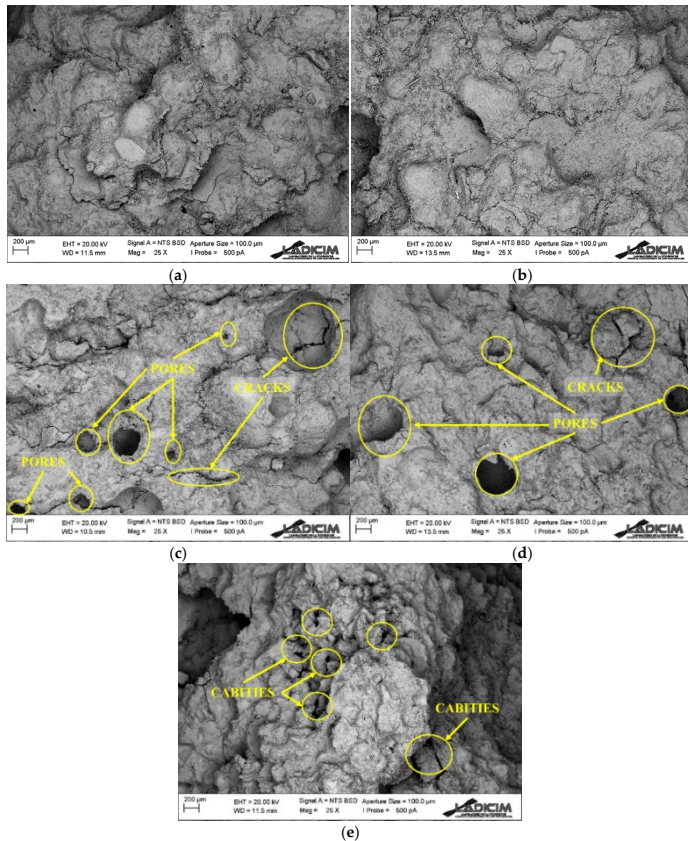


Figure 3.21. Microstructural analysis under 25× magnification: pores, cracks and cavities of UFS mortars with 0% (a), 25% (b), 50% (c), 75% (d) and 100% (e) substitution.

Figure 3.21 shows that mortars with 0% and 25% UFS have a homogeneous paste without any visible pores. This could be because the low UFS replacement allows adequate workability despite the high absorption of the UFS. On the other hand, for 50% and 75% UFS, pores can be observed in the mortar paste. Finally, for 100% UFS, it can be

observed that the paste has large cavities, probably because the UFS absorbed most of the water.

Figure 3.22 shows microstructural figures of samples with a w/c ratio of 0.6 and different FSR ratios for 500 \times magnifications.

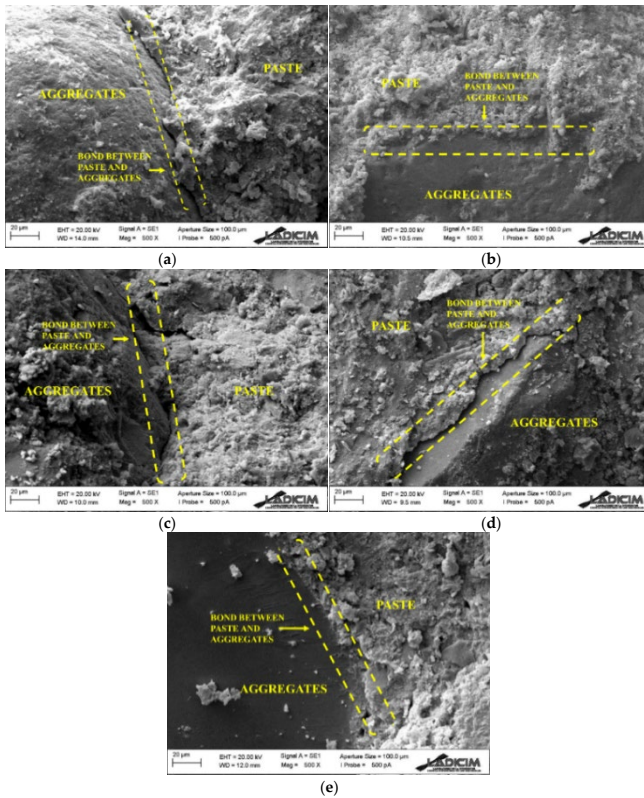


Figure 3.22. Microstructural analysis under 500 \times magnification: bond between paste and aggregates of UFS mortars with 0% (a), 25% (b), 50% (c), 75% (d) and 100% (e) substitution.

Figure 3.22 shows how the paste and aggregate interact in the mixture. For UFS of 0 and 25%, good bonding between the aggregate and the

paste can be observed. It can also be seen that as the UFS replacement increases, the bonding between the paste and the aggregate becomes poorer as the space between the aggregate and the paste increases.

3.5. Partial conclusions and future work

In this research, 32 mix proportions were manufactured to study the effect of the UFS replacement and the water cement ratio (w/c) on the workability, physical and mechanical properties, durability, and microstructural characteristics of mortars. After analysing the results, the following conclusions can be drawn:

- Increasing the UFS replacement reduce the workability of the mixes, making it impractical to manufacture mortars with high UFS replacement and low w/c ratios.
- Increasing the UFS replacement decreases the compactness of the mortars, so it is necessary to increase the w/c ratio, reducing the specific gravity, dry density and bulk density and increasing the porosity and absorption.
- Low quantities of UFS replacement can lead to a slight improvement in mechanical properties, while high UFS replacement require high w/c ratios and, consequently, it is not possible to achieve high values of mechanical properties.
- For the same workability, increasing the UFS replacement increases the wear value obtained. Even with an UFS replacement of 100% the values obtained remain below the most restrictive value which is 20 mm.
- From microstructural characterization it can be concluded that in mortars with low w/c replacement the paste and the aggregate are uniformly distributed without the presence of pores and with good adhesion between the paste and the aggregate. When the UFS replacement increases, pores begin to appear in the mortar.

- From a practical point of view, the authors recommend using up to 25% replacement of UFS because with a minimum amount of extra water, a workability equal to that of a conventional mortar is obtained, it has slightly higher mechanical strengths and the mechanical durability is very similar to that of a control mortar.
- Future studies should be carried out in the field of mortars with UFS to increase the replacement percentage without increasing the w/c ratio, maintaining the same workability.

Author Contributions	Conceptualization, GGDA, PT, CT; methodology, GGDA, JASA, PT, AC, RC, LRP, CT; validation, GGDA, JASA, PT, AC and CT; formal analysis, GGDA, JASA, PT, LRP, AC and CT; investigation, GGDA, JASA, PT, AC; resources, RC, CT; data curation, GGDA, JASA, PT; writing—original draft preparation, GGDA, JASA, PT; writing—review and editing, GGDA, JASA, CT; visualization, RC, LRP, AC and CT; supervision, RC, CT; project administration, RC, CT; funding acquisition, RC, CT.
Funding	This research was partially funded by SODERCAN, Cantabria, Spain.
Acknowledgments	The authors of this research would like to thank Reinoso Forgings & Castings for the foundry sand as well as Mexico board; Consejo Nacional de Ciencia y Tecnología (CONACYT) for support during this project.
Conflicts of Interest	The authors declare no conflict of interest.

Chapter 4. Siderurgical Aggregate Cement Treated Bases and Concrete Using Foundry Sand

This chapter is the result of the experimental campaign to manufacture cement treated bases with foundry sand waste as fine aggregate substitution. This article has been published in the journal Applied Sciences and its reference is presented below:

Del Angel, G.G.; Aghajanian, A.; Tamayo, P.; Rico, J.; Thomas, C. Siderurgical Aggregate Cement-Treated Bases and Concrete Using Foundry Sand. *Appl. Sci.* 2021, 11, 435. <https://doi.org/10.3390/app11010435>

Siderurgical Aggregate Cement Treated Bases and Concrete Using Foundry Sand

Gilberto García Del Angel¹, Ali Aghajanian¹, Pablo Tamayo¹, Jokin Rico² and Carlos Thomas ¹

1. LADICIM (Laboratory of Materials Science and Engineering), University of Cantabria, E.T.S. de Ingenieros de Caminos, Canales y Puertos, Av./Los Castros 44, 39005 Santander, Spain
2. INGECID S.L. (Ingeniería de la Construcción, Investigación y Desarrollo de Proyectos), E.T.S. de Ingenieros de Caminos, Canales y Puertos, Av./Los Castros 44, 39005 Santander, Spain.

Abstract: Cement-treated bases are soils, gravels or manufactured aggregates mixed with certain quantities of cement and water in order to improve the characteristics of a base or sub-base layer. Due to the exploitation of natural aggregates, it is a matter of importance to avoid shortage of natural resources, which is why the use of recycled aggregates is a practical solution. In this paper we studied the feasibility of the use of untreated electric arc furnace slags and foundry sand in the development of cement-treated bases and slag aggregate concrete with a lower quantity of cement. We analysed the physical, mechanical and durability characteristics of the aggregates, followed by the design of mixes to fabricate test specimens. With cement-treated bases, results showed an optimal moisture content of 5% and a dry density of 2.47 g/cm³. Cement-treated bases made with untreated slag aggregate, foundry sand and 4% of cement content showed an unconfined compression strength at seven days of 3.73 MPa. For siderurgical aggregate concrete mixes, compressive strength, modulus of elasticity and flexural strength tests were made. The results showed that the mixes had good mechanical properties but durability properties could be an issue.

Keywords: siderurgical aggregate; foundry sand; cement-treated bases; concrete; mechanical properties

4.1. Introduction

Cement-treated bases (CTB) consists of native soils, gravels, or manufactured aggregates blended with prescribed quantities of cement and water [131]. CTB are also known as cement-treated aggregate base, cement-stabilized base or soil cement, depending on the materials used [132]. The more adequate cements for CTB are those whose hardening time is long enough to assure the workability of the mixture, moderate heat of hydration to limit the effects of cracking by retraction, low development of resistance and stiffness module. According to “Centro de Estudios Experimentales – Ministerios de Obras Públicas” (CEDEX), the amount of cement recommended is 4% or higher [133]. In other cases, depending of the type of soil, it is determined by the soil group type [134,135]. The water content starts the hydration process and facilitates the compaction process. It is recommended to use 5–7% by mass of the aggregate [133].

The use of CTB is due to the shortage of conventional aggregates and energy demands [136]. In addition, the use of CTB improves workability of road materials, increases the strength of the mixture, enhance durability and increases load spreading capacity [137].

The procedure to manufacture laboratory test specimens of CTB involves using the Proctor test procedure [138]. The aggregates are mixed with selected water and cement contents and confined in a mould where confining pressure of the proctor mass compacts the aggregates to obtain maximum dry density and optimal water content.

CTB properties like California bearing ratio (CBR), tensile strength and unconfined compressive strength (UCS) depend on the density, water content and confining pressure, which depend on the conditions to be simulated. There is a linear relationship between the UCS and the cement content [34,139,140]. The moisture content also affects the development of the UCS [34]. The natural aggregates (NA) of the CTB

have to fulfil an adequate grading curve [133], Los Angeles abrasion value, plastic index, flakiness index, sand equivalent and crushing value [34]. The milestone aggregates are the most common NA used for CTB but in recent years there has been an increasing number of studies of CTB with recycled aggregates (RA) as a replacement for the NA.

A RA is a recycled aggregate material that comes from different sources like brick stone [141], burnt rocks [142], concrete [143], reclaimed pavement [144], reclaimed asphalt [145], masonry [146], foundry sand [62] and precast elements [49,50]. The use of these RAs as filler materials has shown they produce an increase of mechanical and durability properties of concrete [147,148]. Their use as recycled aggregate concrete (RAC) and CTB [146,149–151] has also been studied, demonstrating their viability in cement and CTB as they present behaviours similar to those made with NA.

According to World Steel [152], the total global production of crude steel in 2018 was 1808.4 Mt, where 28.8% of the production was from electric furnaces [153]. Electric Arc Furnace Slags EAFS are by-products of the steel-making process, where the electric-arc furnaces (EAF) use high-power electric arcs to produce the heat necessary to melt recycled steel scrap and to convert it into high quality steel [154]. The slag has a lower density than steel and in a liquid state floats on top of the molten steel. It is extracted from the furnace and is air-cooled in order to form crystalline structures [155]. Once the steel has passed the valorisation process it can be called a siderurgical aggregate (SA), which has been shown to have characteristics that can be useful for the civil engineering and has led to its use in concrete [155,156].

Multiple studies [157–159] have demonstrated the potential use of EAFS as SA for concrete, showing that compressive strength increases or is very similar to that in traditional concrete. In self-compacted concrete, SA has a similar mechanical performance to concrete

manufactured with other additions [48,160]. Studies with asphalt mix showed that SAs are an alternative to a coarse fraction [161–163]. Also, studies in high performance concrete where total replacement of coarse aggregate with SA is used, shown an improve of the compressive strength, tensile strength and elastic modulus [164].

The most common aggregate in CTB and concrete is natural sand (NS). In this study, instead of NS, foundry sand (FS) was used. FS comes from the steelmaking process. Foundries successfully recycle and reuse the sand many times, but when the sand can no longer be reused it is removed and is termed spent foundry sand [33]. The physical and chemical properties of FS depend of the type of casting process and the industry sector from which it originates [52]. It has been reported that FS is non-hazardous due its high silica content. It is ideal to encapsulate hazardous materials [4,6,8]. This is especially interesting in cement-based materials, because all the harmful materials are encapsulated within a cement matrix stopping the transport of harmful components, as reported by Dyer et al. [88] and Alekseev et al.[24].

FS could be used conveniently in manufacturing good quality concrete and construction materials [67,72,165]. It should be taken into account that there is an increase in water demand due the presence of binders [15] such as clay binders [62] and polymeric binders[4].

A study reported the use of SA and FS for manufacture CTB, proving that the use of these RAs can achieve the requirements of a CTB [42]. Though there is evidence of the replacement of NA for SA and FS in concretes, there is not much information about the combination of those by-products in the concrete and CTB making process. The background of this research is to reduce waste and, at the same time, reduce the need for natural resources, making CTB and concrete more sustainable. That is why the aim of this study was the development of concrete with only untreated siderurgical aggregates (SAC) and CTB

mixes using SA and FS. For SAC the quantity of FS used was 20% by total weight of concrete in order to use as much FS as possible.

4.2. Materials and methods

4.2.1. Cement

The cement used for the CTB was a CEM-V/A (S-V) 32.5 N/SR, according to the Article 513 in the Spanish Regulations for Road Materials called PG-3. For the SAC, the cement used was a CEM-I-52.5 R from the point of view of the replication of the obtained results and in order to provide optimal performance with the minimum cement content, making it economically viable.

4.2.2. Foundry sand

The density of the FS was 2.58 g/cm^3 , calculated based on the methodology of standard EN-1097-6. The grading curve was determined by standard EN-933-2 and can be observed in the Figure 4.1.

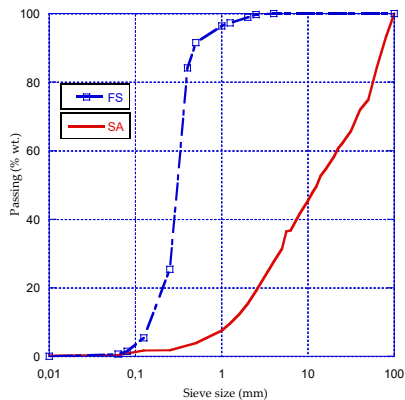


Figure 4.1. Foundry sand (FS) and siderurgical aggregate (SA) grading curve.

25%wt. of the FS was smaller than 0.25 mm. The maximum size matched the size of standardized sand (2 mm). On the other hand, the material had a filler content of less than 80 μm of 1.5% wt. For the FS, an X-ray fluorescence chemical analysis (XRF) was made. The results are shown in the Table 4.1. The main components of the FS are SiO_2 and CaO .

Table 4.1. X-ray fluorescence (XRF) chemical composition analysis of FS (%wt.).

SiO_2	CaO	Al_2O_3	Cr_2O_3	Fe_2O_3	SO_3	K_2O	TiO_2	P_2O_5	Others
83.90	7.83	2.87	1.67	1.40	0.72	0.53	0.13	0.06	<0.05

4.2.3. Siderurgical aggregates

In an initial stage, a sieve analysis was made by standard EN-933-2 (Figure 4.1). Because the material came without grading separation, a representative sample of the SA was taken to determine how much of the material was bigger than 31.5 mm aggregate size. Sizes bigger than 130 mm were observed (Figure 4.2). It was determined that 35% of the total weight of the SA was bigger than 31.5 mm aggregate size, which allowed 65% of the SA for use. The 0/31.5 mm fraction was separated in three different aggregate fractions to manufacture the SAC: 0/4, 4/8 and 8/31.5 mm, respectively. For the CTB, the 0/31.5 mm fraction was used. The grading curves are shown in Figure 4.3.



Figure 4.2. Untreated siderurgical aggregates.

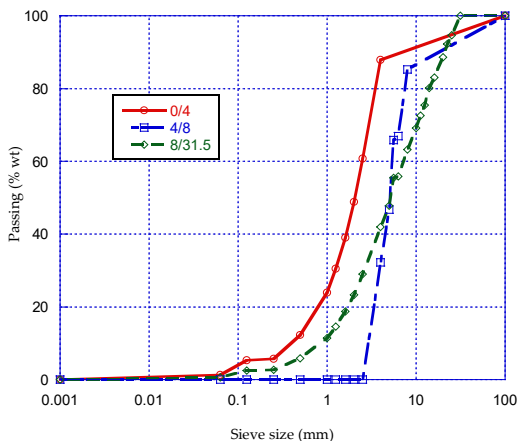


Figure 4.3. SA aggregate fraction grading curves.

Table 4.2 shows the XRF chemical analysis of the SA. The main composition of the SA is Fe_2O_3 and CaO . A study over several years has been carried out comparing the chemical compositions of EAFs. The composition is more less homogeneous in this plant with higher chromium and manganese traces found compared to those from other studies [76]. In any case, the products used in the manufacture of CTB are encapsulated in a cementitious matrix and, therefore, the degree of danger is significantly reduced.

Table 4.2. XRF chemical composition of SA (% wt.).

Fe_2O_3	CaO	SiO_2	MgO	MnO	Al_2O_3	Cr_2O_3	SO_3	TiO_2	P_2O_5	BaO	V_2O_5	Na_2O	Others
37.27	31.00	9.78	5.61	5.12	4.24	4.04	0.36	0.36	0.25	0.06	0.03	0.01	<0.01

Characterization of the physical, mechanical and durability properties of SA was made using European standards (EN-1097-6) for calculating density, porosity and absorption, flakiness index (FI) EN-933-3, Los Angeles wear test (LA) EN-1097-2, sand equivalent (SE) EN-933-8, freezing thawing (F-T) EN-1367-1, humidity-dryness loss (H-D) EN-146510 and crushing value (CVA) EN-83112:1989. The results are

shown in Table 4.3. Density results were similar to values reported, whereas porosity and absorption were higher than in other studies [156,166–168].

Table 4.3. Properties of the SA.

Fraction	Density (g/cm ³)	Porosity (%)	Absorp. (%)	FI (%)	LA (%)	SE (%)	F-T Loss (%)	H-D Loss (%)	CVA (%)
SA (0/31.5)	3.63	-	-	6	45	86	0.64	5.11	45
SA (4/8)	3.76	19.00	5.05	-	-	-	-	-	-
SA (8/31.5)	3.59	12.88	3.59	-	-	-	-	-	-

Freezing-thawing loss of mass was similar to that in other works [162,163] and Los Angeles wear test showed that the SA in this study had a higher value than others SA [169–171]. These results could be due to the fact that the SAs had more pores than conventional siderurgical aggregates.

4.2.4. Mix proportions

4.2.4.1. CTB Mix proportions

Figure 4.4 shows the upper and lower limits of the grading curve skeleton of CTB for a maximum aggregate size of 31.5 mm. The proposed aggregates content for the CTB (CTB-A) was 85% SA and 15% FS. A previous step to calculate the mix proportions of CTB-A was to determine the compaction capacity, establishing the cement and water contents proportions in order to get the optimal moisture content and maximum dry density using the modified Proctor test.

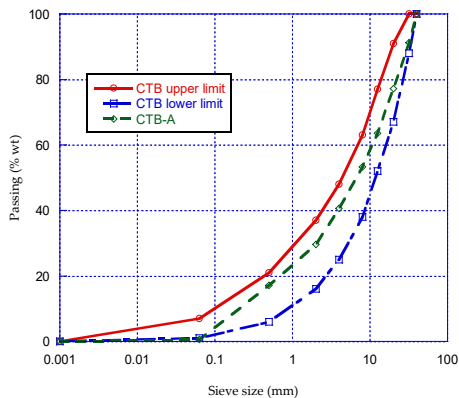


Figure 4.4. Cement-treated bases A (CTB-A) aggregates skeleton.

The recommended initial content of cement is $\geq 4\%$ by mass of SA. In this experimental study, the content of cement was 4, 3 and 2% for CTB-A4, CTB-A3 and CTB-A2, respectively, in order to analyse if the aggregates used in this study could achieve the minimum compression value (4.5 MPa) with less quantity of cement. Recommended water content is an initial value of 5% to 7% by mass. In this study, the tested water content was 4, 5 and 6% for each CTB (A4, A3 and A2). Nine test specimens were manufactured. Each specimen had a dimension of 150 mm \times 125 mm (length and height, respectively). The results are shown in Table 4.4.

Table 4.4. CTB proctor test results.

CTB	Optimal Moisture (%)	Maximum Dry Density (g/cm ³)
CTB-A2	3.1	2.31
	4.6	2.34
	6.2	2.34
CTB-A3	3.6	2.47
	4.9	2.46
	5.6	2.46
CTB-A4	3.8	2.40
	5.1	2.40
	5.2	2.38

Proctor test results showed that CTB-A2 presented the highest density of 2.34 g/cm³ with 4.6% of moisture. For CTB-A3 the highest density obtained was 2.47 g/cm³ with 3.6% of moisture. This result matches a study presented by Autelitano and Giuliani [38] but there is not a big difference between the optimal moisture content of 4.9% and 5.6% because the dry density is the same in both cases (2.46 g/cm³). For CTB-A4, a similar result is presented. The highest density obtained was 2.40 g/cm³ with 5.1% and 3.8% of moisture. Therefore, it can be observed that the optimal moisture is around 5%. Three specimens of each CTB with 5% of optimal moisture were manufactured. Results, with their standard deviations, are shown in Table 4.5.

Table 4.5. CTB proctor test results with optimal moisture.

CTB	Optimal Moisture (%)	Maximum Dry Density (g/cm ³)
CTB-A4	5	2.43 ± 0.03
CTB-A3	5	2.42 ± 0.03
CTB-A2	5	2.36 ± 0.04

4.2.4.2.SAC Mix proportions

The SAC was calculated based on Fuller's grading curve for a maximum aggregate size of 31.5 mm. Two aggregates skeleton were proposed (Figure 4.5). The first (SAC-A) was designed in order to use as much material as possible, and the second (SAC-B) to fit the Fuller curve. It is observed that the two mix proportions had a lack of 0/0.25 mm fraction size, because SA has very few fine grains. SCA-A was designed with a proportion of 20% FS, 15% of 0/4 SA, 15% of 4/8 SA and 50% 8/31.5 SA. SCA-B was designed with a proportion of 20% FS, 25% of 0/4 SA, 25% of 4/8 SA and 30% 8/31.5 SA.

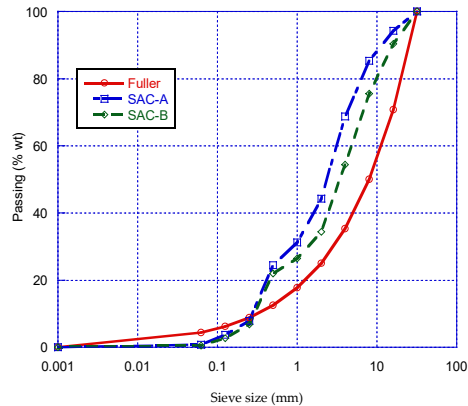


Figure 4.5. SAC aggregates skeleton.

It is observed that the same percent of 0/4 and 4/8 was used in SAC-A and SAC-B (25% and 15%, respectively). That is why it was decided to use the 0/8 mm size for an easier mixing process. SAC-A and SCA-B were calculated with an initial cement content of 280 kg/m^3 and a w/c ratio of 0.40 and 0.50, respectively. When both designs were mixed a lack of fine aggregate and a dry mix was observed so it was necessary to add FS and water. All of the SAC included 1% of super plasticizer additive Master Ease 5025 by cement weight because the FS and SA addition demanded more water, producing poor workability. SAC-A and SAC-B with their respectively adaptations are shown in Table 4.6.

Table 4.6. CTB and SAC mix proportions.

Material (kg/m^3)	CTB-A4	CTB-A3	CTB-A2	SAC-A	SAC-B
SA (0/31.5)	3086	3086	3086	-	-
SA (8/31.5)	-	-	-	617	1090
SA (0/8)	-	-	-	1063	675
FS	387	387	387	583	539
Cement	139	104	69	280	280
Water	181	179	177	222	212
Additive	-	-	-	2.80	2.80
w/c ratio	-	-	-	0.79	0.76

4.2.5. Physical properties of hardened concrete

For the CTB, the density was calculated in the mix proportion phase by the Proctor test. For each SAC, a test specimen of 150 mm × 300 mm (diameter and height, respectively) was fabricated according to EN-12390-2 and physical properties (density, water absorption and accessible porosity for water) of the SAC at seven days of age were determined following the standard EN-83980.

4.2.6. Gas permeability

For each SAC, test specimens of 150 mm × 300 mm (diameter and height, respectively) were performed according to EN-12390-2 and a gas permeability test at seven days of age was determined by the methodology in standards EN-3966 and EN-83981.

4.2.7. Depth of water penetration

The depth of penetration of water under pressure at seven days of age was tested following the standards of EN-12390-2 and EN-12390-8. The pressures used for this test were 0.6, 1.0 and 1.4 bar.

4.2.8. Compressive strength

Three test specimens were manufactured for each CTB-A. The test specimens had a dimension of 150 mm × 125 mm (diameter and height, respectively). The UCS of CTB-A at seven days was tested by the NLT 305/90 standard. When the specimen dimensions were not 152.4 mm × 177.8 mm (diameter and height, respectively), a correction coefficient had to be calculated by interpolation. For this study the correction coefficient was 0.86.

For SAC, three cubic specimens of 100 mm length were performed according to EN-12390-2. The compressive strength of the specimens was tested at seven and 28 days of curing according to EN-12390-3.

4.2.9. Modulus of elasticity

The modulus of elasticity was determined following the standard EN-12390-13 at 28 days, in test specimens of 150 mm × 300 mm (diameter and height respectively) fabricated according to EN-12390-2.

4.2.10. Flexural strength

Flexural strength was determinate following the standard 12390-5 in three prismatic specimens of 100 mm height and 400 mm length at 28 days.

4.3. Results and discussion

4.3.1. Physical properties of hardened concrete

In Table 4.7, the physical properties of SAC-A and SAC-B are shown. SAC-A had a density of 2.46 g/cm³ and SAC-B a density of 2.55 g/cm³. The porosity was 14.89% for SCA-A and 14.19% for SCA-B. The absorption value was higher in SCA-A than SCA-B at 6.10 and 5.57% respectively.

Table 4.7. Physical properties of the SAC.

Mixture	Density (g/cm ³)	Porosity (%)	Absorption (%)
SAC-A	2.46	14.98	6.10
SAC-B	2.55	14.19	5.57

The density values are similar to other presented in different works using EAFS [164,172]. The porosity values could be due the aggregates size fraction of SA utilized in this study with porosities of 12 and 19%. Normal values for conventional concrete porosity range between 9 and 10% [173]. Tamayo et al. [159] presented similar porosity and absorption results with 100% replacement of EAFS. SAC-A could have had the highest porosity because 50% of its volume was the 8/31.5 fraction and 30% volume were the 0/8 fraction, which presented

porosity values of 12.88 and 19% respectively. It was observed that with the increase of porosity, the absorption tended to increase as well.

Table 4.8 shows the result of the gas permeability and water penetration of SAC-A and SAC-B, which were 1.79×10^{-16} and 1.10×10^{-16} , respectively. It can be observed that water penetration was total in both SACs. The depth of water penetration is an indirect parameter that may indicate if the concrete will be durable. According to EHE-08, the water penetration should not be higher than 50 mm [174]. Therefore, both SACs did not fulfil the limit value. Total water penetration could be due porosity of the aggregates which makes water ingress easier, as reported by Gonzalez et al. [166].

Table 4.8. Gas permeability and water penetration of the SAC.

Mixture	$K_{O_2}(\text{m}^2)$	Water Penetration (mm)
SAC-A	1.79×10^{-16}	Total
SAC-B	1.10×10^{-16}	Total

4.3.2. Compressive strength

The compressive strength results of CTB-A and SAC, with their standard deviations, are shown in Table 4.9. CTB-A4 reached the highest compressive strength value with a compressive strength of 4.18 MPa. The compressive strength values for CTB-A3 and CTB-A2 were 3.48 MPa and 2.27 MPa, respectively. It can be observed that there is a relationship between the cement percent and the compressive strength, as other authors demonstrated [34,42,132,134,139,140,162]. In Spain, the minimum compressive strength value at seven days should be 4.5 MPa [133,162]. In order to achieve such a value, a higher cement percent needs to be used in further studies. On the other hand, CTB-A4 did fulfil the requirements of compressive strength in countries like Australia, Brazil, China, UK, Italy and South Africa [162].

Table 4.9. Compressive strength results.

Mixture	Compressive Strength at 7 Days (MPa)	Compressive Strength at 28 Days (MPa)
CTB-A4	3.73 ± 0.36	-
CTB-A3	3.21 ± 0.49	-
CTB-A2	2.93 ± 0.77	-
SAC-A	25.77 ± 1.27	27.75 ± 0.86
SAC-B	33.59 ± 0.51	38.25 ± 0.97

At seven and 28 days, SAC-B obtained the highest compressive values of 33.59 MPa and 38.25 MPa, respectively. On the other hand, SAC-A had lower compressive values of 25.77 and 27.75 MPa, respectively. SAC-B had an increase of 12% compressive strength from seven to 28 days. In addition, SAC-B had 27% higher resistance at compressive strength than SAC-A at 28 days. This could be due the porosity of the main aggregate size and a lower w/c ratio. Similar results of concrete incorporating 100% FS are presented by Khatib et al. [73] and Gholampour et al. [69]. On the other hand, the concrete of this study presented higher compressive strength than those presented by Etxeberria et al. [76], who also analysed concrete mixes with 100% EAFS.

4.3.3. Modulus of elasticity

Figure 4.6 shows the values of the modulus of elasticity at 28 days for SAC-A and SAC-B, which were 33 GPa and 34 GPa, respectively. This could be due a high elastic modulus of the aggregates. Such values match the results reported by Tamayo et al. [159] using 100% replacement of EAFS. SAC-A and SAC-B also presented higher modulus of elasticity values than those reported by Gholampour et al. [69], who reported 20.8 GPa with total replacement of NS by FS. Diverse studies [62,81,175,176] reported inferior modulus of elasticity values than those reported in this study, but none analysed a greater incorporation of FS than 50%.

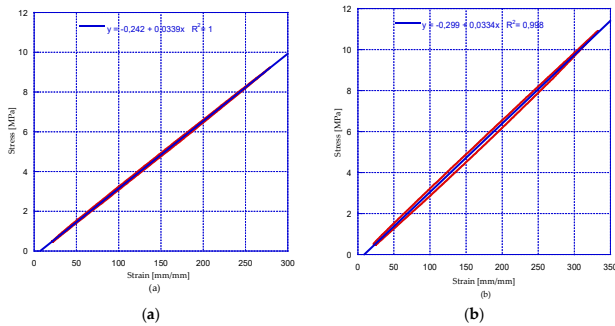


Figure 4.6. Modulus of elasticity of SAC-A (a) and SAC-B (b).

4.3.4. Flexural strength

Table 4.10 shows the flexural strength values of SAC-A and SAC-B were 5.15 and 5.88 MPa at 28 days, respectively. It can be observed that SAC-B was 12% more resistant than SAC-A. This could be due the lower porosity of the main fraction used and a lower w/c ratio. There is not much information about the flexural strength of concrete that incorporates SA and FS. Studies by Ganesh et al. [176] and Gholampour [69] analysed flexural strength with 50% replacement of FS, while in this work 100% of FS was used. The results from this study presented higher flexural strength for those with incorporation of 50% replacement.

Table 4.10. Flexural strength of SAC mixtures.

Mixture	Flexural Strength (MPa)
SAC-A	5.15 ± 1.43
SAC-B	5.88 ± 0.17

4.4. Partial conclusions

This work investigated the development of a CTB and SAC aggregate skeleton composed of untreated SA and FS in order to reduce NA consumption and waste production. The physical, mechanical and

durability properties of the SAC were characterized and compared with results from another authors. The following conclusions were drawn:

- The use of SA and FS for CTB manufacture is feasible, but in order to reach an adequate compression strength (>4.5 MPa) a cement percent higher than 4% needs to be used in order to achieve adequate requirements
- A statistical analysis using Minitab software was made to determine the standard deviation of each CTB, which in this case was 0.416 for CTB-A4, 0.650 for CTB-A3 and 0.866 for CTB-A2. In addition, a Pearson correlation test was made to calculate the correlation between cement percent content and UCS. The result of this test was 0.812 and a p-value of 0.008, which indicates that there is a positive correlation between these variables.
- The physical properties of the SAC presented high porosity and absorption values. This could be due to the high porosity and absorption of the aggregates used and because this was a low cement content concrete.
- The mechanical properties of SAC-A and SAC-B presented a moderated compressive strength at 28 days of 27.75 and 38.25 MPa respectively. Modulus of elasticity presented similar values of 33 and 34 GPa, which were similar to results found in the literature. Flexural strength presented higher values than those in conventional concrete and in concrete with up to 50% of FS addition.
- As to durability properties, total water penetration was occurred in the test specimens. This could be due to the porosity of the SA and the lack of a finer fraction to fill the voids in the concrete matrix. So, in further works, the addition of fillers or a finer FS could be used.

- In future studies, a comparison between SAC and conventional concrete with NA could be of interest to determine the effects of the use of these RAs on concrete behaviour.
- The findings in this work, and the total water penetration in SAC, suggest that SAC could be used as a layer between soil and structural concrete.

Author Contributions

Conceptualization, J.R. and C.T.; methodology, C.T and G.G.D.A., validation, P.T. and A.A.; for-mal analysis, G.G.D.A., P.T and A.A.; investigation, G.G.D.A.; data curation, G.G.D.A.; writing-original draft preparation, G.G.D.A. and A.A; writing-review and editing C.T., J.R. and G.G.D.A.; visualization, G.G.D.A.; supervision, C.T and J.R.; project administration, C.T and J.R. All authors have read and agreed to the published version of the manuscript.

Funding

This research was funded by the company INGECID S.L.

Data Availability Statement:

The data presented in this study are openly available.

Acknowledgments

The authors of this research would like to thanks to INGECID S.L and SIDENOR Reinosa for the steel slags and foundry sand as well to ROCACERO for the for providing the cement and super-plasticizer additive.

Conflicts of Interest

The authors declare no conflict of interest.

Chapter 5. Influence of partial and total replacement of used foundry sand in self-compacting concrete

This chapter is the result of the experimental campaign to manufacture self-compacting concrete with foundry sand waste as fine aggregate substitution. This article has been published in the journal Applied Sciences and its reference is presented below:

Del Angel, G.G.; Aghajanian, A.; Cabrera, R.; Tamayo, P.; Sainz-Aja, J.A.; Thomas, C. Influence of Partial and Total Replacement of Used Foundry Sand in Self-Compacting Concrete. *Appl. Sci.* 2023, 13, 409. <https://doi.org/10.3390/app13010409>

Influence of partial and total replacement of used foundry sand in self-compacting concrete

Gilberto García Del Angel¹, Ali Aghajanian¹, René Cabrera², Pablo Tamayo¹, Jose A. Sainz-Aja¹ and Carlos Thomas¹

1. LADICIM (Laboratory of Materials Science and Engineering), University of Cantabria, E.T.S. de Ingenieros de Caminos, Canales y Puertos, Av./Los Castros 44, 39005 Santander, Spain
2. FI (Faculty of Engineering), Autonomous University of Tamaulipas, Centro Universitario, Tampico 89336, Mexico

Abstract: In this work, the feasibility of partially and totally replacing natural sand with used foundry sand in self-compacting concrete was studied. Natural sand was replaced in 50% and 100% vol. by used foundry sand. The fresh state properties parameters analysed in this study were slump flow, t_{500} , V-funnel, Japanese ring and L-box following EFNARC guidelines. Results indicated an improvement in the fresh state properties when used foundry sand was utilized for partial and total replacement. The mechanical properties compressive strength and splitting ten-sile strength were obtained and analysed at 7 and 28 days. Regarding the compressive strength, used foundry sand enhanced compressive strength by up to 67% compared to control concrete. For splitting tensile strength, the self-compacting concrete with 50% vol. of used foundry sand displayed a slight decrease (2.8%) compared with the control concrete. SEM images showed that the concretes with used foundry sand had a less porous and more compacted matrix than the control concrete. It was concluded that the incorporation of used foundry sand in large volumes can be utilized as a sustainable alternative natural fine aggregate.

Keywords: self-compacting concrete; used foundry sand; siderurgical aggregates; eco-concrete; mechanical properties

5.1. Introduction

Foundry sand is used in the manufacture of mould formwork for the production of ferrous and non-ferrous casting materials and it is mainly made up of silica sand and binders of a natural or chemical nature. The natural binder is mostly bentonite clay mixed with water with a carbonaceous additive to enhance the casting surface [177], while chemical binders include phenolic-urethanes, sodium silicates, epoxy resins and furfuryl alcohol [92]. Depending on the binder additive used, these will receive the name of green foundry sands (GFS) or chemical foundry sands (CFS), respectively [56,92]. During the casting process, the sand from the moulds is reused until its properties are no longer suitable. It has been reported that this use is around 8 to 10 times at temperatures about 1500 °C [57], which is when a by-product known in the literature as waste foundry sand (WFS) or used foundry sand (UFS) is generated. In this research work the term UFS will be used. The UFS generated on an annual basis has been reported to be 100 Mt[79], while Sandhu and Siddique [54] reported 62.64 MT. Dyer et al. [10] reported that 0.60 tons of UFS are generated per 1 ton of steel production.

The physical-chemical properties of UFS will depend of the casting process, type of metal, fines content, number of times that the sand has been reused and the industry sector [92]. Overall, their properties are suitable for the replacement of the fine aggregate fraction [178]. It is because of the high quantities of UFS produced and its good physical and chemical properties that researchers have studied its applications in the civil engineering sector. Researchers have found that UFS is suitable for layers in pavement structures, reducing costs and reducing CO₂ emissions compared with natural sand [88]. It can also be used in subgrade fill [177], pavement structures [178], where chemical composition and leachate analysis show that there is no hazard in their

implementation [178], and cement-treated bases [107], where UFS's feasibility as a fine aggregate has been proved.

Regarding mortars, Cevik et al. [23] found that at early ages (3 days of curing), the partial incorporation of UFS (15% and 30%) increases the compressive strength by 13.51% and 12.35% (respectively) but at 28 days, the compressive strength of the mortars with 15% of UFS decreases 5.45% compared to the reference mortar. In another study, Monosi et al. [30] reported a decrease in the fresh state properties of 8%, 19% and 22% when the UFS replacement in mortars with a w/c ratio of 0.5 was 10%, 20% and 30%, respectively. For the compressive strength, a decrease of 2%, 20% and 30% was reported with WFS replacement of 10%, 20% and 30%, respectively [30]. The loss of properties in the fresh state properties and mechanical properties of mortars when replacing natural sand with UFS is attributed to the loose links between the cement paste and the aggregate due the fine powder of carbon and clay of the binders used [179]. Vazquez et al. [31], reported a decrease of 70% in compressive strength at 7, 14 and 28 days with mortars with total replacement of natural sand by UFS from an aluminium plant. This is due to the reaction between cement and the metalized aluminium, creating hydrogen gas and resulting in microfractures within the cement matrix [31]. UFS has also been used in the manufacture of masonry elements as clay replacement up to 50%wt. [90,91] and total replacement [67]. It also has been reported that the hazardous components are inertised during the firing process [180].

As for conventional concrete, the increase or decrease in fresh state properties and mechanical properties such as compressive strength depends on the type of UFS, whether or not there was a previous treatment and the substitution rate [92]. In relation to fresh state properties, Ahmad et al. [181] stated that the decrease in fresh state properties is due to the fineness of UFS [181]. Bilal et al. [182] reported a decrease of 31.25% in the slump test when 40% of natural sand was

replaced by UFS [182]. For mechanical properties, Ahmad et al. [181] also studied up to 50% replacement of natural sand by UFS, reporting a compressive strength decrease at all ages because of the impurities within the sand [181]. By contrast, Siddique et al. [183] studied up to 20% replacement of natural sand by UFS in concrete, reporting that the mechanical properties increase at all ages as the replacement percentage increased, which is due to the more fine particles in the UFS, creating a denser matrix [183].

Self-compacting concrete (SCC) is a special type of concrete that does not require vibration to be compacted; that is, it can flow under its own weight and, even in the presence of congested reinforcements, it completely fills and compacts the formwork [46]. It has been studied with other by-products such as electric arc furnace slags [47,48], where its feasibility for use as coarse aggregate has been demonstrated, showing adequate fresh state properties and mechanical behaviour. Likewise, SCC with recycled aggregates of precast concrete as coarse aggregates has displayed mechanical properties [49] and durability [50] similar to SCC with natural aggregates. Moreover, SCC with recycled aggregates from railway wastes has shown adequate fresh state properties, mechanical properties and durability [51].

Regarding UFS in SCC, Siddique and Sandhu [52] studied SCC with 5, 10 and 15% replacement of natural sand by UFS, reporting an increase in compressive strength and splitting tensile strength at all ages (7, 28 and 56 days). The slump flow increases 3% with 10% and 15% UFS replacement. By contrast, Parashar et al. [53] reported decreases in fresh state properties, SCC's behaviour and mechanical properties when increasing replacement percentages up to 40%. Ashis and Verma [22] studied SCC with up to 50% replacement of UFS at intervals of 10% and the results indicated that the incorporation of UFS does not affect the passing ability and viscosity, but negatively affects the flowability as the UFS replacement proportion increases. A decrease in the

segregation of the SCC was also reported with an increase in UFS incorporation, due the low specific density of the UFS, avoiding settling [22]. In the same study [22], it was reported that at early ages, UFS negatively affects compressive strength, but for longer ageing it does the contrary. This is due to the presence of a high silica content which slows down the pozzolanic reactions. However, with longer ageing, an improvement in compressive strength was observed. Sandhu and Siddique [54] analysed the replacement rate from 5% to 30% of UFS in SCC. It was reported that the fresh state properties and mechanical properties decreased as the replacement rate increased due to the increase in the specific surface area of UFS, leading to improper hydration and formation of voids. A 100% replacement of natural fine aggregate by UFS can be proposed as a solution to landfill disposal and, at the same time, result in eco-efficient concrete. Makul [55] concluded that UFS can be used in ready mixed concrete plants and precast concrete yards. Moreover, it has been reported that the use of UFS led to 50–60% cost saving compared to natural sand [56].

Because of the high production of UFS, researchers have studied its application in cement-based materials. This has led to the development of more eco-efficient concretes which improve environmental conditions by avoiding the deposit of this by-product in landfills. The replacement of natural sand by UFS in conventional concrete and SCC is usually around 30–50%. Not many studies have experimented with large volumes because it is reported that the properties of fresh and hardened concrete are negatively affected.

In this regard, one study reported in 2011 by Şahmaran et al. [77] shows a total replacement of UFS. In that study, the fresh state and mechanical properties of the SCC decreased compared to the control concrete. In the absence of further studies using full UFS replacement, the authors of this paper considered using chemical UFS to investigate whether its effect on SCC can be beneficial for the mechanical and fresh properties.

The novelty of this work is to contrast the results of other authors who have indicated that the use of large volumes of UFS negatively affects the fresh and hardened properties of SCC. The aim of this work will be to test whether chemical UFS in partial and total proportions are suitable for certain applications in construction based on the determination of their fresh state properties and their mechanical properties.

Therefore, the aim of this work is to investigate whether there can be a contrast in the total replacement of UFS in the manufacture of SCC when the UFS type is CFS. To achieve this, a novel dosing method has been proposed and experiments have been carried out with longer mixing times to ensure the correct homogeneity of the materials.

5.2. Materials and methods

5.2.1. Materials

The cement used was a CEM I-52.5 R with a density of 3 g/cm³ and a Blaine specific surface of 4400 m²/kg. Limestone filler (LF) with a Blaine specific surface of 3720 m²/kg was used as extra powder material according to EFNARC guidelines [46]. Table 5.1 shows the physical properties of the limestone coarse aggregate (LC), limestone sand (LS), silica sand (SS) and UFS. The characterization was performed according to the EN-1097-6 standard [184].

Table 5.1. Physical properties of the aggregates used.

Material	Bulk Density (g/cm ³)	Absorption (% wt.)	Porosity (% vol.)
LF <0.063 mm	2.76	-	-
UFS 0/2 mm	2.66	3.37	8.96
SS 0/1 mm	2.63	0.21	0.55
LS 0/4 mm	2.68	0.15	0.40
LC 4/16 mm	2.66	0.14	0.37

An X-ray fluorescence chemical analysis (XRF) was performed for the cement and UFS. Results show that the three principal components are SiO₂, CaO and Al₂O₃, as can be seen in Table 5.2.

Table 5.2. XRF chemical composition of cement and UFS.

Material	SiO ₂	CaO	Al ₂ O ₃	Cr ₂ O ₃	Fe ₂ O ₃	SO ₃	K ₂ O	MgO	TiO ₂	P ₂ O ₅	Others
Cement	17.81	65.6	4.65	-	3.25	4.50	0.60	1.2	0.2	-	-
UFS	83.9	7.83	2.87	1.67	1.40	0.72	0.70	0.53	0.13	0.06	<0.05

The grading curves of these materials were obtained following the methodology of the EN-933-2 [185] standard and they are shown in Figure 5.1.

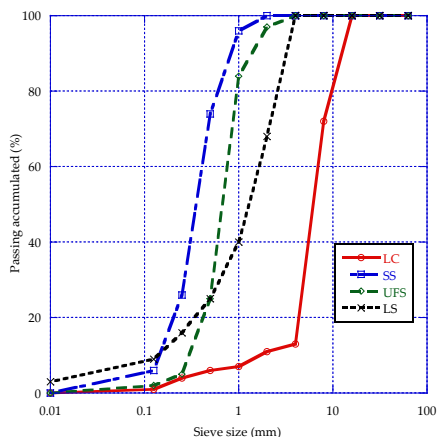


Figure 5.1. Grading curves of the aggregates.

5.2.2. Mix proportions

For this study, three mixes were designed based on the EFNARC guidelines [46] with the amount of coarse aggregate set at 60% vol. All mixes use the same amount of CEM 52.5 R, effective water and Master Ease 5025 superplasticizer. The same amount of LC is also used but a different amount of three types of sand. The three mixes are described below based on the use of one sand or another:

- A control mix (SCC-C) using only LS and SS adjusted by Fuller's method.
- A mix that, without using SS, combines UFS with LS (SCC-UFS-100) to obtain an overall particle size distribution as similar as possible to the SCC-C mix. For this purpose, adjustment equations with the granulometric modulus of the sands were proposed.
- A mix that uses half the UFS of the previous mix (SCC-UFS-50) and allows for the use of SS. The proportion of SS and LS is calculated using the adjustment equations with their granulometric modulus.
- The mix proportions are shown in Table 5.3.

Table 5.3. Mix proportions (kg/m³).

Component	SCC-C	SCC-UFS-50	SCC-UFS-100
CEM 52.5 R	340	340	340
Water	200	200	200
LF	196	196	196
LC 4/16	1060	1060	1060
LS 0/4	450	291	133
SS 0/1	178	89	-
UFS 0/2	-	247	494
Superplasticizer	5.12	5.12	5.12
w/c	0.59	0.59	0.59

The proposed procedure for mixing concrete is necessary because of the use of UFS. Its high absorption compared to LS and SS makes the correct homogenization in the mixture of the materials difficult, so to guarantee this, longer mixing and resting times are proposed. The fabrication procedure of the three SCC mixes is described below (Figure 5.2):

- Determine the moisture content of aggregates.
- Weigh the aggregates, and moisten the concrete mixer beforehand.
- Add the aggregates from the largest to smallest and add the cement and powder material.

- Mix all the materials for 3 min.
- Add half of the mixing water without superplasticizer (this addition will not take longer than 20 s) and mix for 3 min.
- Add the second part of the water with the superplasticizer and mix for 3 min.
- Stop the concrete mixer and allow the concrete to settle for 3 min.
- Finally, start the concrete mixer and mix the concrete for a further 5 min.



Figure 5.2. Mix procedure: dry mix of the aggregates (a); addition of first part of mixing water (b); settling of the SCC mix by 3 min (c).

5.2.3. Fresh state properties

In order to characterize this concrete, the slump flow test and t_{500} were determined following the methodology of the EN-12350-8 standard [186]. This standard describes the method to evaluate the flow capacity and stability of the concrete to be obtained.

V-funnel tests were performed according to the EN-12350-9 standard [187] in order to determine the viscosity and filling capacity of self-compacting concrete. L-box tests were performed according to the EN-12350-10 [188] standard using 3 bars to evaluate how SCC flow through narrow openings such as spaces between reinforcing bars.

Finally, the Japanese ring test was performed according to the EN-12350-12 standard [189] to determine the throughput capacity.

Table 5.4 shows EN-260-1 [190] and EFNARC guidelines [46] range of results of the self-compacting concretes' fresh state properties.

Table 5.4. EN and EFNARC guidelines.

Test	EN Guidelines	EFNARC Guidelines
Slump flow (mm)	550–850	650–800
t_{500} (s)	<2–≥2	2–5
L-box (dimensionless)	≥0.8	0.8–1
Japanese ring (mm)	≤10	0–10
V-funnel (s)	<9–9 to 25	6–12

5.3. Mechanical properties

Cubic specimens of the 100 mm side were produced according to EN-12390-2 [191]. The compressive strength of the specimens was tested at 7 and 28 days of curing according to EN-12390-3 [192] with a SUZPECAR servo hydraulic machine of 1500 kN capacity at the 0.5 MPa/s load rate. Splitting tensile strength EN-12390-6 [193] was performed on three thirds of standard cylindrical specimens of 150 × 300 mm at 28 days with a SUZPECAR servo hydraulic machine of 1500 kN capacity at a 0.05 MPa/s load rate.

5.4. Concrete microstructure

Concrete structural analysis was carried out with a Zeiss EVO MA15 scanning electron microscope. Micrographs were obtained at different magnifications of the paste-aggregate interface to compare the microstructure of each proposed blend.

The samples analysed in the SEM were obtained from the inside centre of the specimens tested at 28 days compressive strength. For this, it was necessary to extract appropriately sized fragments from each mixture and introduce them into the chamber of the device. When selecting samples, care was taken to ensure that they contained at least one coarse aggregate piece.

Before loading the samples into the SEM, they were gold-plated to obtain images at high magnification and good resolution. To compare the microstructure of the three mixes analysed, micrographs of the slurry in contact with the coarse aggregate were taken at 1500, 3000 and 7000 magnifications.

5.5. Results and discussion

5.5.1. Fresh state properties

The results of the fresh state properties tests can be seen in Table 5.5. The replacement of natural sands by UFS resulted in an improvement in the slump flow, as can be seen in Figure 5.3. The SCC-C (a) presented a slump flow of 500 mm, the SCC-UFS-50 (b) a slump flow of 730 mm, while SCC-UFS-100 (c) resulted in a slump flow of 750 mm, improving the fluidity by 46% and 50%, respectively, both corresponding to a SF2 category according to EN-206-1 [190]. This is because LS and SS have more fines than UFS, resulting in a higher absorption of water, thus decreasing the SF value. Siddique and Sandhu [52] also reported an increase in the slump flow when up to 15% replacement of UFS was used.

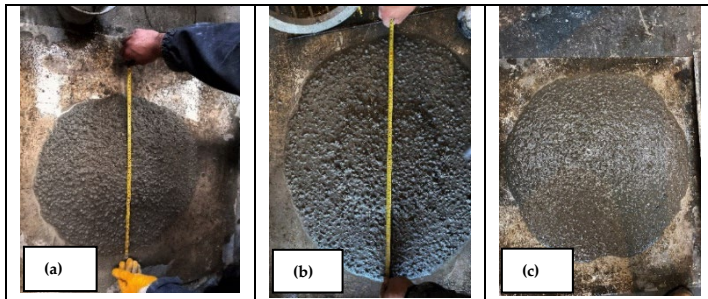


Figure 5.3. Appearance of the slump flow of the three self-compacting mixes; SCC-C (a), SCC-UFS-50 (b) and SCC-UFS-100 (c).

Regarding viscosity, Figure 5.4 shows that the t_{500} test of SCC-C obtained a time of 5 s to reach the 500 mm mark, which classifies it as in class VS2 according to EN-206-1. It is observed that the incorporation of UFS decreased the time in which the SCC reached the 500 mm mark; SCC-UFS-50 achieved a time reduction of 80% (1 s), while SCC-UFS-100 reduced the time by 60% (2 s). These two SCC are catalogued in class VS1 according to EN-206-1. It is observed that there may be a relationship between the analysed parameters, so a fitting formula between the t_{500} and the v-funnel is performed. The equation analysing the correlation between the v-funnel test and t_{500} shows an R^2 result of 0.99, thus concluding a relationship between these parameters. The variation between the V-funnel time and the t_{500} is higher with respect to the lower percentage of replacement. This is more evident in the SCC-C, which has the longest throughput times. The improvement in the t_{500} test result can be attributed to the fact that UFS does not have as many fines as LS and SS, resulting in a less viscous paste.

Figure 5.4 also shows the results of the V-funnel test. It can be observed that partial and total replacement of UFS results in a decrease in the passing times. A reduction of 70% and 50% was found, respectively. The reduction in V-funnel passage times and t_{500} is due to the improved fresh state properties of UFS concretes, which is reflected in the slump diameter. This is because this by-product has less fines than natural sands, leading to a higher flowability of the paste. This is more evident in the SCC-UFS-50, where the V-funnel times and t_{500} decrease significantly compared to the SCC-C. From Figure 5.4, it can also be observed that there is a relationship between the V-funnel test and the t_{500} test, which means that from the result of the t_{500} test, the V-funnel results can be predicted. According to the research presented by Martins et al. [72] where UFS from the automotive industry was used, this is because UFS has sub-angular-to-round-shaped particles, which improves the fluidity of the SCC. Siddique and Sandhu [52] also

reported a decrease in V-funnel time of 10% with the incorporation of up to 15% of UFS.

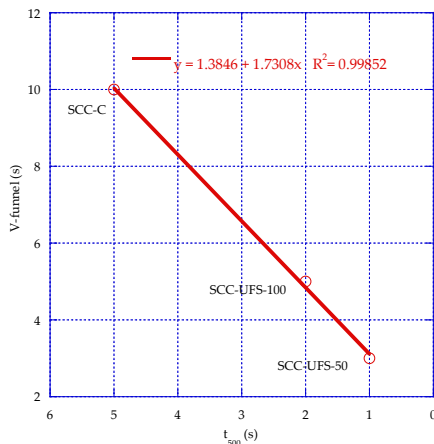


Figure 5.4. Time reduction of t_{500} test and V-funnel test.

The t_{500} time of the SCC-UFS-50 and SCC-UFS-100 was reduced by 60% and 80%, respectively, compared to the SCC-C. Regarding the V-funnel, the SCC-UFS-100 and SCC-UFS-50 presented a decrease in time of 50% and 70% compared to SCC-C. The results presented are in line with the work by Sandhu and Siddique [54], where it is reported that UFS can be incorporated into SCC, while fulfilling EFNARC standards. Şahmaran et al. [77] reported V-funnel time with 100% of UFS similar to those found in this research.

For the Japanese ring test, the SCC-C reached the limit value of 10 mm, whereas SCC-UFS-50 and SCC-UFS-100 were above this limit.

L-box test results show that SCC-C does not have an adequate passing capacity, which could be due to the volume of LC used and to LS and SS having more fines than UFS, creating more friction between the aggregates. On the contrary, SCC-UFS-50 and SCC-UFS-100 fulfil the

standard requirement. Similar results with the incorporation of UFS were reported by Sandhu and Siddique [54].

Table 5.5. Fresh state properties of the self-compacting concretes.

Material	SF (mm)	t ₅₀₀ (s)	V-Funnel (s)	J-Ring (mm)	L-Box
SCC-C	500	5	10	10	0.13
SCC-UFS-50	730	1	5	14	0.80
SCC-UFS-100	750	2	3	16	0.80

5.5.2. Mechanical properties

Figure 5.5 shows the results of the compressive strength of the three self-compacting concretes at 7 and 28 days of age. SCC-C attained a compressive strength of 21.91 MPa after 7 days, while SCC-UFS-100 and SCC-UFS-50 attained 28.94 MPa and 36.61 MPa, respectively. Compared to SCC-C, SCC-UFS-100 obtained a 32% increase in compressive strength, while the SCC-UFS-50 presented an increase of 67%. At 28 days age, SCC-C presented a compressive strength of 35.92 MPa, while SCC-UFS-100 and SCC-UFS-50 attained a compressive strength of 41.25 and 41.76 MPa, resulting in an increase of 15% and 16%, respectively. In general, it is observed that at early ages, SCC-UFS-100 and SCC-UFS-50 have higher compressive strength than SCC-C, with SCC-UFS-50 displaying the highest strength. However, at 28 days the difference between SCC-UFS-100 and SCC-UFS-50 is minimal. The graphical representation of the development of the SCC strength over time can be represented by means of a logarithmic adjustment as reported by other authors [48,51]. From the equations shown in Figure 5.5, it is shown that the correlation of R² analysing the evolution of compressive strength as a function of time is close to 1; therefore, the fit is adequate to observe the strength of the concretes at different ages, allowing a curve fit in which it is observed that the behaviour of SCC-UFS-50 has a higher strength than the other two concretes. The compressive strength differences between the materials studied could be explained by SCC-C fresh state properties being lower than the

other two concretes, leading to poor self-compaction and creating voids within the concrete matrix, resulting in a lower compressive strength.

Comparing the SCC-UFS-50 with the results of the Sua-iam et al. [78] study in which 50% UFS replacement was incorporated along with a rice husk ash cement substitution (0–20%), the compressive strength was higher at all ages.

The compressive strength results match the findings reported by Ashish and Verma [22], where it was observed that with the increase in up to 50% of UFS replacement, the compressive strength increased as well. This was attributed to the high silica content of UFS, thus creating a denser matrix [22].

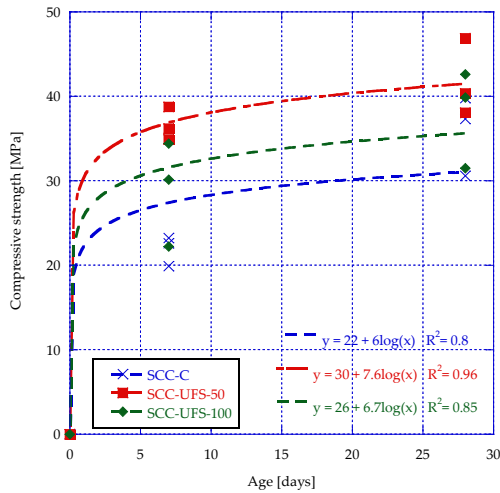


Figure 5.5. Compressive strength of the SCC mixes.

Figure 5.6 shows the appearance of compression cracks at 28 days for SCC-C, SCC-UFS-50 and SCC-UFS-100. The breakage of the SCC-UFS-50 and SCC-UFS-100 specimens was more satisfactory than that of the

SCC-C specimens, which is due to the fact that the applied force propagated through the paste-aggregate interface as stated by Sosa et al. [18], resulting in the observed fracture planes.

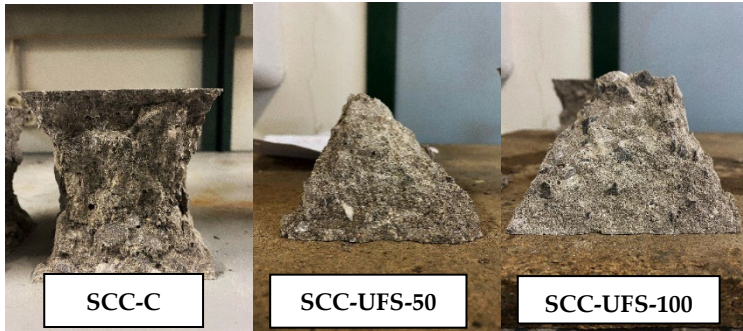


Figure 5.6. Detail of compression fractures at 28 days.

As for splitting tensile strength, Figure 5.7 shows that there is a decrease of 2.8% between SCC-C (2.15 MPa) and SCC-UFS-50 (2.09 MPa). On the other hand, SCC-UFS-100 shows a decrease of 28% (1.53 MPa) compared to SCC-C and a decrease of 26% compared to the SCC-UFS-50. Additionally, the calculation of the standard deviation of the data obtained was performed, resulting in a standard deviation of 0.06 for the SCC-C and 0.07 for both SCC-UFS-50 and SCC-UFS-100.

In general, it is observed that there is no significant difference between SCC-C and SCC-UFS-50. Similar results were reported by Sandhu and Siddique [54], where it was observed that the incorporation of up to 30% of UFS in self-compacting concrete slightly reduced the splitting tensile strength. Parashar et al. [53] reported that the splitting tensile strength is not affected with the incorporation of up to 40% UFS compared to the control concrete.

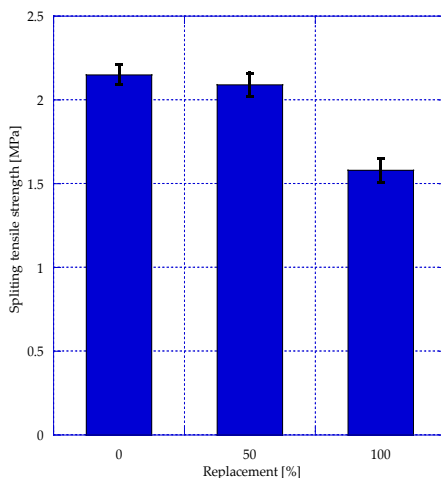


Figure 5.7. Splitting tensile strength of the SCC mixes.

5.5.3. Concrete microstructure

The microstructural analysis of the concrete at 1500 \times magnification is presented in Figure 5.8. It is observed that the SCC-C presents a less compacted and more porous structure than the other two concrete types. This could be related to the lower fresh state properties, where SCC-C presented a lower slump flow and higher t_{500} time compared to the other concretes. On the other hand, the SCC-UFS-100 showed a more compacted and less porous structure compared to the control concrete, which could also be related to the fresh state properties improvement enhancing concrete compaction. Smazewski [14] concluded that the bond between the aggregates and paste of concrete with UFS affects the concrete strength. Sosa et al. [47] reported that the SCC strength is due to the closed microstructure of the matrix. Moreover, Sandhu and Siddique [54] concluded that a denser microstructure of SCC improves the compressive strength.

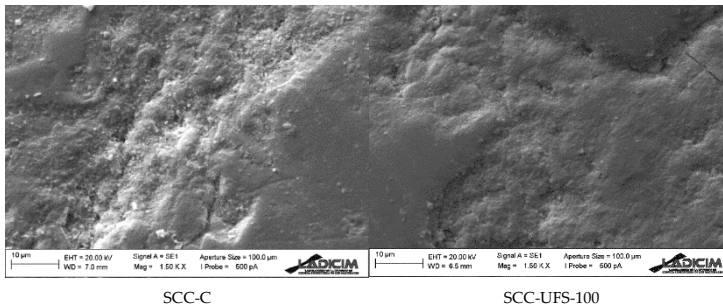
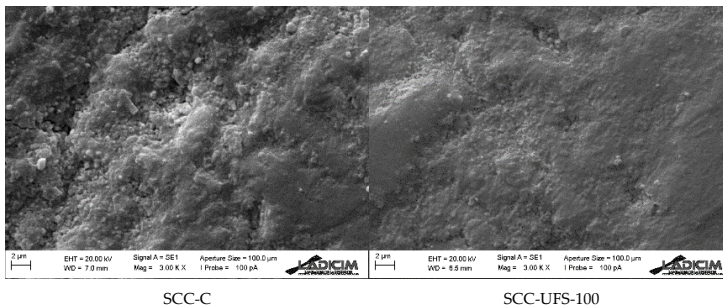


Figure 5.8. Micrographs obtained at 1500 \times .

Figure 5.9 shows magnifications at 3000 \times and 7000 \times comparing SCC-C and SCC-UFS-100. It is observed that SCC-C has a less compact matrix than SCC-UFS-100, which explains why the compressive strength is lower than concrete with UFS. The lack of compaction of the SCC-C increases the porosity of the concrete, so a decrease in the mechanical properties would be expected. This picture confirms the above-mentioned relation of low fresh state properties and lower compressive strength of SCC-C compared to self-compacting concretes containing UFS.



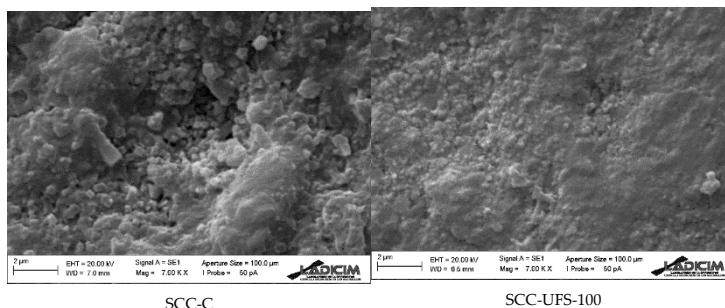


Figure 5.9. Micrographs obtained at 3000 \times and 7000 \times .

5.6. Partial conclusions

In this research, the fresh state properties, mechanical properties and microstructure of self-compacting concrete made with UFS as partial and total replacement for natural fine aggregates was studied. After analysing the results, the following conclusions can be drawn:

- The partial and total replacement of natural fine aggregates by UFS resulted in an increase in the diameter of the SF, by 46% and 50%, respectively, and in a decrease in t_{500} and V-funnel times by 60% and 80%, respectively, which is due to the lack of fines in UFS compared to natural sand, resulting in a decrease in the friction between the aggregates and the cement paste.
- There is a strong relationship between the t_{500} test and V-funnel test, which will help in predicting the results of the V-funnel test based on the t_{500} test. L-box results improve with the partial and total replacement of UFS compared to the control concrete.
- It is observed that at early ages, SCC-UFS-100 and SCC-UFS-50 have higher compressive strength than SCC-C, with SCC-UFS-50 being the one that presents the highest strength at 7

and 28 days, which is due to the lower compaction capacity of SCC-C, resulting in a less resistant material.

- Splitting tensile strength results showed that there is no great difference between SCC-C and SCC-UFS-50, but SCC-UFS-100 shows a decrease of 27%.
- SEM images proved that the incorporation of UFS enhances the concrete, creating a denser and less porous material compared to the control mix. This explains the higher compressive strength of concrete with UFS.
- In general, the partial and total incorporation of UFS in self-compacting concrete resulted in improved fresh state properties and mechanical properties. Self-compacting concrete with 50%vol. showed better mechanical properties and adequate fresh state properties. Likewise, the findings in this study show that total UFS replacement achieves an improvement in the fresh state properties and mechanical properties compared to control concrete, making this by-product a sustainable alternative to the use of natural fine aggregates.
- For the construction industry, the concretes developed in this research have been classified as SF2 and VS1, so they can be used in elements such as walls, columns, tunnel linings, foundation slabs and pavements. In addition, the use of a raw material, in this case natural sand, could be reduced to a lesser proportion.
- For the foundry industry, the use of its by-product creates a solution to avoid landfill contamination and monetary savings by avoiding paying for the deposit to landfill.
- Future studies could be carried out to analyse the durability of these concretes, with water penetration, oxygen permeability and carbonation being of particular interest.

Author Contributions	Conceptualization, G.G.D.A. and C.T.; methodology, G.G.D.A. and J.A.S.-A.; software, P.T.; validation, J.A.S.-A., C.T. and R.C.; formal analysis, C.T., G.G.D.A. and J.A.S.-A.; investigation, G.G.D.A. and A.A.; resources, C.T.; data curation, G.G.D.A. and P.T.; writing—original draft preparation, G.G.D.A., J.A.S.-A. and P.T.; writing—review and editing, P.T., C.T. and A.A.; visualization, C.T. and R.C.; supervision, C.T. and R.C.; project administration, C.T. All authors have read and agreed to the published version of the manuscript.
Funding	This research received no external funding. The authors would like to thank Reinoso Forgings & Castings for the foundry sand used in this study and the Mexican National Council of Science and Technology (CONACYT) for the support granted during the realization of this work.
Acknowledgments	
Conflicts of Interest	The authors declare no conflict of interest.

Chapter 6. General conclusions and future research work

6.1. General conclusions

The main objective of this thesis is the use of siderurgical aggregates in the manufacture of cement-based materials: mortars, cement-treated bases, concrete, and self-compacting concretes. After the extensive valorization process and the experimental campaign, the main conclusions of this Doctoral Thesis are:

The use of RFS in cement-based materials is a viable alternative to mitigate the use of natural silica sand, thus reducing the exploitation of this natural resource and the generation of CO₂. At the same time, cement-based materials are produced that are ecologically more viable and of similar quality to those made with natural aggregates.

As long as its absorption and how it affects the water/cement ratio is taken into account, RFS can be used satisfactorily in the manufacture of mortars, cement-treated bases, concretes and self-compacting concretes.

For each of these materials, several conclusions have been obtained, which are shown below:

Regarding the mortars with recycled foundry sand:

1. Small amounts of recycled foundry sand replacement improve the compressive strength compared to the control mortar. However, due to the high absorption of recycled foundry sand, when using higher replacement percentages, the w/c ratio must increase so that adequate mechanical properties cannot be achieved.
2. The abrasion resistance of mortars with 100% recycled foundry sand complies with the relevant standards.
3. Recycled foundry sand can be used as a substitute for natural sand in manufacturing mortars. The high absorption of

recycled foundry sand and its effect on the workability of the mortar must be considered.

4. From a practical point of view, the authors recommend using up to 25% replacement of recycled foundry sand because with a minimum amount of extra water, a workability equal to that of a control mortar is obtained, it has slightly higher mechanical strengths, and the mechanical durability is very similar to that of a control mortar.

Regarding cement-treated bases and concrete with steel slags and recycled foundry sand:

1. The use of recycled foundry sand and steel slags for manufacturing CTB can be a suitable solution for fully utilizing these materials.
2. For CTBs made from these materials to comply with the standard (compressive strength higher than 4.5 MPa at 7 days), a higher percentage of cement must be used.
3. The concrete made with these aggregates presents high porosity and absorption. This is due to the characteristics of the slag, which was untreated. On the other hand, the mechanical properties were acceptable. However, the durability in terms of water penetration does not comply with the Structural Code regulations so that this material could be suitable as a cleaning concrete.

Regarding self-compacting concrete with recycled foundry sand:

1. The partial and total substitution of the recycled foundry sand improved the fresh properties of the control SCC.
2. Regarding the mechanical properties, the SCC with 50 and 100% substitution improved compressive strength compared to the control SCC.

3. SEM images showed that incorporating recycled foundry sand enhances the concrete, creating a denser and less porous material than the control mix.
4. The findings in this thesis show that recycled foundry sand can be used in higher replacement amounts without negatively affecting its workability and mechanical properties.

6.2. Future research work

This thesis has demonstrated the feasibility of recycled foundry sand in manufacturing mortars, cement-treated bases, conventional concretes, and self-compacting concrete. As this work has developed, new ideas and projects have been proposed:

- ITZ analysis of conventional and self-compacting concretes with recycled foundry sand.
- The durability of conventional and self-compacting concretes with recycled foundry sand.
- Development of self-compacting concretes using recycled foundry sand as a replacement for fine aggregate and vitreous enamel residue for limestone filler.

Chapter 7. References

1. Zheng, J.; Chen, A.; Zheng, W.; Zhou, X.; Bai, B.; Wu, J.; Ling, W.; Ma, H.; Wang, W. Effectiveness Analysis of Resources Consumption, Environmental Impact and Production Efficiency in Traditional Manufacturing Using New Technologies: Case from Sand Casting. *Energy Convers. Manag.* **2020**, *209*, 112671, doi:10.1016/j.enconman.2020.112671.
2. García Chacón, J.A. Estudio de La Influencia de Diferentes Diseños de Los Sistemas de Alimentación y Compensación En La Fundición En Arena, Universidad de Sevilla, 2013.
3. Siddique, R.; Schutter, G. d.; Noumowe, A. Effect of Used-Foundry Sand on the Mechanical Properties of Concrete. *Constr. Build. Mater.* **2009**, *23*, 976–980, doi:10.1016/j.conbuildmat.2008.05.005.
4. Foundry Industry Recycling Starts Today (FIRST); United States. Environmental Protection Agency *Foundry Sand Facts for Civil Engineers*; Federal Highway Administration, 2004;
5. Siddique, R.; Singh, G. Utilization of Waste Foundry Sand (WFS) in Concrete Manufacturing. *Resour. Conserv. Recycl.* **2011**, *55*, 885–892, doi:10.1016/j.resconrec.2011.05.001.
6. Miguel, R.E.; Ippolito, J.A.; Leytem, A.B.; Porta, A.A.; Banda Noriega, R.B.; Dungan, R.S. Analysis of Total Metals in Waste Molding and Core Sands from Ferrous and Non-Ferrous Foundries. *J. Environ. Manage.* **2012**, *110*, 77–81, doi:10.1016/j.jenvman.2012.05.025.
7. Abichou, T.; B. Edil, T.; H. Benson, C. Beneficial Use of Foundry By-Products in Highway Construction. *Am. Soc. Civ. Eng.* **2004**.
8. Winkler, E.S.; Bolshakov, A. *Characterization of Foundry Sand Waste*; Massachusetts, 2000;
9. Gupta, N.; Siddique, R.; Belarbi, R. Sustainable and Greener Self-Compacting Concrete Incorporating Industrial By-Products: A Review. *J. Clean. Prod.* **2021**, *284*, doi:10.1016/j.jclepro.2020.124803.
10. Dyer, P.P.O.L.; Gutierrez Klinsky, L.M.; Silva, S.A.; e Silva, R.A.; de Lima, M.G. Macro and Microstructural Characterisation of Waste Foundry Sand Reused as Aggregate. *Road Mater. Pavement Des.* **2021**, *22*, 464–477, doi:10.1080/14680629.2019.1625807.
11. Sabour, M.R.; Derhamjani, G.; Akbari, M.; Hatami, A.M. Global Trends and Status in Waste Foundry Sand Management Research during the Years 1971–2020: A Systematic Analysis. *Environ. Sci. Pollut. Res.* **2021**, *28*, 37312–37321, doi:10.1007/s11356-021-13251-8.

12. Domingues, L.G.F.; Santos Ferreira, G.C. dos; Pires, M.S.G. Waste Foundry Sand Used to Cover Organic Waste in Landfills. *J. Mater. Cycles Waste Manag.* **2022**, *24*, 378–385, doi:10.1007/s10163-021-01327-z.
13. Iloh, P.; Fanourakis, G.; Ogra, A. Evaluation of Physical and Chemical Properties of South African Waste Foundry Sand (WFS) for Concrete Use. *Sustain.* **2019**, *11*, doi:10.3390/su11010193.
14. Smarzewski, P. Mechanical Properties of Ultra-High Performance Concrete with Partial Utilization of Waste Foundry Sand. *Buildings* **2020**, *10*, doi:10.3390/buildings10010011.
15. Bhardwaj, B.; Kumar, P. Waste Foundry Sand in Concrete: A Review. *Constr. Build. Mater.* **2017**, *156*, 661–674, doi:10.1016/j.conbuildmat.2017.09.010.
16. Monosi, S.; Tittarelli, F.; Giosuè, C.; Ruello, M.L. Effect of Two Different Sources and Washing Treatment on the Properties of UFS By-Products for Mortar and Concrete Production. *Constr. Build. Mater.* **2013**, *44*, 260–266, doi:10.1016/j.conbuildmat.2013.02.029.
17. Tittarelli, F. *Waste Foundry Sand*; Elsevier Ltd, 2018; ISBN 9780081021569.
18. Smarzewski, P.; Barnat-Hunek, D. Mechanical and Durability Related Properties of High Performance Concrete Made with Coal Cinder and Waste Foundry Sand. *Constr. Build. Mater.* **2016**, *121*, 9–17, doi:10.1016/j.conbuildmat.2016.05.148.
19. Dayton, E.A.; Whitacre, S.D.; Dungan, R.S.; Basta, N.T. Characterization of Physical and Chemical Properties of Spent Foundry Sands Pertinent to Beneficial Use in Manufactured Soils. *Plant Soil* **2010**, *329*, 27–33, doi:10.1007/s11104-009-0120-0.
20. Sandhu, R.K.; Siddique, R. Durability Performance of Self-Compacting Concrete Made with Waste Foundry Sand. *Struct. Concr.* **2022**, *23*, 722–738, doi:10.1002/suco.202100164.
21. Priyadarshini, M.; Giri, J.P. Use of Recycled Foundry Sand for the Development of Green Concrete and Its Quantification. *J. Build. Eng.* **2022**, *52*, 104474, doi:10.1016/j.jobe.2022.104474.
22. Ashish, D.K.; Verma, S.K. Robustness of Self-Compacting Concrete Containing Waste Foundry Sand and Metakaolin: A Sustainable Approach. *J. Hazard. Mater.* **2021**, *401*, 123329, doi:10.1016/j.jhazmat.2020.123329.
23. Çevik, S.; Mutuk, T.; Oktay, B.M.; Demirbaş, A.K. Mechanical and Microstructural Characterization of Cement Mortars Prepared by Waste Foundry Sand (WFS). *J. Aust. Ceram. Soc.* **2017**, *53*, 829–837, doi:10.1007/s41779-

- 017-0096-9.
24. Alekseev, K.; Mymrin, V.; Avanci, M.A.; Klitzke, W.; Magalhães, W.L.E.; Silva, P.R.; Catai, R.E.; Silva, D.A.; Ferraz, F.A. Environmentally Clean Construction Materials from Hazardous Bauxite Waste Red Mud and Spent Foundry Sand. *Constr. Build. Mater.* **2019**, *229*, 116860, doi:10.1016/j.conbuildmat.2019.116860.
 25. Alonso-Santurde, R.; Coz, A.; Viguri, J.R.; Andrés, A. Recycling of Foundry By-Products in the Ceramic Industry: Green and Core Sand in Clay Bricks. *Constr. Build. Mater.* **2012**, *27*, 97–106, doi:10.1016/j.conbuildmat.2011.08.022.
 26. Apithanyasai, S.; Supakata, N.; Papong, S. The Potential of Industrial Waste: Using Foundry Sand with Fly Ash and Electric Arc Furnace Slag for Geopolymer Brick Production. *Heliyon* **2020**, *6*, doi:10.1016/j.heliyon.2020.e03697.
 27. Arulrajah, A.; Yaghoubi, E.; Imteaz, M.; Horpibulsuk, S. Recycled Waste Foundry Sand as a Sustainable Subgrade Fill and Pipe-Bedding Construction Material: Engineering and Environmental Evaluation. *Sustain. Cities Soc.* **2017**, *28*, 343–349, doi:10.1016/j.scs.2016.10.009.
 28. Basar, H.M.; Deveci Aksoy, N. The Effect of Waste Foundry Sand (WFS) as Partial Replacement of Sand on the Mechanical, Leaching and Micro-Structural Characteristics of Ready-Mixed Concrete. *Constr. Build. Mater.* **2012**, *35*, 508–515, doi:10.1016/j.conbuildmat.2012.04.078.
 29. EN 998-2. Specification for Mortar for Masonry - Part 2: Masonry Mortar 2018, 1–31.
 30. Monosi, S.; Sani, D.; Tittarelli, F. Used Foundry Sand in Cement Mortars and Concrete Production. *Open Waste Manag. J.* **2010**, *3*, 18–25, doi:10.2174/1876400201003010018.
 31. Vázquez-Rodríguez, F.J.; Valadez-Ramos, J.; Puente-Ornelas, R.; Contreras, J.E.; Arato, A.; Rodríguez, E.A. Nonferrous Waste Foundry Sand and Milling Fly Ash as Alternative Low Mechanical Strength Materials for Construction Industry: Effect on Mortars at Early Ages. *Rev. Rom. Mater. Rom. J. Mater.* **2018**, *48*, 338–345.
 32. Matos, P.R. de; Marcon, M.F.; Schankoski, R.A.; Prudêncio Jr., L.R. Novel Applications of Waste Foundry Sand in Conventional and Dry-Mix Concretes. *J. Environ. Manage.* **2019**, *244*, 294–303, doi:10.1016/J.JENVMAN.2019.04.048.
 33. Siddique, R.; Noumowe, A. Utilization of Spent Foundry Sand in Controlled Low-Strength Materials and Concrete. *Resour. Conserv. Recycl.* **2008**, *53*, 27–35, doi:10.1016/J.RESCONREC.2008.09.007.
 34. Xuan, D.X.; Houben, L.J.M.; Molenaar, A.A.A.; Shui, Z.H. Mechanical Properties

- of Cement-Treated Aggregate Material - A Review. *Mater. Des.* **2012**, *33*, 496–502, doi:10.1016/j.matdes.2011.04.055.
35. Ebrahim Abu El-Maaty Behiry, A. Utilization of Cement Treated Recycled Concrete Aggregates as Base or Subbase Layer in Egypt. *Ain Shams Eng. J.* **2013**, *4*, 661–673, doi:10.1016/j.asej.2013.02.005.
 36. CEDEX *Manual de Firmes Con Capas Tratadas Con Cemento*; Manuales y recomendaciones; Ministerio de Fomento, Cedex, 2009; ISBN 9788477904892.
 37. PG-3 Pliego de Prescripciones Técnicas Generales Para Obras de Carreteras y Puentes (PG-3). Parte 5: Firmes y Pavimentos. **2015**, 690–695.
 38. Li, Y.; Ma, S.; Chen, G.; Wang, S. Mechanical Properties and Durability of Cement-Stabilised Macadam Incorporating Waste Foundry Sand. *Int. J. Pavement Eng.* **2021**, *0*, 1–15, doi:10.1080/10298436.2021.2011278.
 39. Vinoth, M.; Sinha, A.K.; Guruvittal, U.K.; Havanagi, V.G. Strength of Stabilised Waste Foundry Sand Material. *Indian Geotech. J.* **2022**, *52*, 707–719, doi:10.1007/s40098-021-00586-9.
 40. Bhardwaj, A.; Sharma, R.K. Designing Thickness of Subgrade for Flexible Pavements Incorporating Waste Foundry Sand, Molasses, and Lime. *Innov. Infrastruct. Solut.* **2022**, *7*, doi:10.1007/s41062-021-00723-6.
 41. Iqbal, M.F.; Liu, Q.F.; Azim, I. Experimental Study on the Utilization of Waste Foundry Sand as Embankment and Structural Fill. *IOP Conf. Ser. Mater. Sci. Eng.* **2019**, *474*, doi:10.1088/1757-899X/474/1/012042.
 42. Pasetto, M.; Baldo, N. Experimental Analysis of Hydraulically Bound Mixtures Made with Waste Foundry Sand and Steel Slag. *Mater. Struct. Constr.* **2015**, *48*, 2489–2503, doi:10.1617/s11527-014-0333-4.
 43. Okamura, H.; Ozawa, K. Self-Compacting High Performance Concrete. *Struct. Eng. Int. J. Int. Assoc. Bridg. Struct. Eng.* **1996**, *6*, 269–270.
 44. Ozawa, K. High-Performance Concrete Based on the Durability Design of Concrete Structures. In Proceedings of the Proc. of the Second East Asia-Pacific Conference on Structural Engineering and Construction, 1989; 1989.
 45. Shi, C.; Wu, Z.; Lv, K.; Wu, L. A Review on Mixture Design Methods for Self-Compacting Concrete. *Constr. Build. Mater.* **2015**, *84*, 387–398, doi:10.1016/j.conbuildmat.2015.03.079.
 46. EFNARC The European Guidelines for Self-Compacting Concrete. *Eur. Guidel. Self Compact. Concr.* **2005**, 63.

47. Sosa, I.; Tamayo, P.; Sainz-Aja, J.A.; Thomas, C.; Setién, J.; Polanco, J.A. Durability Aspects in Self-Compacting Siderurgical Aggregate Concrete. *J. Build. Eng.* **2021**, *39*, doi:10.1016/j.job.2021.102268.
48. Sosa, I.; Thomas, C.; Polanco, J.A.; Setién, J.; Tamayo, P. High Performance Self-Compacting Concrete with Electric Arc Furnace Slag Aggregate and Cupola Slag Powder. *Appl. Sci.* **2020**, *10*, 773, doi:10.3390/app10030773.
49. Fiol, F.; Thomas, C.; Muñoz, C.; Ortega-López, V.; Manso, J.M. The Influence of Recycled Aggregates from Precast Elements on the Mechanical Properties of Structural Self-Compacting Concrete. *Constr. Build. Mater.* **2018**, *182*, 309–323, doi:10.1016/j.conbuildmat.2018.06.132.
50. Fiol, F.; Thomas, C.; Manso, J.M.; López, I. Transport Mechanisms as Indicators of the Durability of Precast Recycled Concrete. *Constr. Build. Mater.* **2020**, 121263, doi:10.1016/j.conbuildmat.2020.121263.
51. Sainz-Aja, J.; Carrascal, I.; Polanco, J.A.; Thomas, C.; Sosa, I.; Casado, J.; Diego, S. Self-Compacting Recycled Aggregate Concrete Using out-of-Service Railway Superstructure Wastes. *J. Clean. Prod.* **2019**, *230*, 945–955, doi:10.1016/j.jclepro.2019.04.386.
52. Siddique, R.; Sandhu, R.K. Properties of Self-Compacting Concrete Incorporating Waste Foundry Sand. *Leonardo J. Sci.* **2013**, *23*, 105–124.
53. Parashar, A.; Aggarwal, P.; Saini, B.; Aggarwal, Y.; Bishnoi, S. Study on Performance Enhancement of Self-Compacting Concrete Incorporating Waste Foundry Sand. *Constr. Build. Mater.* **2020**, *251*, doi:10.1016/j.conbuildmat.2020.118875.
54. Sandhu, R.K.; Siddique, R. Strength Properties and Microstructural Analysis of Self-Compacting Concrete Incorporating Waste Foundry Sand. *Constr. Build. Mater.* **2019**, *225*, 371–383, doi:10.1016/j.conbuildmat.2019.07.216.
55. Makul, N. Combined Use of Untreated-Waste Rice Husk Ash and Foundry Sand Waste in High-Performance Self-Consolidating Concrete. *Results Mater.* **2019**, *1*, 100014, doi:10.1016/j.rinma.2019.100014.
56. Thiruvenkita, M.; Pandian, S.; Santra, M.; Subramanian, D. Use of Waste Foundry Sand as a Partial Replacement to Produce Green Concrete: Mechanical Properties, Durability Attributes and Its Economical Assessment. *Environ. Technol. Innov.* **2020**, *19*, doi:10.1016/j.eti.2020.101022.
57. Guney, Y.; Sari, Y.D.; Yalcin, M.; Tuncan, A.; Donmez, S. Re-Usage of Waste Foundry Sand in High-Strength Concrete. *Waste Manag.* **2010**, *30*, 1705–1713, doi:10.1016/j.wasman.2010.02.018.

-
58. Dungan, R.S.; Dees, N.H. The Characterization of Total and Leachable Metals in Foundry Molding Sands. *J. Environ. Manage.* **2009**, *90*, 539–548, doi:10.1016/j.jenvman.2007.12.004.
59. Yazoghli-Marzouk, O.; Vulcano-Greullet, N.; Cantegrit, L.; Friteyre, L.; Jullien, A. Recycling Foundry Sand in Road Construction-Field Assessment. *Constr. Build. Mater.* **2014**, *61*, 69–78, doi:10.1016/j.conbuildmat.2014.02.055.
60. Ganesh Prabhu, G.; Hwan Hyun, J.; Yong Kim, Y. Effects of Foundry Sand as a Fine Aggregate in Concrete Production. **2014**, doi:10.1016/j.conbuildmat.2014.07.070.
61. Javed, S. *Use of Waste Foundry Sand in Highway Construction*; West Lafayette, Indiana, 1992; Vol. 1;
62. Siddique, R.; Schutter, G. de; Noumowe, A. Effect of Used-Foundry Sand on the Mechanical Properties of Concrete. *Constr. Build. Mater.* **2009**, *23*, 976–980, doi:10.1016/J.CONBUILDMAT.2008.05.005.
63. *FIRST Foundry Sand Facts for Civil Engineers*; 2004;
64. Bralower, P. The Use and Misuse of Foundry Sand Additives, Part 2. *Mod. Cast.* **1988**, *126*, 1174–1183.
65. Siddique, R.; Kunal; Mehta, A. *Utilization of Industrial By-Products and Natural Ashes in Mortar and Concrete Development of Sustainable Construction Materials*; Elsevier Ltd, 2019; ISBN 9780081027042.
66. Naik, T.R.; Kraus, R.N.; Ramme, B.W.; Canpolat, F. Effects of Fly Ash and Foundry Sand on Performance of Architectural Precast Concrete. *J. Mater. Civ. Eng.* **2012**, *24*, 851–859, doi:10.1061/(asce)mt.1943-5533.0000432.
67. Matos, P.R. de; Marcon, M.F.; Schankoski, R.A.; Prudêncio, L.R. Novel Applications of Waste Foundry Sand in Conventional and Dry-Mix Concretes. *J. Environ. Manage.* **2019**, *244*, 294–303, doi:10.1016/j.jenvman.2019.04.048.
68. Gurumoorthy, N.; Arunachalam, K. Durability Studies on Concrete Containing Treated Used Foundry Sand. *Constr. Build. Mater.* **2019**, *201*, 651–661, doi:10.1016/j.conbuildmat.2019.01.014.
69. Gholampour, A.; Zheng, J.; Ozbakkaloglu, T. Development of Waste-Based Concretes Containing Foundry Sand, Recycled Fine Aggregate, Ground Granulated Blast Furnace Slag and Fly Ash. *Constr. Build. Mater.* **2020**, doi:10.1016/j.conbuildmat.2020.121004.
70. Díaz Pace, D.M.; Miguel, R.E.; Di Rocco, H.O.; Anabitarte García, F.; Pardini, L.;
-

- Legnaioli, S.; Lorenzetti, G.; Palleschi, V. Quantitative Analysis of Metals in Waste Foundry Sands by Calibration Free-Laser Induced Breakdown Spectroscopy. *Spectrochim. Acta - Part B At. Spectrosc.* **2017**, *131*, 58–65, doi:10.1016/j.sab.2017.03.007.
71. Naik, T.R.; Patel, V.M.; Parikh, D.M.; Tharaniyii, M.P. *Utilization of Used Foundry Sand in Concrete*; 1994;
72. Martins, M.A. de B.; Barros, R.M.; Silva, G.; Santos, I.F.S. dos Study on Waste Foundry Exhaust Sand, WFES, as a Partial Substitute of Fine Aggregates in Conventional Concrete. *Sustain. Cities Soc.* **2019**, *45*, 187–196, doi:10.1016/j.scs.2018.11.017.
73. Khatib, J.M.; Baig, S.; Bougara, A.; Booth, C. Foundry Sand Utilisation in Concrete Production. *2nd Int. Conf. Sustain. Constr. Mater. Technol.* **2010**, 931–935.
74. Siddique, R.; Aggarwal, Y.; Aggarwal, P.; Kadri, E.-H.; Bennacer, R. Strength, Durability, and Micro-Structural Properties of Concrete Made with Used-Foundry Sand (UFS). *Constr. Build. Mater.* **2011**, *25*, 1916–1925, doi:10.1016/j.conbuildmat.2010.11.065.
75. Kaur, G.; Siddique, R.; Rajor, A. Micro-Structural and Metal Leachate Analysis of Concrete Made with Fungal Treated Waste Foundry Sand. *Constr. Build. Mater.* **2013**, *38*, 94–100, doi:10.1016/j.conbuildmat.2012.07.112.
76. Etxeberria, M.; Pacheco, C.; Meneses, J.M.; Berridi, I. Properties of Concrete Using Metallurgical Industrial By-Products as Aggregates. *Constr. Build. Mater.* **2010**, *24*, 1594–1600, doi:10.1016/j.CONBUILDMAT.2010.02.034.
77. Şahmaran, M.; Lachemi, M.; Erdem, T.K.; Yücel, H.E. Use of Spent Foundry Sand and Fly Ash for the Development of Green Self-Consolidating Concrete. *Mater. Struct. Constr.* **2011**, *44*, 1193–1204, doi:10.1617/s11527-010-9692-7.
78. Sua-iam, G.; Makul, N.; Cheng, S.; Sokrai, P. Workability and Compressive Strength Development of Self-Consolidating Concrete Incorporating Rice Husk Ash and Foundry Sand Waste – A Preliminary Experimental Study. *Constr. Build. Mater.* **2019**, *228*, 116813, doi:10.1016/j.conbuildmat.2019.116813.
79. Gupta, N.; Siddique, R.; Belarbi, R. Sustainable and Greener Self-Compacting Concrete Incorporating Industrial By-Products: A Review. *J. Clean. Prod.* **2020**, 124803, doi:10.1016/j.jclepro.2020.124803.
80. EFCA The European Guidelines for Self-Compacting Concrete. **2006**.
81. Basar, H.M.; Deveci Aksoy, N. The Effect of Waste Foundry Sand (WFS) as Partial Replacement of Sand on the Mechanical, Leaching and Micro-Structural

-
- Characteristics of Ready-Mixed Concrete. *Constr. Build. Mater.* **2012**, *35*, 508–515, doi:10.1016/j.conbuildmat.2012.04.078.
82. Kumar, A.; Pratheba, S.; Rajendran, R.; Perumal, K.; Lingeshwaran, N.; Sambaraju, S. An Experimental Study on the Mechanical Properties of Concrete Replacing Sand with Quarry Dust and Waste Foundry Sand. *Mater. Today Proc.* **2020**, doi:10.1016/j.matpr.2020.06.271.
83. Ganesh Prabhu, G.; Bang, J.W.; Lee, B.J.; Hyun, J.H.; Kim, Y.Y. Mechanical and Durability Properties of Concrete Made with Used Foundry Sand as Fine Aggregate. *Adv. Mater. Sci. Eng.* **2015**, *2015*, doi:10.1155/2015/161753.
84. American Society for Testing and Materials ASTM C 1012: Standard Test Method for Length Change of Hydraulic Cement Mortars Exposed to a Sulfate Solution.
85. American Society for Testing and Materials ASTM C 1202 – 12: Standard Test Method for Electrical Indication of Concretes Ability to Resist Chloride- Ion Penetration. **2012**.
86. United States Environmental Protection Agency (US EPA) *Waste and Materials—Flow Benchmark Sector Report: Beneficial Use of Secondary Materials—Foundry Sand*; Washington, DC, 2008;
87. Li, X.; Chertow, M.; Guo, S.; Johnson, E.; Jiang, D. Estimating Non-Hazardous Industrial Waste Generation by Sector, Location, and Year in the United States: A Methodological Framework and Case Example of Spent Foundry Sand. *Waste Manag.* **2020**, *118*, 563–572, doi:10.1016/j.wasman.2020.08.056.
88. Dyer, P.P.O.L.; de Lima, M.G.; Klinsky, L.M.G.; Silva, S.A.; Coppio, G.J.L. Environmental Characterization of Foundry Waste Sand (WFS) in Hot Mix Asphalt (HMA) Mixtures. *Constr. Build. Mater.* **2018**, *171*, 474–484, doi:10.1016/j.conbuildmat.2018.03.151.
89. Benson, C.H.; Bradshaw, S. *User Guideline for Foundry Sand in Green Infrastructure Construction*; Wisconsin, 2011;
90. Jitendra, K.; Khed, V.C. Optimization of Concrete Blocks with High Volume Fly Ash and Foundry Sand. In *Proceedings of the Materials Today: Proceedings*; Elsevier Ltd, January 1 2020; Vol. 27, pp. 1172–1179.
91. Hossiney, N.; Das, P.; Mohan, M.K.; George, J. In-Plant Production of Bricks Containing Waste Foundry Sand—A Study with Belgaum Foundry Industry. *Case Stud. Constr. Mater.* **2018**, *9*, e00170, doi:10.1016/j.cscm.2018.e00170.
92. Garcia Del Angel, G.; Thomas, C. The Use of Foundry Sand for Recycled Aggregate Concrete. In *The Structural Integrity of Recycled Aggregate Concrete*
-

Produced with Fillers and Pozzolans; 2022; pp. 3–24 ISBN 9780128241059.

93. Jesus, C.; Arruda Junior, E.; Braga, N.S.; Silva Junior, J.; Barata, M.S. Coloured Concrete Produced from Low-Carbon Cements: Mechanical Properties, Chromatic Stability and Sustainability. *J. Build. Eng.* **2023**, *67*, 21, doi:10.2139/ssrn.4244563.
94. Cui, K.; Chang, J. Hydration, Reinforcing Mechanism, and Macro Performance of Multi-Layer Graphene-Modified Cement Composites. *J. Build. Eng.* **2022**, *57*, 104880, doi:10.1016/j.job.2022.104880.
95. Aksoylu, C.; Özkılıç, Y.O.; Hadzima-Nyarko, M.; Işık, E.; Arslan, M.H. Investigation on Improvement in Shear Performance of Reinforced-Concrete Beams Produced with Recycled Steel Wires from Waste Tires. *Sustain.* **2022**, *14*, doi:10.3390/su142013360.
96. Zeybek, Ö.; Özkılıç, Y.O.; Çelik, A.İ.; Deifalla, A.F.; Ahmad, M.; Sabri Sabri, M.M. Performance Evaluation of Fiber-Reinforced Concrete Produced with Steel Fibers Extracted from Waste Tire. *Front. Mater.* **2022**, *9*, 1–15, doi:10.3389/fmats.2022.1057128.
97. Basaran, B.; Kalkan, I.; Aksoylu, C.; Özkılıç, Y.O.; Sabri, M.M.S. Effects of Waste Powder, Fine and Coarse Marble Aggregates on Concrete Compressive Strength. *Sustainability* **2022**, *14*, 14388, doi:10.3390/su142114388.
98. Karalar, M.; Özkılıç, Y.O.; Aksoylu, C.; Sabri Sabri, M.M.; Beskopylny, A.N.; Stel'makh, S.A.; Shcherban', E.M. Flexural Behavior of Reinforced Concrete Beams Using Waste Marble Powder towards Application of Sustainable Concrete. *Front. Mater.* **2022**, *9*, 1–14, doi:10.3389/fmats.2022.1068791.
99. Çelik, A.İ.; Özkılıç, Y.O.; Zeybek, Ö.; Özdöner, N.; Tayeh, B.A. Performance Assessment of Fiber-Reinforced Concrete Produced with Waste Lathe Fibers. *Sustain.* **2022**, *14*, doi:10.3390/su141911817.
100. Karalar, M.; Özkılıç, Y.O.; Deifalla, A.F.; Aksoylu, C.; Arslan, M.H.; Ahmad, M.; Sabri, M.M.S. Improvement in Bending Performance of Reinforced Concrete Beams Produced with Waste Lathe Scraps. *Sustain.* **2022**, *14*, 1–17, doi:10.3390/su141912660.
101. Çelik, A.İ.; Özkılıç, Y.O.; Zeybek, Ö.; Karalar, M.; Qaidi, S.; Ahmad, J.; Burduhos-Nergis, D.D.; Bejinariu, C. Mechanical Behavior of Crushed Waste Glass as Replacement of Aggregates. *Materials (Basel)*. **2022**, *15*, doi:10.3390/ma15228093.
102. Qaidi, S.; Najm, H.M.; Abed, S.M.; Özkılıç, Y.O.; Al Dughaiishi, H.; Alost, M.; Sabri, M.M.S.; Alkhatib, F.; Milad, A. Concrete Containing Waste Glass as an Environmentally Friendly Aggregate: A Review on Fresh and Mechanical

- Characteristics. *Materials (Basel)*. **2022**, *15*, 1–16, doi:10.3390/ma15186222.
103. Karalar, M.; Bilir, T.; Çavuşlu, M.; Özkiliç, Y.O.; Sabri Sabri, M.M. Use of Recycled Coal Bottom Ash in Reinforced Concrete Beams as Replacement for Aggregate. *Front. Mater.* **2022**, *9*, doi:10.3389/fmats.2022.1064604.
104. Qaidi, S.; Al-Kamaki, Y.; Hakeem, I.; Dulaimi, A.F.; Özkılıç, Y.; Sabri, M.; Sergeev, V. Investigation of the Physical-Mechanical Properties and Durability of High-Strength Concrete with Recycled PET as a Partial Replacement for Fine Aggregates. *Front. Mater.* **2023**, *10*, 1–17, doi:10.3389/fmats.2023.1101146.
105. Tittarelli, F. 4 - Waste Foundry Sand. In *Waste and Supplementary Cementitious Materials in Concrete*; Siddique, R., Cachim, P., Eds.; Woodhead Publishing Series in Civil and Structural Engineering; Woodhead Publishing, 2018; pp. 121–147 ISBN 978-0-08-102156-9.
106. Mavroulidou, M.; Lawrence, D. Can Waste Foundry Sand Fully Replace Structural Concrete Sand? *J. Mater. Cycles Waste Manag.* **2019**, *21*, 594–605, doi:10.1007/s10163-018-00821-1.
107. Garcia Del Angel, G.; Aghajanian, A.; Tamayo, P.; Rico, J.; Thomas, C. Siderurgical Aggregate Cement-Treated Bases and Concrete Using Foundry Sand. *Appl. Sci.* **2021**, *11*, 1–13, doi:10.3390/app11010435.
108. Etxeberria, M.; Vazquez, E.; Mari, A.; Barra, M. Influence of Amount of Recycled Coarse Aggregates and Production Process on Properties of Recycled Aggregate Concrete. *Cem. Concr. Res.* **2007**, *37*, 735–742.
109. Cunha, S.; Tavares, A.; Aguiar, J.B.; Castro, F. Cement Mortars with Ceramic Molds Shells and Paraffin Waxes Wastes: Physical and Mechanical Behavior. *Constr. Build. Mater.* **2022**, *342*, 1–13, doi:10.1016/j.conbuildmat.2022.127949.
110. Ramon Roque da Silva, L.; Cirino Gaspar, F.; Cesar Gonçalves, P.; Claret dos Santos, V.; de Lourdes Noronha Motta Melo, M.; Ferreira Gomes, G. An Experimental Dynamic Study of Cement Mortar with Polyurethane Residues and Foundry Sand. *Eng. Struct.* **2023**, *274*, 115107, doi:10.1016/j.engstruct.2022.115107.
111. de Paiva, F.F.G.; dos Santos, L.F.; Tamashiro, J.R.; Pereira Silva, L.H.; Teixeira, S.R.; Galvín, A.P.; López-Uceda, A.; Kinoshita, A. Effect of Phenolic Resin Content in Waste Foundry Sand on Mechanical Properties of Cement Mortars and Leaching of Phenols Behaviour. *Sustain. Chem. Pharm.* **2023**, *31*, 100955, doi:10.1016/j.scp.2022.100955.
112. Sabour, M.R.; Derhamjani, G.; Akbari, M. Mechanical, Durability Properties, and Environmental Assessment of Geopolymer Mortars Containing Waste Foundry

- Sand. *Environ. Sci. Pollut. Res.* **2022**, 29, 24322–24333, doi:10.1007/s11356-021-17692-z.
113. Cui, K.; Liang, K.; Chang, J.; Lau, D. Investigation of the Macro Performance, Mechanism, and Durability of Multiscale Steel Fiber Reinforced Low-Carbon Ecological UHPC. *Constr. Build. Mater.* **2022**, 327, 126921, doi:10.1016/j.conbuildmat.2022.126921.
 114. EN 197-1. Cement Part 1: Composition, Specifications and Conformity Criteria for Common Cements 2011, 1–40.
 115. EN 80103:2013 Test Methods of Cements. Physical Analysis. Actual Density Determination 2013, 1–14.
 116. EN 196-6:2019 196-6:2019. Methods of Testing Cement - Part 6: Determination of Fineness 2010, 1–22.
 117. Paul, P.; Belhaj, E.; Diliberto, C.; Apedo, K.L.; Feugeas, F. Comprehensive Characterization of Spent Chemical Foundry Sand for Use in Concrete. *Sustain.* **2021**, 13, 1–19, doi:10.3390/su132212881.
 118. EN 1015-3:2000. Methods of Test for Mortar for Masonry. Part 3: Determination of Consistence of Fresh Mortar (by Flow Table) 2000, 1–12.
 119. EN 12390-7:2020. Testing Hardened Concrete - Part 7: Density of Hardened Concrete 2020, 1–15.
 120. EN 83980:2014. Concrete Durability. Test Methods. Determination of the Water Absorption, Density and Accessible Porosity for Water in Concrete. 2014, 1–8.
 121. EN 1015-11:2020. Methods of Test for Mortar for Masonry - Part 11: Determination of Flexural and Compressive Strength of Hardened Mortar 2020.
 122. EN 1338:2004. Concrete Paving Blocks - Requirements and Test Methods. **2004**, 1–72.
 123. Pandas Pearson Correlation Available online: <https://pandas.pydata.org/docs/reference/api/pandas.DataFrame.corr.html> (accessed on 9 February 2023).
 124. Srivastava, A.; Singh, S.K. Utilization of Alternative Sand for Preparation of Sustainable Mortar: A Review. *J. Clean. Prod.* **2020**, 253, 119706, doi:10.1016/j.jclepro.2019.119706.
 125. Khanduri, A. Properties of Mortar Incorporating Waste Foundry Sand. Master Degree Thesis., Thapar University, Patiala, 2010.

-
126. Mushtaq, S.M.; Siddique, R.; Goyal, S.; Kaur, K. Experimental Studies and Drying Shrinkage Prediction Model for Concrete Containing Waste Foundry Sand. *Clean. Eng. Technol.* **2021**, *2*, 100071, doi:10.1016/j.clet.2021.100071.
 127. Thomas, C.; Setién, J.; Polanco, J.A.A.Ja.; Alaejos, P.; Sánchez De Juan, M.; De Juan, M.S.; Sánchez De Juan, M. Durability of Recycled Aggregate Concrete. *Constr. Build. Mater.* **2013**, *40*, 1054–1065, doi:10.1016/j.conbuildmat.2012.11.106.
 128. Sainz-Aja, J.; Carrascal, I.; Polanco, J.; Thomas, C.; Sosa, I.; Casado, J.; Diego, S. Self-Compacting Recycled Aggregate Concrete Using out-of-Service Railway Superstructure Wastes. *J. Clean. Prod.* **2019**, *230*, 945–955, doi:10.1016/j.jclepro.2019.04.386.
 129. Laplante, P.; Aitcin, P.C.; Vézina, D. Abrasion Resistance of Concrete. *J. Mater. Civ. Eng.* **1991**, *3*, 19–28, doi:10.1061/(ASCE)0899-1561(1991)3:1(19).
 130. Warudkar, A.; Elavenil, S.; Arunkumar, A. Assessment of Abrasion Resistance of Concrete Pavement for Durability. *Int. J. Civ. Eng. Technol.* **2018**, *9*, 1176–1181.
 131. Portland Cement Association Cement-Treated Base Available online: <https://www.cement.org/docs/default-source/th-paving-pdfs/ctb-cement-treated-base/cement-treated-base-pca-logo.pdf?sfvrsn=2> (accessed on 10 May 2020).
 132. Lim, S.; Zollinger, D.G. Estimation of the Compressive Strength and Modulus of Elasticity of Cement-Treated Aggregate Base Materials. *Transp. Res. Rec.* **2003**, *30–38*, doi:10.3141/1837-04.
 133. CEDEX *Manual de Firmes Con Capas Tratadas Con Cemento*; Publicaciones, C. de P., Técnica, S.G.T., Fomento, M. de F., Eds.; ARTEGRAF, S.A.: Madrid, 2003; ISBN 84-7790-393-X.
 134. Ismail, A.; Baghini, M.S.; Karim, M.R.; Shokri, F.; Al-Mansob, R.A.; Firoozi, A.A.; Firoozi, A.A. Laboratory Investigation on the Strength Characteristics of Cement-Treated Base. *Appl. Mech. Mater.* **2014**, *507*, 353–360, doi:10.4028/www.scientific.net/amm.507.353.
 135. Molenaar, A.A.A. Design of Flexible Pavement, Lecture Note CT 4860 Structural Pavement Design. *Delft Univ. Technol. Delft Netherlands* **2007**.
 136. Terrel, R.L.; Epps, J.A.; Barenberg, E.J.; Mitchell, J.K.; Thompson, M.R. *Soil Stabilization in Pavement Structures: A User's Manual. Volume 1: Pavement Design and Construcion Considerations*; Washington, DC, 1979; Vol. 1.
 137. National Institute for Transport and Road Research *Cementitious Stabilizers in*

- Road Construction. Pretoria, South Africa: Committee of State Road Authorities. Report No.: TRH 13.; 1986;*
138. European Committee for Standardization 103501: Geotechnic. Compaction Test. Modified Proctor. **1994**.
 139. Terrel, R.L.; Epps, J.A.; Barenberg, E.J.; Mitchell, J.K.; Thompson, M.R. *Soil Stabilization in Pavement Structures: A User's Manual. Volume 2: Mixture Design Considerations*; 1979; ISBN 1111111111.
 140. Davis, K.A.; Warr, L.S.; Burns, S.E.; Hoppe, E.J. Physical and Chemical Behavior of Four Cement-Treated Aggregates. *J. Mater. Civ. Eng.* **2007**, *19*, 891–897, doi:10.1061/(ASCE)0899-1561(2007)19:10(891).
 141. Mohammadinia, A.; Arulrajah, A.; Sanjayan, J.; Disfani, M.M.; Bo, M.W.; Darmawan, S. Laboratory Evaluation of the Use of Cement-Treated Construction and Demolition Materials in Pavement Base and Subbase Applications. *J. Mater. Civ. Eng.* **2015**, *27*, 1–12, doi:10.1061/(ASCE)MT.1943-5533.0001148.
 142. Kuz'min, M.P.; Larionov, L.M.; Kondratiev, V. V.; Kuz'mina, M.Y.; Grigoriev, V.G.; Kuz'mina, A.S. Use of the Burnt Rock of Coal Deposits Slag Heaps in the Concrete Products Manufacturing. *Constr. Build. Mater.* **2018**, *179*, 117–124, doi:10.1016/j.conbuildmat.2018.05.222.
 143. Molenaar, A.; Xuan, D.; Houben, L.; Shui, Z. Prediction of the Mechanical Characteristics of Cement Treated Demolition Waste for Road Bases and Subbases. In Proceedings of the 10th conference on asphalt pavements for Southern Africa; KwaZulu-Natal, South Africa, 2011.
 144. Isola, M.; Betti, G.; Marradi, A.; Tebaldi, G. Evaluation of Cement Treated Mixtures with High Percentage of Reclaimed Asphalt Pavement. *Constr. Build. Mater.* **2013**, *48*, 238–247, doi:10.1016/J.CONBUILDMAT.2013.06.042.
 145. Grilli, A.; Bocci, M.; Tarantino, A.M. Experimental Investigation on Fibre-Reinforced Cement-Treated Materials Using Reclaimed Asphalt. *Constr. Build. Mater.* **2013**, *38*, 491–496, doi:10.1016/J.CONBUILDMAT.2012.08.040.
 146. Xuan, D.X.; Houben, L.J.M.; Molenaar, A.A.A.; Shui, Z.H. Mixture Optimization of Cement Treated Demolition Waste with Recycled Masonry and Concrete. *Mater. Struct. Constr.* **2012**, *45*, 143–151, doi:10.1617/s11527-011-9756-3.
 147. Nagrockienė, D.; Girskas, G.; Skripkiūnas, G. Properties of Concrete Modified with Mineral Additives. *Constr. Build. Mater.* **2017**, *135*, 37–42, doi:10.1016/j.conbuildmat.2016.12.215.
 148. Kuz'min, M.P.; Chu, P.K.; Qasim, A.M.; Larionov, L.M.; Kuz'mina, M.Y.;

- Kuz'min, P.B. Obtaining of Al-Si Foundry Alloys Using Amorphous Microsilica – Crystalline Silicon Production Waste. *J. Alloys Compd.* **2019**, *806*, 806–813, doi:10.1016/j.jallcom.2019.07.312.
149. Thomas, C.; Setién, J.; Polanco, J.A.; de Brito, J.; Fiol, F. Micro- and Macro-Porosity of Dry- and Saturated-State Recycled Aggregate Concrete. *J. Clean. Prod.* **2019**, *211*, 932–940, doi:10.1016/j.jclepro.2018.11.243.
150. Pérez, P.; Agrela, F.; Herrador, R.; Ordoñez, J. Application of Cement-Treated Recycled Materials in the Construction of a Section of Road in Malaga, Spain. *Constr. Build. Mater.* **2013**, *44*, 593–599, doi:10.1016/j.conbuildmat.2013.02.034.
151. Xuan, D.; Houben, L.J.M.; Molenaar, A.A.A.; Shui, Z. Cement Treated Recycled Demolition Waste as a Road Base Material. *J. Wuhan Univ. Technol. Sci. Ed.* **2010**, *25*, 696–699.
152. World Steel Association Web Page.
153. World Steel Association World Steel in Figures. **2019**.
154. Yıldırım, I.Z.; Prezzi, M. Chemical, Mineralogical, and Morphological Properties of Steel Slag. *Adv. Civ. Eng.* **2011**, *2011*, 13.
155. Thomas, C.; Rosales, J.; Polanco, J.A.; Agrela, F. *Steel Slags*; Elsevier Ltd, 2018; ISBN 9780081024805.
156. Monosi, S.; Ruello, M.L.; Sani, D. Electric Arc Furnace Slag as Natural Aggregate Replacement in Concrete Production. *Cem. Concr. Compos.* **2016**, *66*, 66–72, doi:10.1016/j.cemconcomp.2015.10.004.
157. Manso, J.M.; Polanco, J.A.; Losanez, M.; Gonzalez, J.J. Durability of Concrete Made with EAF Slag as Aggregate. *Cem. Concr. Compos.* **2006**, *28*, 528–534.
158. Pellegrino, C.; Cavagnis, P.; Faleschini, F.; Brunelli, K. Properties of Concretes with Black/Oxidizing Electric Arc Furnace Slag Aggregate. *Cem. Concr. Compos.* **2013**, *37*, 232–240.
159. Tamayo, P.; Pacheco, J.; Thomas, C.; de Brito, J.; Rico, J. Mechanical and Durability Properties of Concrete with Coarse Recycled Aggregate Produced with Electric Arc Furnace Slag Concrete. *Appl. Sci.* **2020**, *10*, doi:10.3390/app10010216.
160. Sosa Yépez, I. Incorporación de Escorias Siderúrgicas En Hormigones Autocompactantes de Altas Prestaciones, Universidad de Cantabria, 2017.
161. Rodríguez-Fernández, I.; Lastra-González, P.; Indacochea-Vega, I.; Castro-Fresno, D. Recyclability Potential of Asphalt Mixes Containing Reclaimed

- Asphalt Pavement and Industrial By-Products. *Constr. Build. Mater.* **2019**, *195*, 148–155, doi:10.1016/J.CONBUILDMAT.2018.11.069.
162. Autelitano, F.; Giuliani, F. Electric Arc Furnace Slags in Cement-Treated Materials for Road Construction: Mechanical and Durability Properties. *Constr. Build. Mater.* **2016**, *113*, 280–289, doi:10.1016/J.CONBUILDMAT.2016.03.054.
163. Fuente-Alonso, J.A.; Ortega-López, V.; Skaf, M.; Aragón, Á.; San-José, J.T. Performance of Fiber-Reinforced EAF Slag Concrete for Use in Pavements. *Constr. Build. Mater.* **2017**, *149*, 629–638, doi:10.1016/J.CONBUILDMAT.2017.05.174.
164. Faleschini, F.; Alejandro Fernández-Ruiz, M.; Zanini, M.A.; Brunelli, K.; Pellegrino, C.; Hernández-Montes, E. High Performance Concrete with Electric Arc Furnace Slag as Aggregate: Mechanical and Durability Properties. *Constr. Build. Mater.* **2015**, *101*, 113–121, doi:10.1016/J.CONBUILDMAT.2015.10.022.
165. Siddique R. Klaus, J. Influence of Metakaolin on the Properties of Mortar and Concrete: A Review. *Appl. Clay Sci.* **2009**, *43*, Pages 392–400.
166. González-Ortega, M.A.; Cavalaro, S.H.P.; Rodríguez de Sensale, G.; Aguado, A. Durability of Concrete with Electric Arc Furnace Slag Aggregate. *Constr. Build. Mater.* **2019**, *217*, 543–556, doi:10.1016/J.CONBUILDMAT.2019.05.082.
167. Arribas, I.; Santamaría, A.; Ruiz, E.; Ortega-López, V.; Manso, J.M. Electric Arc Furnace Slag and Its Use in Hydraulic Concrete. *Constr. Build. Mater.* **2015**, *90*, 68–79, doi:10.1016/j.conbuildmat.2015.05.003.
168. Coppola, L.; Buoso, A.; Coffetti, D.; Kara, P.; Lorenzi, S. Electric Arc Furnace Granulated Slag for Sustainable Concrete. *Constr. Build. Mater.* **2016**, *123*, 115–119, doi:10.1016/J.CONBUILDMAT.2016.06.142.
169. Pellegrino, C.; Gaddo, V. Mechanical and Durability Characteristics of Concrete Containing EAF Slag as Aggregate. *Cem. Concr. Compos.* **2009**, *31*, 663–671, doi:10.1016/J.CEMCONCOMP.2009.05.006.
170. Faleschini, F.; De Marzi, P.; Pellegrino, C. Recycled Concrete Containing EAF Slag: Environmental Assessment through LCA. *Eur. J. Environ. Civ. Eng.* **2014**, *18*, 1009–1024, doi:10.1080/19648189.2014.922505.
171. Qasrawi, H. The Use of Steel Slag Aggregate to Enhance the Mechanical Properties of Recycled Aggregate Concrete and Retain the Environment. *Constr. Build. Mater.* **2014**, *54*, 298–304, doi:10.1016/J.CONBUILDMAT.2013.12.063.
172. Faleschini, F.; Santamaria, A.; Zanini, M.A.; San José, J.-T.; Pellegrino, C. Bond between Steel Reinforcement Bars and Electric Arc Furnace Slag Concrete. *Mater.*

- Struct.* **2017**, *50*, 170.
173. de La Cruz, J.C.; del Campo, J.M.; Colorado, D. Comparative Study on Porosity and Permeability of Conventional Concrete and Concrete with Variable Proportions of Natural Zeolite Additions. *Rev. la Constr.* **2015**, *14*, 72–78, doi:10.4067/s0718-915x2015000300009.
174. Ministerio de Fomento *Instrucción de Hormigón Estructural (EHE-08)*; 2008;
175. Thiruvenkita, M.; Pandian, S.; Santra, M.; Subramanian, D. Use of Waste Foundry Sand as a Partial Replacement to Produce Green Concrete: Mechanical Properties, Durability Attributes and Its Economical Assessment. *Environ. Technol. Innov.* **2020**, *19*, 101022, doi:10.1016/j.eti.2020.101022.
176. Ganesh Prabhu, G.; Hyun, J.H.; Kim, Y.Y. Effects of Foundry Sand as a Fine Aggregate in Concrete Production. *Constr. Build. Mater.* **2014**, *70*, 514–521, doi:10.1016/j.conbuildmat.2014.07.070.
177. Siddique, R.; Kunal; Mehta, A. Utilization of Industrial By-Products and Natural Ashes in Mortar and Concrete Development of Sustainable Construction Materials. In *Nonconventional and Vernacular Construction Materials: Characterisation, Properties and Applications*; Elsevier Ltd, 2019; pp. 247–303 ISBN 9780081027042.
178. Zhang, Y.; Sappinen, T.; Korkiala-Tanttu, L.; Vilenius, M.; Juuti, E. Investigations into Stabilized Waste Foundry Sand for Applications in Pavement Structures. *Resour. Conserv. Recycl.* **2021**, *170*, 105585, doi:10.1016/j.resconrec.2021.105585.
179. Friol Guedes de Paiva, F.; Tamashiro, J.R.; Pereira Silva, L.H.; Kinoshita, A. Utilization of Inorganic Solid Wastes in Cementitious Materials – A Systematic Literature Review. *Constr. Build. Mater.* **2021**, *285*, doi:10.1016/j.conbuildmat.2021.122833.
180. Alonso-Santurde, R.; Andrés, A.; Viguri, J.R.; Raimondo, M.; Guarini, G.; Zanelli, C.; Dondi, M. Technological Behaviour and Recycling Potential of Spent Foundry Sands in Clay Bricks. *J. Environ. Manage.* **2011**, *92*, 994–1002, doi:10.1016/j.jenvman.2010.11.004.
181. Ahmad, J.; Aslam, F.; Zaid, O.; Alyousef, R.; Alabduljabbar, H. Mechanical and Durability Characteristics of Sustainable Concrete Modified with Partial Substitution of Waste Foundry Sand. *Struct. Concr.* **2021**, *22*, 2775–2790, doi:10.1002/suco.202000830.
182. Bilal, H.; Yaqub, M.; Ur Rehman, S.K.; Abid, M.; Alyousef, R.; Alabduljabbar, H.; Aslam, F. Performance of Foundry Sand Concrete under Ambient and Elevated Temperatures. *Materials (Basel)*. **2019**, *12*, doi:10.3390/ma12162645.

183. Siddique, R.; Singh, G.; Singh, M. Recycle Option for Metallurgical By-Product (Spent Foundry Sand) in Green Concrete for Sustainable Construction. *J. Clean. Prod.* **2018**, *172*, 1111–1120, doi:10.1016/j.jclepro.2017.10.255.
184. EN 1097-6 Tests for Mechanical and Physical Properties of Aggregates - Part 6: Determination of Particle Density and Water Absorption. **2014**.
185. EN 933-2 Tests for Geometrical Properties of Aggregates. Determination of Particle Size Distribution. Test Sieves, Nominal Size of Apertures. **1999**.
186. EN 12350-8 Testing Fresh Concrete - Part 8: Self-Compacting Concrete - Slump-Flow Test. **2020**.
187. EN 12350-9:2011 Testing Fresh Concrete - Part 9: Self-Compacting Concrete - V-Funnel Test. **2011**.
188. EN 12350-10:2011 Testing Fresh Concrete - Part 10: Self-Compacting Concrete - L Box Test. **2011**.
189. EN 12350-12:2011 Testing Fresh Concrete - Part 12: Self-Compacting Concrete - J-Ring Test. **2011**.
190. EN 206-1 Concrete - Specification, Performance, Production and Conformity. **2021**.
191. EN 12390-2 Testing Hardened Concrete. Part 2: Making and Curing Specimens for Strength Tests. **2015**.
192. EN 12390-3 Testing Hardened Concrete - Part 3: Compressive Strength of Test Specimens. **2011**.
193. EN 12390-6 Testing Hardened Concrete - Part 6: Tensile Splitting Strength of Test Specimens. **2010**.

Annexes

Index of tables and figures

Table 1.1. Physical properties of RFS according to different authors. .	5
Table 1.2. Chemical composition of RFS (% by weight) according to different authors.	6
Table 2.1. Physical properties of UFS according to several authors. .	22
Table 2.2. Compressive strength (MPa) with different replacement percent of UFS at 28 days according to different authors.	27
Table 2.3. Flexural strength (MPa) with different replacement percent of UFS at 28 days according to different authors.	31
Table 3.1. Cement chemical composition.	46
Table 3.2. Physical properties of the aggregates used.	48
Table 3.3. UFS chemical composition.....	48
Table 3.4. Mortar mix proportion descriptions.....	48
Table 4.1. X-ray fluorescence (XRF) chemical composition analysis of FS (%wt.).....	77
Table 4.2. XRF chemical composition of SA (% wt.).	78
Table 4.3. Properties of the SA.....	79
Table 4.4. CTB proctor test results.....	80
Table 4.5. CTB proctor test results with optimal moisture.....	81
Table 4.6. CTB and SAC mix proportions.	82
Table 4.7. Physical properties of the SAC.....	84
Table 4.8. Gas permeability and water penetration of the SAC.	85
Table 4.9. Compressive strength results.	86
Table 4.10. Flexural strength of SAC mixtures.	87
Table 5.1. Physical properties of the aggregates used.	97
Table 5.2. XRF chemical composition of cement and UFS.	98
Table 5.3. Mix proportions (kg/m ³).	99
Table 5.4. EN and EFNARC guidelines.	101
Table 5.5. Fresh state properties of the self-compacting concretes. .	105

Figure 1.1. Doctoral Thesis outline.....	14
Figure 2.1. Foundry sand generation.....	19
Figure 2.2. Green foundry sand (left) and Chemical foundry sand. Source: [65]......	20
Figure 2.3. Chemical composition of UFS (%wt.) according to different authors.	23
Figure 2.4. Slump test results according to different authors.....	26
Figure 2.5. Carbonation depth of concrete with different UFS replacements according to different authors.	32
Figure 2.6. Bricks manufactured with UFS. Source: [91].	37
Figure 3.1. Aggregates grading curve.....	47
Figure 3.2. Used foundry (a) sand and silica sand (b).	47
Figure 3.3. Set up of the flexural (a) and compression strength test (b).	49
Figure 3.4. Set up of the abrasion wear resistance test.	50
Figure 3.5. Sample preparation for SEM analysis. (a) oven drying at 70 °C. (b) Samples after metallization.....	51
Figure 3.6. Mortar workability: slump table test results in cm (a) and comparative example for a fixed UFS value (b).	52
Figure 3.7. Mortar workability: slump table test results in cm (a); effect of UFS in mortar workability with w/c = 0.5 (b).	53
Figure 3.8. Mortar workability: slump table test results. Comparative example for a fixed w/c ratio.	54
Figure 3.9. Specific gravity (g/cm^3) of the mortar mixes (a) and decrease in the specific gravity (%) (b).	54
Figure 3.10. Dry density (g/cm^3) of the mortar mixes (a) and dry density decrease (%) (b).	55
Figure 3.11. Bulk density of the mortar mixes (g/cm^3) (a) and bulk density decrease (%) (b).	56
Figure 3.12. Accessible porosity of mortars with UFS (% vol.).....	57
Figure 3.13. Absorption coefficient of mortars with UFS (% wt.).	58

Figure 3.14. Flexural strength (MPa) as function of w/c ratio and UFS replacement.....	59
Figure 3.15. Compressive Strength (MPa) as function of w/c ratio and UFS replacement.....	59
Figure 3.16. Mortar specimens with UFS, from 0 to 100%.	60
Figure 3.17. Compressive strength of mortars (MPa) (a) and w/c ratio influence on compressive strength of UFS mortars (b).	60
Figure 3.18. Wear resistance.....	62
Figure 3.19. Examples of the specimen surface after the wear resistance tests.....	63
Figure 3.20. Correlation matrix of analysed parameters.	64
Figure 3.21. Microstructural analysis under 25× magnification: pores, cracks and cavities of UFS mortars with 0% (a), 25% (b), 50% (c), 75% (d) and 100% (e) substitution.	66
Figure 3.22. Microstructural analysis under 500× magnification: bond between paste and aggregates of UFS mortars with 0% (a), 25% (b), 50% (c), 75% (d) and 100% (e) substitution.	67
Figure 4.1. Foundry sand (FS) and siderurgical aggregate (SA) grading curve.....	76
Figure 4.2. Untreated siderurgical aggregates.....	77
Figure 4.3. SA aggregate fraction grading curves.	78
Figure 4.4. Cement-treated bases A (CTB-A) aggregates skeleton.	80
Figure 4.5. SAC aggregates skeleton.....	82
Figure 4.6. Modulus of elasticity of SAC-A (a) and SAC-B (b).....	87
Figure 5.1. Grading curves of the aggregates.	98
Figure 5.2. Mix procedure: dry mix of the aggregates (a); addition of first part of mixing water (b); settling of the SCC mix by 3 min (c)..	100
Figure 5.3. Appearance of the slump flow of the three self-compacting mixes; SCC-C (a), SCC-UFS-50 (b) and SCC-UFS-100 (c).....	102
Figure 5.4. Time reduction of t ₅₀₀ test and V-funnel test.....	104
Figure 5.5. Compressive strength of the SCC mixes.	106
Figure 5.6. Detail of compression fractures at 28 days.	107

Figure 5.7. Splitting tensile strength of the SCC mixes..... 108
Figure 5.8. Micrographs obtained at 1500×. 109
Figure 5.9. Micrographs obtained at 3000× and 7000×..... 110